1969

Spherical antenna array

Narong Yoothanom

Department: Electrical and Computer Engineering

SPHERICAL ANTENNA ARRAY

by 54

NARONG YOOTHANOM, 1942

A DISSERTATION

Presented to the Faculty of the Graduate School of the

UNIVERSITY OF MISSOURI -- ROLLA

In Partial Fulfillment of the Requirement for the Degree of

DOCTOR OF PHILOSOPHY

in

ELECTRICAL ENGINEERING

Rolla, Missouri

1969

W. H. Sketek (Advisor)	E C Bertnolli
J Rivers	J. K. Foote
Norman Dillman	J. G. Smith

ABSTRACT

The far field radiation pattern of an isotropic spherical antenna array with two types of element distributions, a latitude-longitude distribution and an approximately equally-spaced distribution, has been analyzed using Poisson's Sum Formula. Beamwidth expressions of both element distributions are found in various planes. All numerical results are given only for the case of 21 rings.

ACKNOWLEDGEMENTS

The author would like to acknowledge with sincere respect the guidance and invaluable comments and discussions provided for him by Professor Gabriel G. Skitek throughout his graduate study at the University of Missouri - Rolla.

He would also like to acknowledge both the Anandhamahidol Foundation under the patronage of the King of Thailand and the University of Missouri - Rolla for the financial support throughout his graduate work.

Much of the appreciation goes to the Department of Computer Science for granting a project number and the extensive use of the IBM/360 computer in the department.

Thanks go to Muriel Johnson for typing the manuscript.

TABLE OF CONTENTS

LIST OF SYMBOLS

a	radius of the sphere
A_s	s^{th} weight of the s_{max}-point Gaussian Quadrature integration formula
$\bar{a}_x, \bar{a}_y, \bar{a}_z$	unit vectors in Cartesian coordinates
AR	axial ratio of an elliptical polarization ellipse
BW	beamwidth of the LL distribution
BWA	beamwidth of the AES distribution
C_s	s^{th} pattern harmonic coefficient
d	ring spacing
d_m	antenna spacing in the m^{th} ring
d_{eq}	equator spacing
dx	differential of x
$\bar{e}_\theta, \bar{e}_\phi, \bar{e}_r$	unit vectors in spherical coordinates
E	electric far field pattern
E_A	electric far field pattern of the AES distribution
$f(n)$	n^{th} term of n-summation
$f(\theta_m)$	resultant of n-summation
$g(\theta,\phi,m)$	m^{th} term of m-summation
I_s	s^{th} pattern harmonic
I_{sA}	s^{th} pattern harmonic of the AES distribution
I_{mn}	mn^{th} antenna current amplitude
j	$\sqrt{-1}$
$J_m(x)$	m^{th} order Bessel function of argument x
k	wave propagation constant
M	total number of rings less one

$\overline{M}$	unit vector in the direction of the mo^{th} antenna
N	total number of antennas in each ring in the LL distribution
N_{eq}	number of antennas in the equator
N_m	number of antennas in the m^{th} ring
$[[N_m]]$	the integer nearest to N_m
$P_m(x)$	m^{th} order Legendre polynomial of argument x
r_m	radius of the m^{th} ring, measured from the polar axis
$\overline{R}$	unit vector in the direction of the observation point
R	distance from the observation point to the origin of the spherical coordinates
s_n	distance from the n^{th} element to the reference point in a linear array
t_s	zeros of the Legendre polynomial of order s_{max}
x,y,z	Cartesian coordinates
π	3.14159
θ,ϕ,r	spherical coordinates
θ_m	elevation angle of the m^{th} ring
θ_0	elevation angle of the mainbeam
θ_b	elevation angle of the beamwidth
ϕ_n	azimuth angle of the n^{th} antenna
ϕ_0	azimuth angle of the mainbeam
ϕ_b	azimuth angle of the beamwidth
λ	wavelength
ρ_e	element density

μ	arbitrary constant
σ	percentage spacing deviation
ψ_{mn}	mn^{th} antenna current phasing
ξ_{mn}	angle subtended by the observation point and the mn^{th} antenna at the reference point
ε	positive number less than unity

LIST OF FIGURES

LIST OF TABLES

CHAPTER I

INTRODUCTION TO THE SPHERICAL ANTENNA ARRAY PROBLEM

A. Introduction

Since the early days of antennas, which traces back to the time prior to World War II, it has been recognized that antenna arrays play an essential role in the world of communication, being a transmitting device as well as a receiver of an electromagnetic signal.

The antenna array is given a great deal of interest since it possesses at least two particularly attractive features, directability with a well-defined beam and electronical scannability. These features are exhibited clearly in the radiation pattern of a linear or planar phased array, whether it is uniformly or non-uniformly spaced.

In space communication and space tracking, it is found desirable for antenna arrays to beam scan through a hemisphere or even the whole sphere. For a large array, however, it would be preferable if the antenna array could remain fixed during operation. A spherical antenna array that is electronically scanned can satisfy the requirements of a spaced fixed and beam scanning into a complete spherical space. This is due to the fact that

radiation in any spherical space direction requires an antenna of spherical symmetry. Furthermore, from a specific direction, the spherical array does not look different to an observer at a far point providing that the spherical array contains a large number of antenna elements. This fact seems to guarantee that its radiation pattern will not alter very significantly when the main beam is electronically scanned. This makes the spherical array very challenging for beam scanning over a complete sphere.

B. Definition of a Spherical Antenna Array

A spherical antenna array consists of radiators (antenna elements) positioned either uniformly or non-uniformly on the surface of an imaginary sphere. An element of the spherical antenna array, due to the curved surface of the imaginary sphere, is positioned on the plane tangent to the sphere. Figure 1-1 illustrates an example of an equally-spaced spherical array which contains 20 elements [3]. This is the only spherical antenna array that has elements spaced precisely uniform. It can be shown that a uniformly spherical antenna array can have only 20 elements. The element locations were found through the use of the icosahedron. If the number of elements exceeds 20, the spherical antenna array will no longer be uniform.

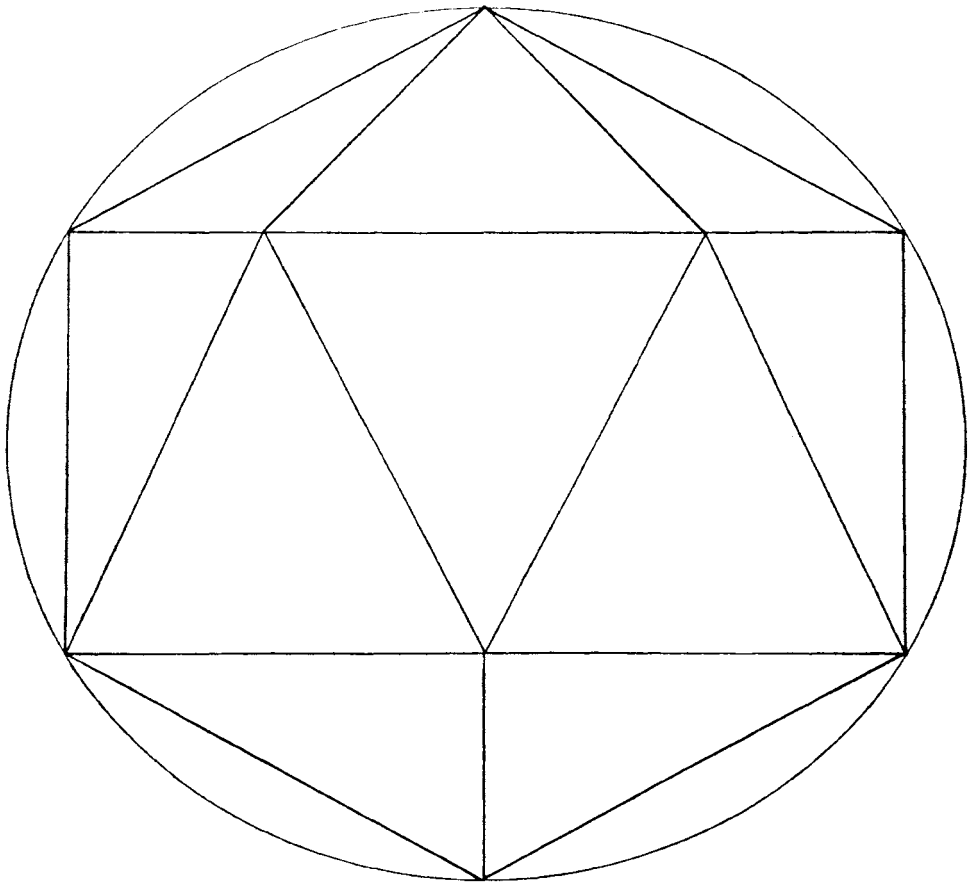

Figure 1-1. The Icosahedron Distribution

C. Review of the Literature

Prior to 1963, all antenna arrays were arranged into two classifications, linear and planar arrays. In 1963, conventions for the analysis of spherical arrays were proposed by Hoffman [1]. His analysis was made possible by direct computation of the pattern summation on a computer. Wolff [2] discussed the general analysis of spherical arrays of linearly polarized elements and concluded that a spherical array can produce a well-defined beam with deep nulls in its radiation pattern. Du and Tai [17] studied the radiation pattern of an array of four symmetrically located elementary sources on a perfectly conducting sphere. Sengupta, et al. [3] presented a paper on radiation characteristics of a spherical array of circularly polarized elements. Their array was formed by first dividing each face of a circumscribed icosahedron into four equitriangles. Then all vertices of the triangles were moved along the radius of the sphere to its surface where the elements were located. By doing so, the symmetry of the array is lost since only the triangle constructed at the center stays equitriangular. Consequently, the array is not equally-spaced any more. The pattern computation was made through the use of a computer by evaluating the location of each antenna in terms of spherical coordinates and substituting it into the summation equation of the pattern.

In addition to this literature, Smith [24] reported an approximation of a spherical array by a continuous field distribution in a spherical aperture. Unfortunately, this report is rated as classified information; it can not be circulated to the public.

D. Scope of This Dissertation

The motivation for this research is generated by the fact that the study of a spherical antenna array, to date, has been limited to a few cases of element distribution which contained only a small number of elements. Though the distributions were simple, no rigorous theoretical radiation characteristics of the array were formulated in an explicit form. All analyses were made possible by direct substitution of the geometrical location of each antenna into the field pattern equations and, through a great deal of help from a computer, the radiation pattern was analyzed. This computer approach might be handy, but it is not suited to a speedy computation, especially when a very large number of elements are concerned.

Therefore, this research has been conducted with the goal to analyze the radiation characteristics (i.e., field pattern, beamwidth, etc.) of a spherical antenna array which has an element distribution other than the icosahedron. The element distribution considered has three favorable characteristics when compared to the one obtained through the use of an icosahedron: simpler, easier to locate

elements, and the number of elements can be increased to a very large number without losing the equally-spaced fundamental character of the array. No experimental work was performed due to a lack of facilities and instrumentation.

Two types of element distributions were considered. One was the latitude-longitude type and the other was the approximately equally-spaced distribution. Both of them have a similar physical appearance. Antennas were arranged into rings whose centers are on the polar axis of the sphere. The number of antennas in each ring is assumed to be very large.

All elements were identical and were assumed to be isotropic. The amplitude of the current distribution throughout the array was assumed uniform. Although the mutual coupling among elements existed everywhere in the array, it was not taken into account in this dissertation.

Both element distributions of the array are discussed in Chapter II. Chapter III deals with the formulation as well as the simplification of the far field pattern. Chapter IV gives the theoretical analysis (the radiation patterns as well as the beamwidths) of both distributions.

Chapter V analyzes the radiation characteristics numerically. Various graphical presentations of both patterns and beamwidths in various planes can be found in this chapter. The results are summarized in Chapter VI,

and recommendations for further study in this area are given in this chapter.

CHAPTER II

ELEMENT DISTRIBUTION

A. The Latitude-Longitude Distribution

1. Spacing

One of the element distributions of the spherical array used in this study is of the latitude-longitude type. It is precisely the conventional one employed in geographical study of the world. Figure 2-1 shows the intersections of the sphere latitudes and longitudes. At each intersection, an identical radiation element, which is assumed isotropic in this study, is placed.

The latitudes or rings on the sphere are arranged in such a way that they are equally spaced*. Let d be the ring spacing, a be the radius of the sphere, and M+1 be the total number of rings. Then the ring spacing is found by dividing the circumferential distance from the north pole to the south pole by the number of ring intervals.

$$d = \frac{\pi a}{M} \quad . \tag{2-1}$$

---

*For simplicity in the case of non-planar array, the element spacing is defined as the distance between two adjacent elements along the curved surface.

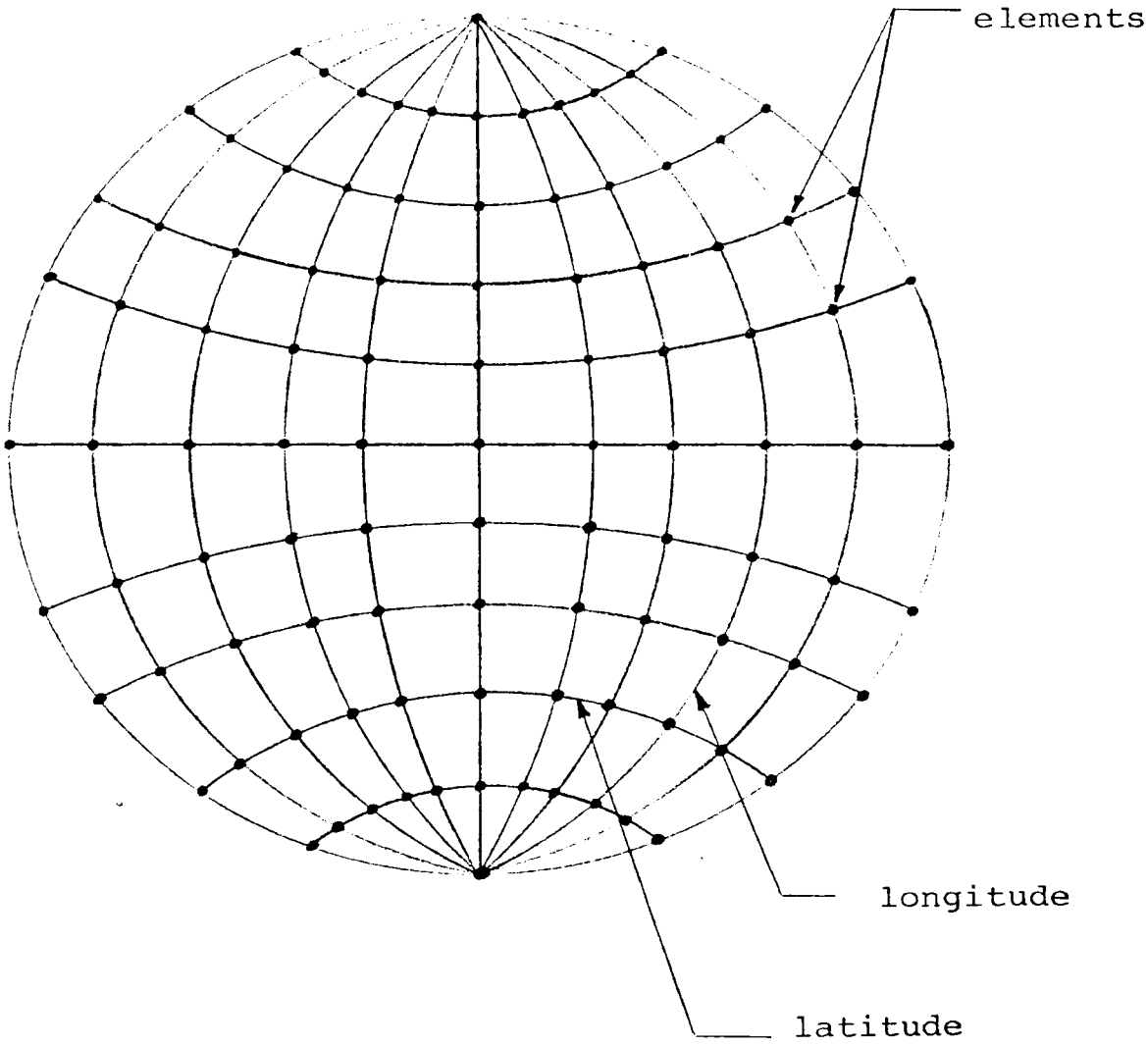

Figure 2-1. The Latitude-Longitude Distribution

The longitudes of the sphere are arranged such that they divide each latitude ring into a number of equal intervals. Therefore, the antennas in each ring are uniformly spaced. Obviously, due to the difference in ring sizes, the antenna spacing from ring to ring is not equal. One characteristic of this distribution is that every ring contains the same number of antennas.

Let N be the total number of antennas in each ring and d_m be the antenna spacing in the m^{th} ring. With the help of Figure 2-2, the antenna spacing in the m^{th} ring is found to be

$$d_m = \frac{2\pi a}{N} \sin \theta_m \quad , \tag{2-2}$$

where

$$\theta_m = \frac{m\pi}{M} \tag{2-3}$$

and m = 0, 1, 2, 3, $\cdots$, M.

At $\theta_m = \pi/2$, Equation (2-2) gives the element spacing at the equator of the sphere, which is

$$d_{eq} = \frac{2\pi a}{N} \quad . \tag{2-4}$$

In terms of d_{eq}, the general expression of d_m can be placed in the form

$$\begin{aligned} d_m &= d_{eq} \sin \theta_m \\ &= d_{eq} \sin \left(\frac{m\pi}{M}\right) \end{aligned} \tag{2-5}$$

Equation (2-5) is valid for all M, both odd and even. When M is even, one ring will fall on the equator of the sphere. When M is odd, however, no ring falls on the equator.

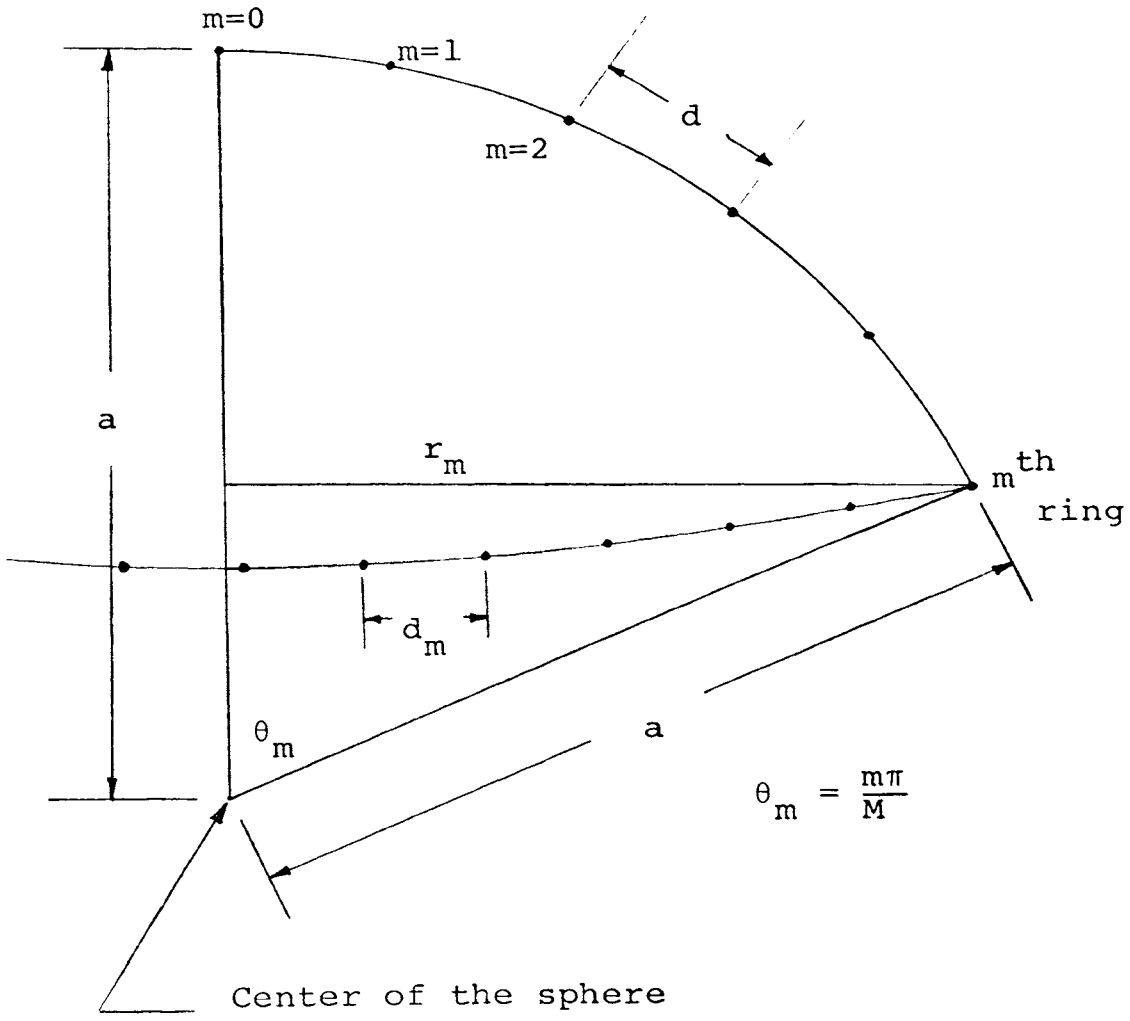

Figure 2-2. Element Spacing Computation

In this type of element location, it is assumed that

$$d = d_{eq} \quad . \tag{2-6}$$

Thus, only near the equator will the elements be relatively equally spaced.

From Equation (2-6) it follows that

$$\frac{\pi a}{M} = \frac{2\pi a}{N}$$

which simplifies to

$$N = 2M \; . \tag{2-7}$$

Equation (2-7) indicates that path length at the equator equals twice the path length from pole to pole along the spherical surface. It also shows that the number of antennas at the equator, as well as in the other rings, is always an even number, for M odd or even.

Let us generalize so that

$$d = \mu\lambda \tag{2-8}$$

where μ is an arbitrary constant, then

$$\frac{\pi a}{M} = \mu\lambda \; .$$

The radius of the sphere in wavelength becomes

$$a = \frac{\mu M}{\pi} \lambda \; . \tag{2-9}$$

Multiplying through by the propagation constant k, and using the well-known relation of $k\lambda = 2\pi$, we finally obtain

$$ka = 2\mu M \; , \tag{2-10}$$

which reduces to

$$ka = M \tag{2-11}$$

for the case of half-wavelength spacing ($\mu = 1/2$).

2. Element Density

The element density is defined as the ratio of total number of elements in the array to the surface area of the sphere. For the latitude-longitude element distribution, the total number of elements is (M+1)N. Therefore,

$$\rho_e = (M + 1)N/4\pi a^2 . \tag{2-12}$$

Substituting Equations (2-7) and (2-9) into (2-12) and simplifying gives

$$\rho_e = 2\pi/\lambda^2 . \tag{2-13}$$

This is approximately 6.28 elements per square wavelength.

In the study of linear and planar arrays, it has been found that the element of the array should be spaced at half-wavelengths apart, otherwise the grating lobes in the field pattern would appear. With the element density greater than this critical value, the spherical array having this type of element distribution appears to have one or more high grating lobes in its pattern.

For the case of an average spacing of half-wavelength (i.e., an element density of 4 per square wavelength), the equator spacing must be

$$d_{eq} = \frac{2\pi a}{N} = \frac{2\pi}{N} \cdot \sqrt{\frac{(M + 1)N}{16\pi}} \quad \lambda$$

$$\simeq 0.628 \ \lambda .$$

B. Approximately Equally-Spaced Array

1. Element Distribution

For the element distribution discussed in Section A, the element spacing in the rings away from the equator becomes smaller. This can be easily verified in Equation (2-4) by setting the values of m which are much smaller or greater than M/2. For example, the spacing of the first ring is calculated by setting m = 1 in Equation (2-5), which gives

$$d_1 = d_{eq} \sin (\pi/M) \quad . \tag{2-14a}$$

For M = 20 and $d_{eq} = 0.628\lambda$,

$$d_1 = 0.0984\lambda \quad . \tag{2-14b}$$

It is shown by Equation (2-14b) that the element spacing in the first ring is very small compared to the spacing at the equator. For this case, the element spacing is 6.4 times smaller. The element spacings on other rings for the case of M = 20 are plotted in Figure 2-3.

Thus one drawback of the latitude-longitude distribution is that the element spacing becomes quite small in the rings close to the poles of the sphere. The mutual coupling between elements in those rings can no longer be neglected in practice. In this work, however, as has been stated earlier, the main purpose is to find the first order of approximation and some method of theoretical

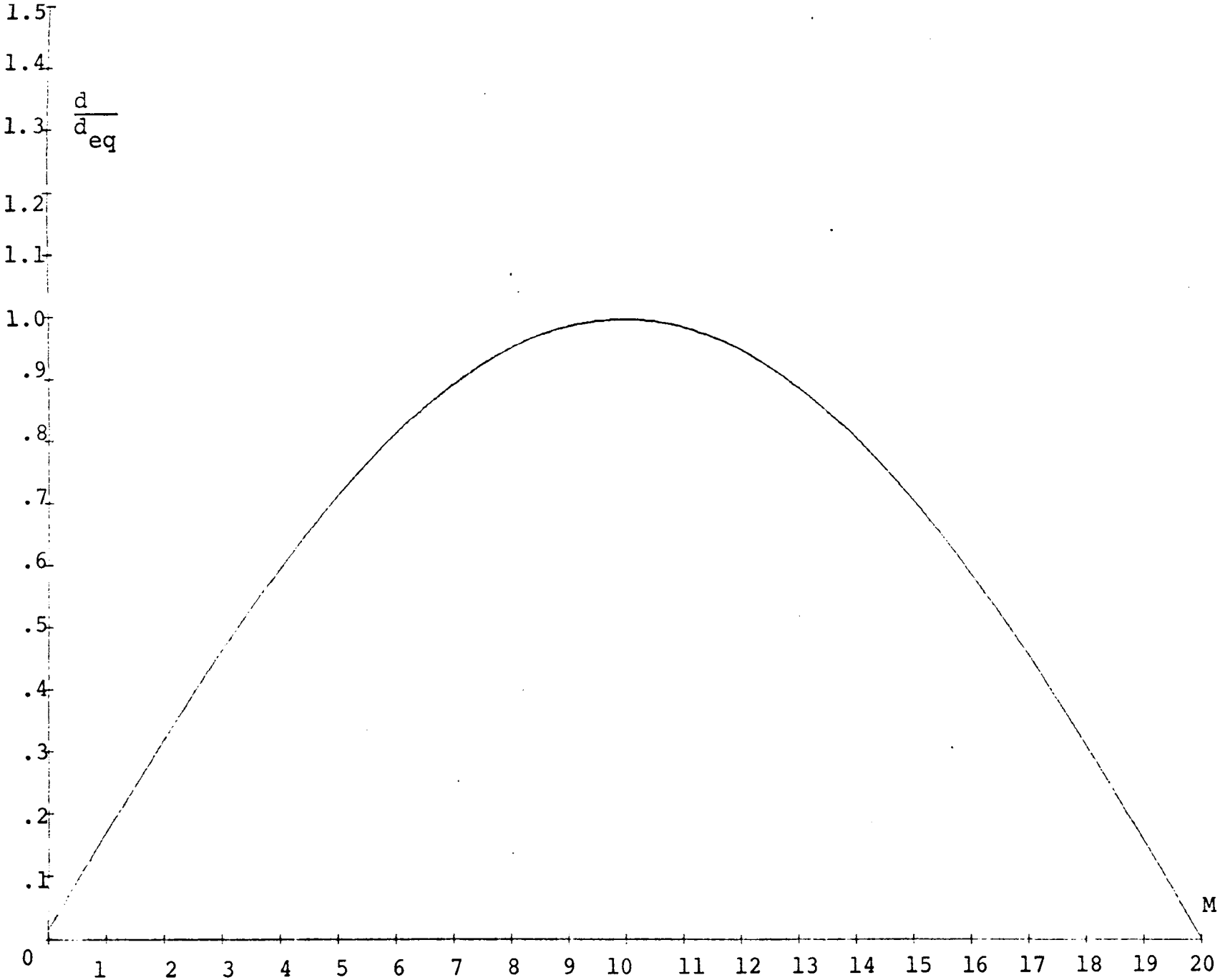

Figure 2-3. Element Spacing in Various Rings in the Latitude-Longitude Distribution for M = 20

analysis of a spherical array. Thus mutual coupling between elements will not be considered in this dissertation.

One way to avoid the mutual coupling effects in the rings is to force the antenna spacing to be greater than $\lambda/2$ and constant in every ring. By this restriction, the rings no longer contain the same number of antennas. Furthermore, the elements of different rings are not in general colinear except on the reference plane ($\phi = 0$), where, for the matter of convenience, they are forced to be colinear.

For the approximately equally-spaced array, the spacing in each ring is said to be equal. It does not imply this in a precise sense since a sphere can not be divided into equal identical areas except for the case of an icosahedron or a polygon of a smaller number of sides (see Appendix A).

Thus the spacing in the approximately equally-spaced distribution fluctuates around the average spacing, which at the beginning is assumed to take the value of halfwavelength. Some of the element spacings will take on values less than, while others will take on values greater than, halfwavelength.

The rings are kept at halfwavelength apart to insure the element density to be around 4 elements per square wavelength. Let N_{eq} be the number of elements on the equatorial ring. Then

$$N_{eq} = 2M \ . \tag{2-15}$$

By the condition that the element spacing is kept constant for all rings and equal to the ring spacing,

$$d = d_m \ ,$$

the number of elements in the m^{th} ring is found to be

$$N_m = 2M \sin \left(\frac{m\pi}{M}\right) \tag{2-16}$$

for $m \neq 0, M$. $N_m = 1$ for $m = 0, M$.

In general, the value of N_m obtained from Equation (2-16) is not an integer. Physically, the number of elements in each ring, however, must be an integer. To compromise this condition, Equation (2-16) is modified to be

$$\text{the number of elements in the } m^{th} \text{ ring} = [[N_m]] \tag{2-17}$$

where the double bracket symbol has been introduced to indicate that only the integer nearest to the value N_m is picked.

Under this modification, the spacing in the m^{th} ring is now given by

$$d_m = \frac{2\pi a}{[[N_m]]} \sin \left(\frac{m\pi}{M}\right) \tag{2-18}$$

or, in terms of the equator spacing, d_{eq},

$$\frac{d_m}{d_{eq}} = \frac{2M}{[[N_m]]} \sin \left(\frac{m\pi}{M}\right) \ . \tag{2-19}$$

The percentage of the deviation of element spacing is

$$\sigma = \frac{d_m - d_{eq}}{d_{eq}} \times 100\% \ . \qquad (2\text{-}20)$$

An example of the element distribution of this type is shown in Tables 1 and 2 for M = 20 and 25, respectively. In the σ column, the negative sign shows that the spacing of the antennas in that ring is less than d_{eq}. The spacing deviation is small in the rings containing a large number of elements, but grows to large values in the rings of a few elements. Fortunately, the rings whose element spacing deviate more significantly are very few compared to the total number of rings.

Since the spacing deviation varies with the rings, it is useful to derive the upperbound of the element spacing deviation. To evaluate it, it is noticed that the large deviation always occurs in the ring nearest the poles, that is, in the ring which corresponds to m = 1. Setting m = 1 in Equation (2-19) gives

$$\frac{d_1}{d_{eq}} = \frac{2M \sin\left(\frac{\pi}{M}\right)}{[[2M \sin\left(\frac{\pi}{M}\right)]]} \ . \qquad (2\text{-}21)$$

For large M, the approximation $\sin(\pi/M) \doteq \pi/M$ can be used. Then

$$\frac{d_1}{d_{eq}} = \frac{2\pi}{[[2\pi]]}$$

$$= \frac{\pi}{[[\pi]]}$$

$$= \frac{\pi}{3} \ . \qquad (2\text{-}22)$$

M = 20

m	N_m	$[[N_m]]$	$\frac{d_m}{d_{eq}}$	σ %
0	1.	1.		
1	6.2574	6.	1.0429	4.289
2	12.3607	12	1.0301	3.0055
3	18.1596	18	1.0089	0.8865
4	23.5114	24	0.9796	-2.0359
5	28.2842	28	1.0102	1.0151
6	32.3606	32	1.0113	1.1270
7	35.6402	36	.9900	-0.9994
8	38.0422	38	1.0011	0.1111
9	39.5075	40	.9877	-1.2312
10	40.000	40	1.000	0.000
11	39.5075	40	0.9877	-1.2312
12	38.0423	38	1.0011	0.1112
13	35.6403	36	.9900	-0.9992
14	32.3607	32	1.0113	1.1272
15	28.2843	28	1.0102	1.0155
16	23.5115	24	0.9796	-2.0355
17	18.1597	18	1.0089	0.8873
18	12.3608	12	1.0301	3.0065
19	6.2575	6	1.0429	4.2919
20	1.	1.		

Table 1. The AES Element Distribution for M = 20

M = 25

m	N_m	$[[N_m]]$	$\frac{d_m}{d_{eq}}$	σ %
0	1	1		
1	6.2667	6	1.0444	4.4422
2	12.4345	12	1.0362	3.6206
3	18.4062	18	1.0226	2.2567
4	24.0876	24	1.0037	0.3652
5	29.3892	29	1.0134	1.3421
6	34.2273	34	1.0067	0.6685
7	38.5256	39	0.9878	-1.2164
8	42.2164	42	1.0052	0.5151
9	45.2413	45	1.0054	0.5363
10	47.5528	48	0.9907	-0.9317
11	49.1143	49	1.0023	0.2333
12	49.9013	50	0.9980	-0.1974
13	49.9013	50	0.9980	-0.1974
14	49.1144	49	1.0023	0.2334
15	47.5529	48	0.9907	-0.9315
16	45.2414	45	1.0054	0.5363
17	42.2164	42	1.0052	0.5153
18	38.5257	39	0.9878	-1.2160
19	34.2274	34	1.0067	0.6689
20	29.3894	29	1.0134	1.3426
21	24.0878	24	1.0037	0.3658

Table 2. The AES Element Distribution for M = 25

22	18.4063	18	1.0226	2.2574
23	6.2668	6	1.0445	4.4464
25	1.	1.		

Table 2. The AES Element Distribution for M = 25

(Continued)

Therefore, the maximum spacing deviation of the antenna is

$$\sigma_{max} = \frac{d_1 - d_{eq}}{d_{eq}} \times 100\%$$

$$= \frac{\pi - 3}{3} \times 100\%$$

$$= 4.7197\% \qquad (2\text{-}23)$$

The variation of the spacing deviation versus ring number on the sphere for 21 rings is plotted in Figure 2-4. Figure 2-5 illustrates one of the element and ring arrangements on a sphere.

It was mentioned at the introduction of the approximately equally-spaced array that elements in the array need be distributed equally. The first reason is to reduce the mutual coupling among elements by keeping them more than half-wavelength apart or to have a uniform mutual coupling among them for the case of less than half-wavelength spacing. The second reason is to have an array which looks uniform to an observer at a far point in not only a certain direction but in all directions. This is very important for the array since it is needed to beam scan with the same performance in all directions.

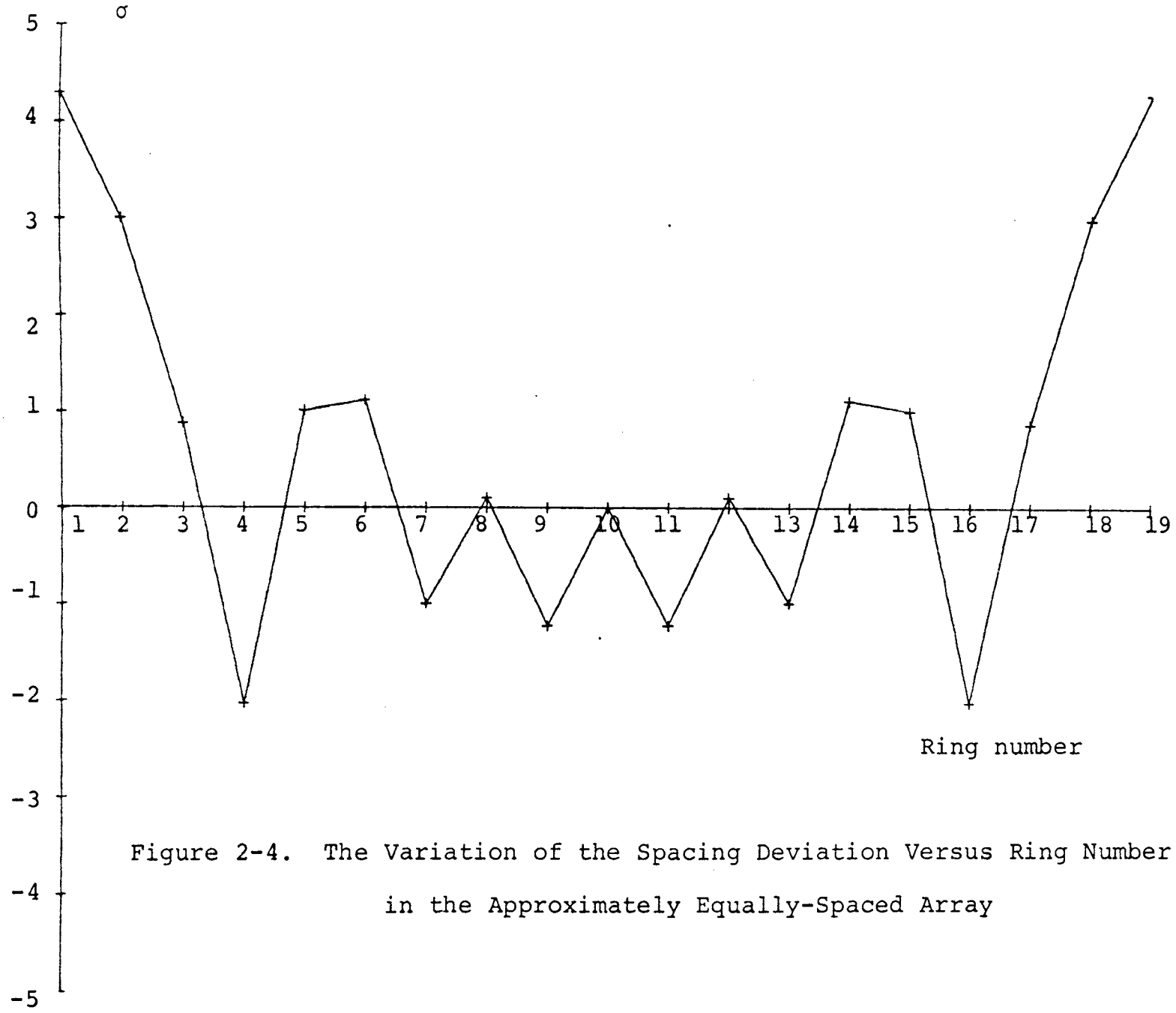

Figure 2-4. The Variation of the Spacing Deviation Versus Ring Number in the Approximately Equally-Spaced Array

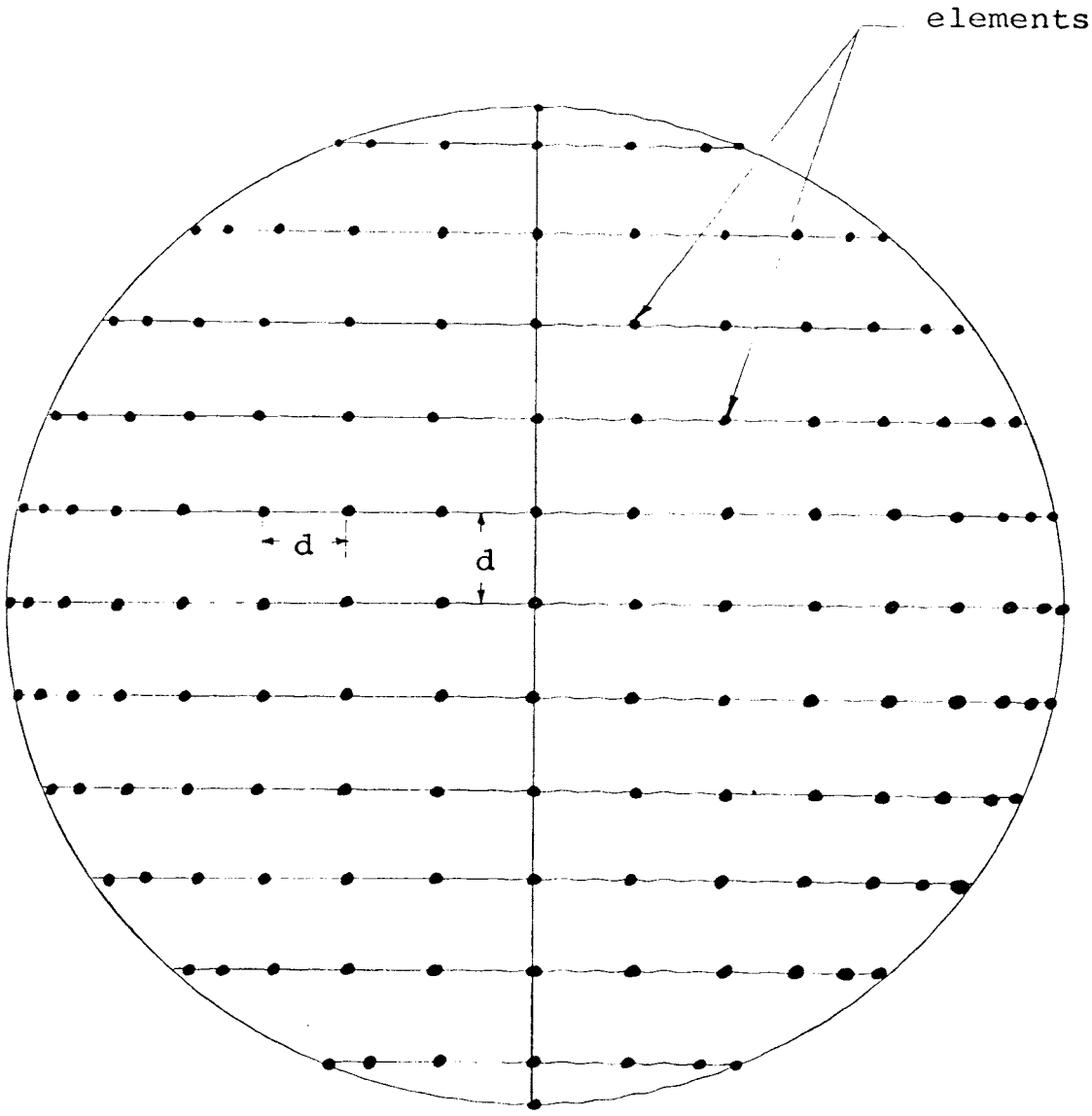

Figure 2-5. The Approximately Equally-Spaced Array

CHAPTER III

FAR FIELD PATTERN

A. Formulation of the Far Field Pattern

Figures 3-1a and b show the front and top view of a spherical array, respectively. The elements are drawn as if they were on a two-dimensional plane in order to show distinctively the element positions. This scheme will be used throughout this work. The element arrangement is still in its general form except that they are formed in rings. The geometrical diagram of the mn^{th} element is shown in Figure 3-2. The subscript m is employed in connection with the elevation angle direction, starting at the polar axis of the sphere; while n is in connection with the azimuthal angle direction, starting from the XZ plane. Consequently, the position of the mn^{th} element in the spherical coordinate system is (a, θ_m, ϕ_n).

Throughout this analysis the origin of the spherical coordinate system, which is placed at the center of the sphere, is taken as the reference. At the far observation point, $P(R, \theta, \phi)$, the relative total field pattern is given by

$$E(\theta,\phi) = \sum_{m=0}^{M} \sum_{n=1}^{N_m} I_{mn} e^{j\psi_{mn}} e^{jka\cos\xi_{mn}(\theta,\phi)} \qquad (3\text{-}1)$$

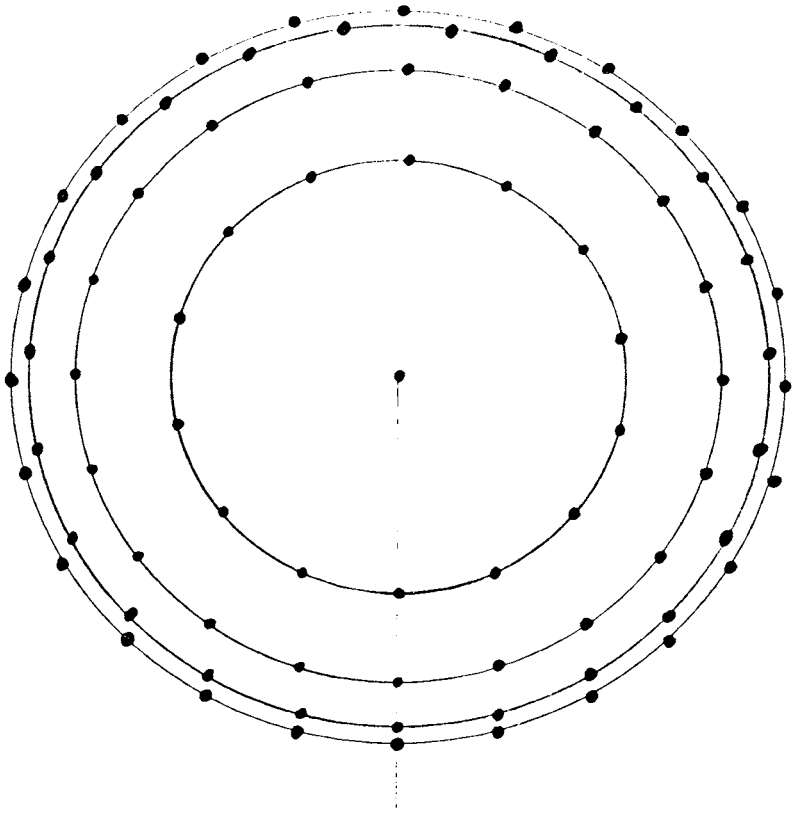

Figure 3-1a. Top View

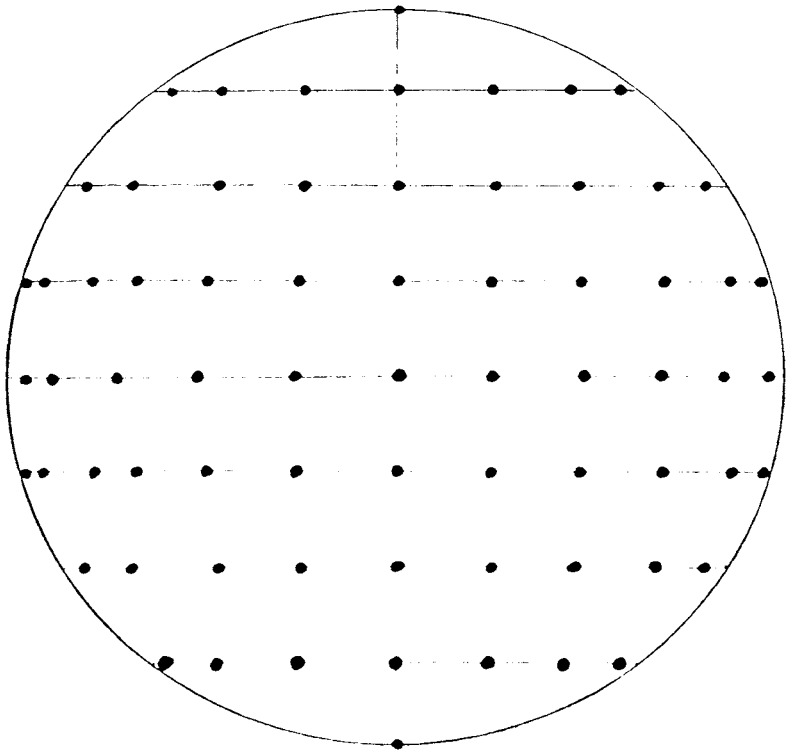

Figure 3-1b. Front View

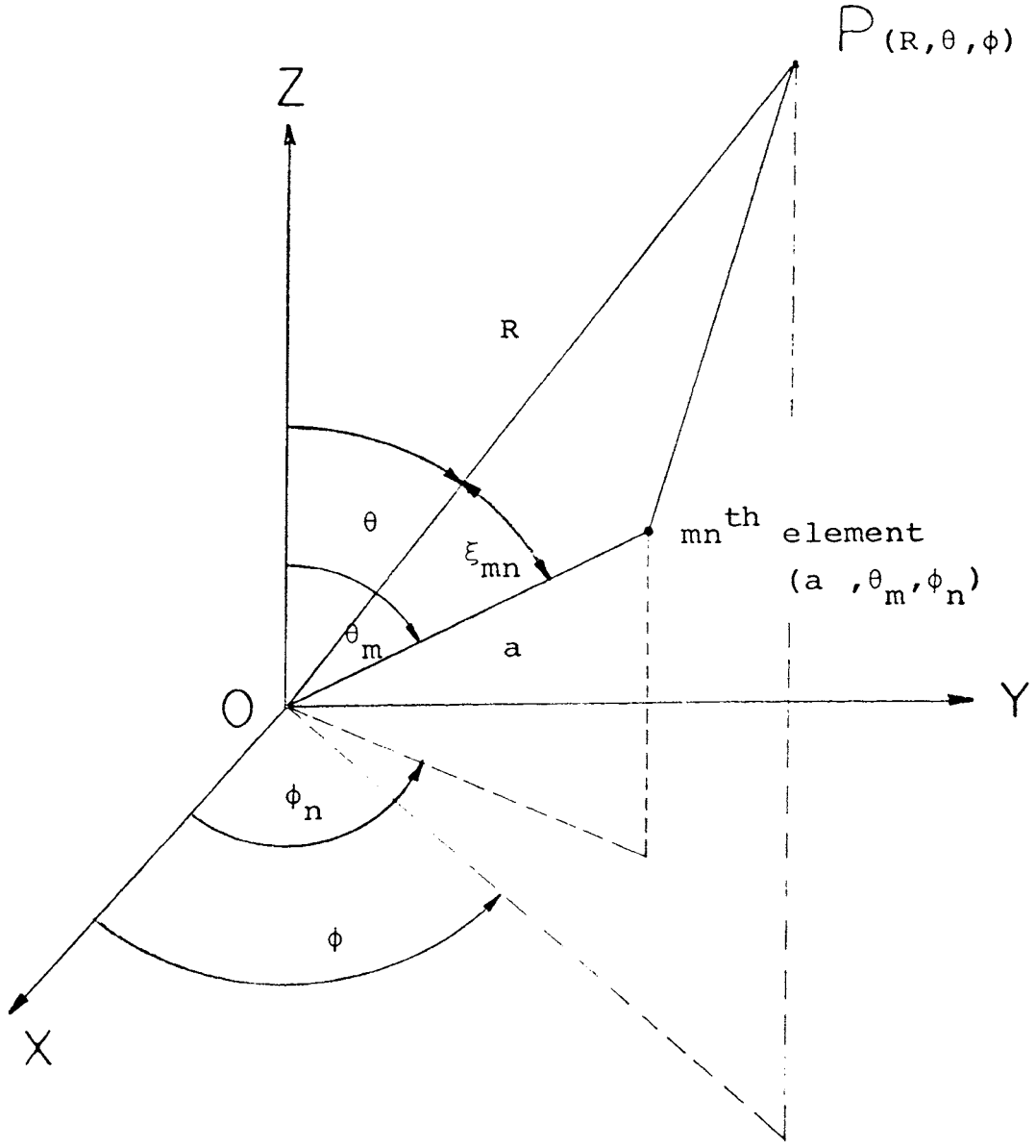

Figure 3-2. The Geometrical Diagram of the mn^{th} Element

where

I_{mn} = the current amplitude of the mn^{th} antenna

ψ_{mn} = the current phasing of the mn^{th} antenna

ξ_{mn} = the angle subtended by the radius position of P and the mn^{th} element at the reference point

k = space propagation constant .

Let the main beam of the array pattern be phased to the direction (θ_o, ϕ_o). At the observation point in this direction, the radiated fields from all elements of the array must be in phase. Hence, the pattern becomes

$$E(\theta_o, \phi_o) = \sum_{m=0}^{M} \sum_{n=1}^{N_m} I_{mn} \quad . \tag{3-2}$$

In order to satisfy Equation (3-2), the phase of the mn^{th} element must be adjusted such that

$$\psi_{mn} = - ka \cos \xi_{mn} (\theta_o, \phi_o) \tag{3-3}$$

Substituting Equation (3-3) into Equation (3-1) gives the pattern in an arbitrary direction in terms of the main beam position.

$$E(\theta,\phi) = \sum_{m=0}^{M} \sum_{n=1}^{N_m} I_{mn} e^{jka\{\cos \xi_{mn}(\theta,\phi) - \cos \xi_{mn}(\theta_o,\phi_o)\}} \quad . \tag{3-4}$$

The angle ξ_{mn}, formed by the lines joining the center of the sphere with the mn^{th} element and with the far field point P, should be expressed in terms of spherical coordinates. To accomplish this, Figure 3-3 is employed.

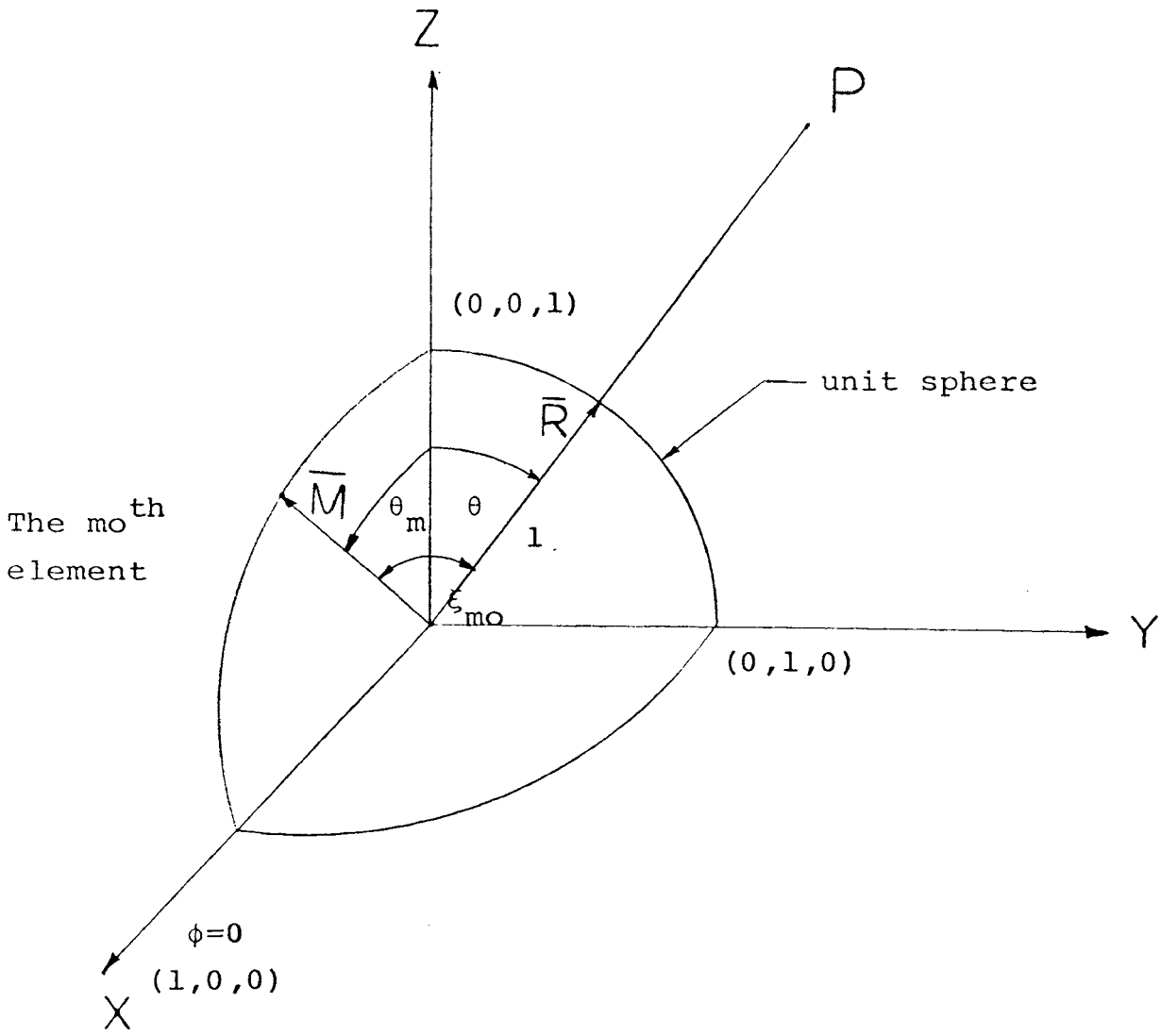

Figure 3-3. The Geometrical Diagram of $\xi_{mo}(\theta,\phi)$ in the Unit Sphere

To simplify the procedure, let us assume that the sphere under consideration has the radius of unity. Let the element being considered be on the plane $\phi = 0$, forming the angle θ_m to the polar axis. This is the mo^{th} element.

Let $\bar{R}$ and $\bar{M}$ be the two unit vectors pointing from the center of the sphere toward the observation point P and the element location respectively. The cosine of the angle formed by the two unit vectors at the origin, which is, in this case, $\xi_{mo}(\theta,\phi)$, is the scalar product of the two unit vectors.

$$\cos \xi_{mo}(\theta,\phi) = \bar{R},\bar{M} \quad . \tag{3-5}$$

Expressing the vectors $\bar{R}$ and $\bar{M}$ in terms of the cartesian coordinates gives the following equations:

$$\bar{M} = \sin \theta_m \bar{a}_x + \cos \theta_m \bar{a}_z \tag{3-5a}$$

$$\bar{R} = \sin \theta \cos \phi \bar{a}_x + \sin \theta \sin \phi \bar{a}_y + \cos \theta \bar{a}_z \tag{3-5b}$$

Therefore, Equation (3-4) becomes

$$\cos \xi_{mo}(\theta,\phi) = \sin \theta_m \sin \theta \cos \phi + \cos \theta_m \cos \theta \tag{3-6}$$

Now the mn^{th} element is in the $\phi = \phi_n$ plane instead of in the $\phi = 0$ plane, but it still makes the same angle θ_m with the polar axis. The expression of $\cos \xi_{mn}(\theta,\phi)$, therefore, remains the same as $\cos \xi_{mo}(\theta,\phi)$, except the azimuth angle is shifted to $(\phi - \phi_n)$.

$$\cos \xi_{mn}(\theta,\phi) = \sin \theta_m \sin \theta \cos(\phi - \phi_n) + \cos \theta_m \cos \theta \quad . \tag{3-7}$$

B. Simplification of the Far Field Pattern

In this section, the difference of the two cosines in the exponent of the far field pattern is simplified. Using the properties of the cosines of different angles, it can be expressed as follows:

$$\cos \xi_{mn}(\theta,\phi) - \cos \xi_{mn}(\theta_o,\phi_o)$$

$$= \sin \theta_m \sin \theta \cos(\phi-\phi_n) + \cos \theta_m \cos \theta$$

$$- \sin \theta_m \sin \theta_o \cos(\phi_o-\phi_n) - \cos \theta_m \cos \theta_o$$

$$= \sin \theta_m\{\sin \theta \cos(\phi-\phi_n) - \sin \theta_o \cos(\phi_o-\phi_n)\}$$

$$+ \cos \theta_m(\cos \theta - \cos \theta_o) \cdot \qquad (3\text{-}8)$$

The first bracket can further be expanded, by using the principles of trigonometry.

$$\sin \theta \cos(\phi-\phi_n) - \sin \theta_o \cos(\phi_o-\phi_n)$$

$$= \sin \theta(\cos \phi \cos \phi_n + \sin \phi \sin \phi_n)$$

$$- \sin \theta_o(\cos \phi_o \cos \phi_n + \sin \phi_o \sin \phi_n)$$

$$= \cos \phi_n(\sin \theta \cos \phi - \sin \theta_o \cos \phi_o)$$

$$+ \sin \phi_n(\sin \theta \sin \phi - \sin \theta_o \sin \phi_o)$$

$$= \cos \phi_n \cos \alpha + \sin \phi_n \sin \alpha$$

$$= \cos(\phi_n - \alpha) \cdot \qquad (3\text{-}9)$$

Where the terms cos α and sin α have been introduced so as to make the forming of the cosine of different angles possible, and given by

$$\cos \alpha = (\sin \theta \cos \phi - \sin \theta_o \cos \phi_o)/\rho \qquad (3\text{-}10a)$$

$$\sin \alpha = (\sin \theta \sin \phi - \sin \theta_o \sin \phi_o)/\rho \qquad (3\text{-}10b)$$

and

$$\rho^2 = (\sin \theta \cos \phi - \sin \theta_o \cos \phi_o)^2 + (\sin \theta \sin \phi - \sin \theta_o \sin \phi_o)^2$$

$$= \sin^2 \theta + \sin^2 \theta_o - 2\sin \theta \sin \theta_o \cos(\phi - \phi_o) \qquad (3\text{-}11)$$

Substituting Equations (3-9) and (3-8) into (3-4) gives the radiation pattern in its general form.

$$E(\theta,\phi) = \sum_{m=0}^{M} \sum_{n=1}^{N_m} I_{mn} e^{jka\{\cos \theta_m(\cos \theta - \cos \theta_o) + \rho \sin \theta_m \cos(\phi - \alpha)\}} . \qquad (3\text{-}12)$$

To simplify the analysis for the far field, a uniform current distribution of unity is assumed in this study.

$$I_{mn} = 1 . \qquad (3\text{-}13)$$

With the above conditions, the expression for the far field pattern is reduced to,

$$E(\theta,\phi) = \sum_{m=0}^{M} \sum_{n=1}^{N_m} e^{jka\{\cos \theta_m(\cos \theta - \cos \theta_o) + \rho \sin \theta_m \cos(\phi_n - \alpha)\}}$$

$$= \sum_{m=0}^{M} e^{jka \cos \theta_m (\cos \theta - \cos \theta_o)}$$

$$\cdot \sum_{n=1}^{N_m} e^{jka \rho \sin \theta_m \cos(\phi_n - \alpha)} \qquad (3\text{-}14)$$

Equation (3-14) is simply the product of two series, one in terms of m and the other in n.

CHAPTER IV

ARRAY ANALYSIS

A. The Application of the Poisson's Sum Formula

In his paper, "Theory of Non-Uniformly Spaced Array", Ishimaru [4] pointed out that the radiation pattern of a linear array of N elements, which normally takes the form

$$E(\theta) = \sum_{n=1}^{N} I_n e^{jks_n \{\substack{\sin \\ \cos}\}\theta} \tag{4-1}$$

where

I_n = the current in the n^{th} element

s_n = the position of the n^{th} element as measured from the reference point of the system

can be rewritten as the summation of a general function $f(n,\theta)$,

$$E(\theta) = \sum_{n=1}^{N} f(n,\theta). \tag{4-2}$$

The Poisson's Sum Formula, which is defined as [5]

$$\sum_{n=-\infty}^{\infty} f(n) = \sum_{h=-\infty}^{\infty} \int_{-\infty}^{\infty} f(\nu)\, e^{j2h\pi\nu}\, d\nu\ , \tag{4-3}$$

is then applied to Equation (4-2), which becomes

$$E(\theta) = \sum_{h=-\infty}^{\infty} \int_{-\infty}^{\infty} f(\nu,\theta)\ e^{j2\pi h\nu}\ d\nu$$

$$= \sum_{h=-\infty}^{\infty} \int_{0}^{N} f(\nu,\theta)\ e^{j2\pi h\nu}\ d\nu\ . \qquad (4\text{-}4)$$

The limits of the integration changes from $(-\infty, \infty)$ to $(0,N)$ because $f(n,\theta)$ does not exist when $\nu < 0$ and $\nu > N$; that is to say, there is no element beyond this range to contribute to the field pattern. In fact, the limit on Equation (4-4) is not the only one that can be used. Any range that covers 1 to N is sufficient to be the range of the integration since the array is a discrete system. Therefore, in general, Equation (4-4) can be placed in the form

$$E(\theta) = \sum_{h=-\infty}^{\infty} \int_{\varepsilon}^{\varepsilon+N} f(\nu,\theta)\ e^{j2\pi h\nu}\ d\nu \qquad (4\text{-}5)$$

provided that $0 \leq \varepsilon < 1$.

Now let us consider the far field pattern of the spherical array which is a product of two series as given by Equation (3-14). For convenience, it is rewritten as

$$E(\theta,\phi) = \sum_{m=0}^{M} e^{jka \cos \theta_m(\cos \theta - \cos \theta_o)}$$

$$\cdot \sum_{n=1}^{N_m} e^{jka\ \rho \sin \theta_m \cos(\phi_n - \alpha)}\ . \qquad (3\text{-}14)$$

It should be noted that, in the second summation, m behaves as a constant with respect to n. Therefore, for the n-summation, Equation (3-14) can be written as

$$\sum_{n=1}^{N_m} e^{jka\ \rho\ \sin\ \theta_m\ \cos(\phi_n - \alpha)} = \sum_{n=1}^{N_m} f(\theta_m, n) \qquad (4\text{-}6)$$

where

$$f(\theta_m, n) = e^{jka\ \rho\ \sin\ \theta_m\ \cos(\phi_n - \alpha)} .$$

Let

$$F(\theta_m) = \sum_{n=1}^{N_m} f(\theta_m, n) \qquad (4\text{-}7)$$

so that Equation (3-14) becomes

$$E(\theta,\phi) = \sum_{m=0}^{M} F(\theta_m)\ e^{jka\ \cos\ \theta_m(\cos\ \theta - \cos\ \theta_o)} . \qquad (4\text{-}8)$$

It is obvious that Equation (4-6) is just the form of the radiation pattern of an array, which in this case is the m^{th} ring.

Now Equations (4-2) and (4-5) are applied directly to Equation (4-7), where ε, for simplicity, is assumed to take the value of zero. Such application results in

$$F(\theta_m) = \sum_{h=-\infty}^{\infty} \int_0^{N_m} f(\theta_m, \nu)\ e^{j2\pi h\nu}\ d\nu$$

$$= \sum_{h=-\infty}^{\infty} \int_0^{N_m} e^{jka\ \rho\ \sin\ \theta_m\ \cos(\phi_\nu - \alpha) + j2\pi h\nu}\ d\nu \qquad (4\text{-}9)$$

In the above equation, the azimuth angle ϕ_n of the n^{th} element in the m^{th} ring becomes a function of ν. The

behavior of this function depends on the arrangement of the elements in the ring. It is linear if the elements are uniformly spaced, but nonlinear otherwise. However, due to the fact that this function is the argument of a cosine function, which is transcendental, it becomes totally necessary that the variables be changed from ν to ϕ in order to avoid a composite function. To accomplish the variable changing, the chain rule for the differential holds since both ν and ϕ are continuous and one is just a function of another [6].

$$d\nu = \frac{d\nu}{d\phi} \cdot d\phi \quad . \tag{4-10}$$

Consequently, the limits of the integration change to $[0, \phi(N_m)]$. Then, with the new variable ϕ, the summation becomes

$$F(\theta_m) = \sum_{h=-\infty}^{\infty} \int_0^{\phi(N_m)} e^{jka\,\rho \sin\theta_m \cos(\phi - \alpha) + j2\pi h\nu(\phi)} \cdot \frac{d\nu}{d\phi}\, d\phi \quad . \tag{4-11}$$

In a ring, the elements are equally-spaced. Therefore, the ν function is linear with respect to ϕ, as shown in Figure 4-1. The linear relation between ν and ϕ is

$$\frac{\nu}{\phi} = \frac{N_m}{2\pi} \cdot \tag{4-12}$$

The derivative of ν with respect to ϕ becomes

$$\frac{d\nu}{d\phi} = \frac{N_m}{2\pi} \quad . \tag{4-13}$$

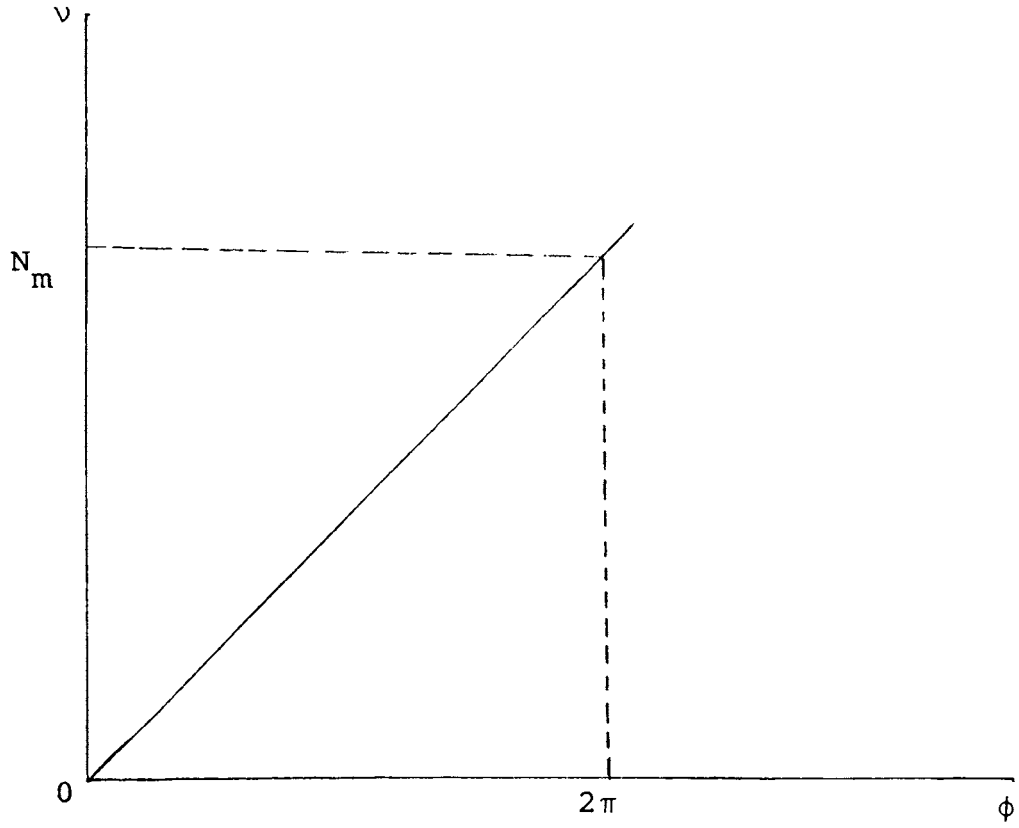

Figure 4-1. The Linear Relation Between ν and ϕ´

$$\nu = \frac{N_m}{2\pi} \phi .$$

Substituting Equations (4-12) and (4-13) in (4-11) results in

$$F(\theta_m) = \sum_{h=-\infty}^{\infty} \int_0^{2\pi} e^{jka\,\rho \sin\theta_m \cos(\phi - \alpha) + jhN_m\phi} \cdot \frac{N_m}{2\pi}\, d\phi$$

$$= \frac{N_m}{2\pi} \sum_{h=-\infty}^{\infty} \int_0^{2\pi} e^{jka\,\rho \sin\theta_m \cos(\phi - \alpha) + jhN_m\,\phi}\, d\phi \qquad (4\text{-}14)$$

The limits of the integration are 0 and 2π since by the time ν goes around and completes a ring, the angle ϕ, which is at the center of the ring, changes by 2π radians simultaneously. It is obvious from Equation (4-13).

It should be noted that the number N_m which represents the number of elements in the m^{th} ring has not been restricted to either a constant or variable. The number of elements in two adjacent rings may or may not be the same. If they are the same, it is the case of the latitude-longitude distribution, and not for the approximately equally-spaced distribution. Let us substitute into the integral part of Equation (4-14),

$$\frac{1}{2\pi} \int_0^{2\pi} e^{jka\,\rho \sin\theta_m \cos(\phi - \alpha) + jhN_m\,\phi}\, d\phi$$

the following

$$\chi_m = ka\ \rho\ \sin\ \theta_m \tag{4-15}$$

$$\phi - \alpha = \gamma + \frac{\pi}{2} \tag{4-16}$$

$$\beta = -(\frac{\pi}{2} + \alpha) \tag{4-17}$$

$$\cos(\phi - \alpha) = \cos(\frac{\pi}{2} + \gamma)$$

$$= -\sin\gamma$$

and

$$d\phi = d\gamma\ .$$

The integral becomes

$$\frac{1}{2\pi}\int_0^{2\pi} e^{jka\ \rho\ \sin\ \theta_m\ \cos(\phi - \alpha)\ +\ jhN_m\ \phi}\ d\phi$$

$$= \frac{1}{2\pi}\int_{-(\frac{\pi}{2}+\alpha)}^{2\pi-(\frac{\pi}{2}+\alpha)} e^{-jx_m \sin\ \gamma + jhN_m(\frac{\pi}{2}\ +\ \gamma\ +\ \alpha)}\ d\gamma$$

$$= \frac{1}{2\pi}\ e^{ihN_m\beta}\int_{\beta}^{2\pi+\beta} e^{jhN_m\gamma\ -\ j\chi_m\ \sin\ \gamma}\ d\gamma \tag{4-18}$$

Equation (4-18) can be expressed as

$$e^{ihN_m\beta}\ J_{hN_m}(\chi_m) \tag{4-19}$$

where the Bessel function $J_{hN_m}(x_m)$ has been defined by G. N. Watson [7].

Therefore,

$$F(\theta_m) = N_m \sum_{h=-\infty}^{\infty} e^{jhN_m\beta} J_{hN_m}(\chi_m) \quad . \tag{4-20}$$

In general, at least for the purpose of this analysis, the number of elements in each ring is assumed to be very large. From the properties of Bessel function, the magnitude of this function of very large order is much smaller than that of zero order. Furthermore, the magnitude of the exponential with a complex exponent is unity. Therefore, for the first approximation, the summation of the Bessel functions in Equation (4-20) is made equal to $J_0(\chi_m)$. Thus

$$F(\theta_m) \simeq N_m J_0(\chi_m) . \tag{4-21}$$

In the latitude-longitude distribution of the array, this approximation should be excellent since every ring contains the same large number of elements. In the approximately equally-spaced distribution, on the other hand, not every ring contains a large number of elements, especially those which are in the regions of the poles. However, after investigating the element arrangement in all rings, the number of rings which contain few elements are much less than the number of rings which have many antennas. For the case of 25 rings, for instance, there are only two rings (one ring at each pole) which contain less than ten elements, while the rest contain elements up to 50. Therefore, the approximation of the Bessel

function made above should not affect the far field pattern significantly.

With $F(\theta_m)$ given by Equation (4-21), the far field pattern now becomes

$$E(\theta,\phi) = \sum_{m=0}^{M} N_m J_o(\chi_m) e^{jka \cos \theta_m(\cos \theta - \cos \theta_o)} \qquad (4\text{-}22)$$

where χ_m is defined by Equation (4-15).

B. The Latitude-Longitude Distribution Array

By the characteristic of this type of distribution, in which the longitudes divide every latitude or rings into N equal subintervals, the number of elements in one ring is the same as the number in others. Hence

$$\begin{aligned} N_m &= N_{m\pm1} \\ &= N \end{aligned} \qquad (4\text{-}23)$$

which is not a function of m. Factoring N out leaves the far field pattern in the form

$$E(\theta,\phi) = N \sum_{m=0}^{M} J_o(\chi_m)\ e^{jka \cos \theta_m(\cos \theta - \cos \theta_o)} \qquad (4\text{-}24)$$

Let $g(\theta,\phi,m)$ represent the m^{th} term of the above series,

$$g(\theta,\phi,m) = J_o(\chi_m)\ e^{jka \cos \theta_m(\cos \theta - \cos \theta_o)} \qquad (4\text{-}25)$$

so that the far field pattern becomes

$$E(\theta,\phi) = N \sum_{m=0}^{M} g(\theta,\phi,m) \qquad (4\text{-}26)$$

Now applying Equation (4-5), with ε taking the value of zero, to Equation (4-26) gives

$$E(\theta,\phi) = N \sum_{h=-\infty}^{\infty} \int_0^M g(\theta,\phi,\nu)\, e^{j2\pi h\nu}\, d\nu$$

$$= N \sum_{h=-\infty}^{\infty} \int_0^M J_o(ka\,\rho \sin\theta(\nu))\, e^{jka\cos\theta(\nu)(\cos\theta-\cos\theta_o)}$$

$$e^{j2\pi h\nu}\, d\nu \,. \qquad (4\text{-}27)$$

It is helpful to note that in Equation (4-27) there are two θ functions, θ and $\theta(\nu)$. The former indicates the direction in which the field pattern is being evaluated and, of course, has nothing to do with either the integral or the summation. The latter, being transformed through Poisson's Sum Formula from θ_m to $\theta(\nu)$, is a function of the variable ν. It indicates the positions of the rings when N varies from 0 to M.

Again, since $\theta(\nu)$ is the argument of sine and cosine functions which are the argument and exponent of the Bessel and exponential functions, respectively, it is more convenient to change the variable of the integration from ν to θ'.* Employing the chain rule of differentials of two continuous functions, ν and θ',

$$d\nu = \frac{d\nu}{d\theta'} \cdot d\theta' \qquad (4\text{-}28)$$

Equation (4-27) is changed to

---

*The prime is used here to prevent any confusion with the unprimed.

$$E(\theta,\phi) = N \sum_{h=-\infty}^{\infty} \int_{0}^{\theta'(M)} J_o(ka\ \rho \sin\theta')$$

$$\cdot\ e^{jka\ \cos\theta'(\cos\theta - \cos\theta_o) + j2\pi h\nu(\theta')} \cdot \frac{d\nu}{d\theta'} \cdot d\theta' \qquad (4\text{-}29)$$

As was stated earlier, the array consists of rings which are equally spaced. Therefore,

$$\frac{\nu}{M} = \frac{\theta'}{\pi} \qquad (4\text{-}30)$$

and

$$\frac{d\nu}{d\theta'} = \frac{M}{\pi} \qquad (4\text{-}31)$$

Furthermore,

$$\theta'(M) = \pi \qquad (4\text{-}32)$$

since the rings are placed on the whole sphere. Substituting these equations into (4-29) gives

$$E(\theta,\phi) = \frac{MN}{\pi} \sum_{h=-\infty}^{\infty} \int_{0}^{\pi} J_o(ka\ \rho \sin\theta')$$

$$\cdot\ e^{jka\ \cos\theta'(\cos\theta - \cos\theta_o)}\ e^{j2Mh\theta'}\ d\theta' \qquad (4\text{-}33)$$

Equation (4-33) presents quite a complicated integral that must be evaluated. To integrate it, the far field pattern is expanded into a series of terms. A term and its corresponding negative are grouped together, using the complex notation of cosine function,

$$\cos Z = \frac{e^{iZ} + e^{-iZ}}{2} \qquad (4\text{-}34)$$

Hence,

$$E(\theta,\phi) = \frac{MN}{\pi} \left\{ \int_0^{\pi} I(\theta')\, d\theta' + 2 \int_0^{\pi} I(\theta') \cos (2Mh\ \theta')\, d\theta' \right.$$

$$\left. + \cdots + 2 \int_0^{\pi} I(\theta') \cos (2Mh\ \theta')\, d\theta' + \cdots \right\} \qquad (4\text{-}35)$$

where

$$I(\theta') = J_o(ka\ \rho \sin \theta')\ e^{jka \cos \theta'(\cos \theta - \cos \theta_o)} \qquad (4\text{-}36)$$

1. Pattern Series and Its Coefficients

Now let us consider the first integral of the pattern series. Let us call it I_o. To evaluate it, let

$$x = \cos \theta' \qquad (4\text{-}37)$$

$$A = ka(\cos \theta - \cos \theta_o) \qquad (4\text{-}38)$$

and

$$B = ka\ \rho \qquad (4\text{-}39)$$

Then, by differentiating Equation (4-36) with respect to θ',

$$dx = - \sin \theta'\, d\theta'$$

or

$$d\theta' = \frac{dx}{\sqrt{1 - x^2}} \quad . \qquad (4\text{-}40)$$

The I_o integral becomes, after substitution and change in the limits

$$I_o = \int_{-1}^{1} \frac{e^{jAx}\, J_o(B\sqrt{1 - x^2})\,dx}{\sqrt{1 - x^2}}$$

$$= \int_{-1}^{1} \frac{J_o(B\sqrt{1 - x^2})\cos Ax\,dx}{\sqrt{1 - x^2}} + j \int_{-1}^{1} \frac{J_o(B\sqrt{1 - x^2})\sin Ax\,dx}{\sqrt{1 - x^2}}$$

$$= 2 \int_{0}^{1} \frac{J_o(B\sqrt{1 - x^2})\cos Ax\,dx}{\sqrt{1 - x^2}} \quad . \tag{4-41}$$

The imaginary part of the integral vanishes because the integrand is an odd function, while the real part is an even one. Thus, it can be written as twice the integral whose limits are only half of the original limits.

Let the variable be changed one more time to y through the relation

$$x^2 + y^2 = 1 \quad . \tag{4-42}$$

Then

$$dx = \frac{-y\,dy}{\sqrt{1 - y^2}} \quad . \tag{4-43}$$

The I_o equation becomes

$$I_o = 2 \int_{0}^{1} \frac{J_o(By)\cos(A\sqrt{1 - y^2})\,dy}{\sqrt{1 - y^2}} \quad . \tag{4-44}$$

This can be integrated in a closed form by applying the identity [8]

$$\int_0^a J_\nu(cx)\ \frac{\cos(b\sqrt{a^2 - x^2})}{\sqrt{a^2 - x^2}}\ dx$$

$$\equiv \frac{\pi}{2}\ J_{\frac{1}{2}\nu}\ (\frac{a}{2}\sqrt{b^2 + c^2} - b)\ J_{\frac{\nu}{2}}\ (\frac{a}{2}\sqrt{b^2 + c^2} + b)\ . \qquad (4\text{-}45)$$

Therefore,

$$I_o = \pi J_o(\frac{1}{2}\sqrt{A^2 + B^2} - A)\ J_o(\frac{1}{2}\sqrt{A^2 + B^2} + A) \qquad (4\text{-}46)$$

Manipulation on the arguments of the Bessel functions in the above equation gives (see Appendix B)

$$I_o = \pi J_o\{ka(\sin\omega - \cos\theta + \cos\theta_o)\}\ J_o\{ka(\sin\omega + \cos\theta - \cos\theta_o)\} \qquad (4\text{-}47)$$

where ω is given by

$$\omega = \frac{1}{2}\cos^{-1}\{\cos\theta\cos\theta_o + \sin\theta\sin\theta_o\cos(\phi - \phi_o)\}. \qquad (4\text{-}48)$$

A study of the expression for I_o reveals that the main part of the far field pattern is just the product of two Bessel functions of zero order. Although both have different arguments, they attain the maximum value at $\theta = \theta_o$. This means that the location of the main beam is unique. Thus there will be only one main beam in the far field pattern. This statement is supported by the following example.

In the plane $\phi = \phi_o$, in which the far field pattern is considered (another case would be on the plane $\theta = \theta_o$), the expression for ω is reduced to

$$\omega = \frac{1}{2} \cos^{-1} \{\cos \theta \cos \theta_o + \sin \theta \sin \theta_o\}$$

$$= \frac{1}{2} \cos^{-1} \{\cos(\theta - \theta_o)\}$$

$$= \frac{1}{2} (\theta - \theta_o) \quad \text{at} \quad \phi = \phi_o \tag{4-49}$$

which is obviously zero at the main beam. It might be argued that there seems to be another main beam on the opposite side, that is, at $\phi = \phi_o \pm \pi$ and $\theta = \pi - \theta_o$. By looking at Equation (4-49), ω would be $\pi/2$, which gives sin ω the value of unity. The cosine of θ would take the negative value of cos θ_o. One argument of the Bessel function would be small, but another would be very large, since ka always takes large values. The Bessel function for a small argument would take the value near unity, while the other would be a very small value because of the large argument. The product of the two would, of course, be very small. This confirms that there is only one main beam from the sphere.

Now let us come back to the H^{th} term of the far field pattern series, which is given by,

$$I_H = 2 \int_0^{\pi} I(\theta') \cos (2MH\theta') \, d\theta' \quad . \tag{4-50}$$

The presence of cos(2MHθ') in the integral complicates the integral. However, it has been noted that I(θ') is a function of trigonometric and Bessel functions, so it is likely to be fruitful to expand cos(2MHθ') into infinite

series of some orthogonal functions. Several types of functions have been unsuccessfully tried, except for the associated Legendre polynomials. Therefore, let us expand $\cos(2MH\theta')$ into an infinite series of Legendre polynomials. Because of the even characteristic of cosine function, the series should contain only the terms of $P_n(x)$ of even index [9]. Hence

$$\cos(2MH\theta') = \sum_{\ell=0}^{\infty} A_\ell(MH)\, P_{2\ell}(\cos\theta') \tag{4-51}$$

where $A_\ell(MH)$ is the ℓ^{th} coefficient of the series.

Now let us multiply both sides by $P_{2m}(\cos\theta')$ and integrate with respect to $\cos\theta'$ under the limit of $(-1,1)$. The coefficient $A_m(MH)$ of the m^{th} term is given, after applying the orthogonal properties of the Legendre polynomials [10], by

$$\int_{-1}^{1} \cos(2MH\theta')\, P_{2m}(\cos\theta')\, d(\cos\theta')$$

$$= \sum_{\ell=0}^{\infty} A_\ell(MH) \int_{-1}^{1} P_{2\ell}(\cos\theta')\, P_{2m}(\cos\theta')\, d(\cos\theta')$$

$$= A_m(MH)\, \frac{2}{4m+1}$$

or

$$A_m(MH) = \frac{4m+1}{2} \int_{-1}^{1} \cos(2MH\theta')\, P_{2m}(\cos\theta')\, d(\cos\theta') \tag{4-52}$$

Differentiating cos θ' and applying laws of the product of two trigonometric functions gives the integrand in terms of two sine functions.

$$A_m(MH) = \frac{4m + 1}{2} \int_0^{\pi} \cos(2MH\theta') \sin\theta' P_{2m}(\cos\theta') d\theta'$$

$$= \frac{4m + 1}{4} \int_0^{\pi} [\sin(2MH + 1)\theta'$$

$$- \sin(2MH - 1)\theta'] P_{2m}(\cos\theta') d\theta'$$

$$= \frac{4m + 1}{4} \int_0^{\pi} \sin(2MH + 1)\theta' P_{2m}(\cos\theta') d\theta'$$

$$- \frac{4m + 1}{4} \int_0^{\pi} \sin(2MH - 1)\theta' P_{2m}(\cos\theta') d\theta' . \qquad (4\text{-}53)$$

Using the identity [11]

$$\int_0^{\pi} \sin n\theta' P_m(\cos\theta') d\theta'$$

$$= \frac{2(n - m + 1)(n - m + 3) \cdots (n + m - 1)}{(n - m)(n - m + 2) \cdots (n + m)} \qquad (4\text{-}54)$$

with the condition that $n > m$ and $n + m$ must be odd.

For the case of Equation (4-53), we have $2m + 2MH \pm 1$ which is strictly odd. Therefore, the last condition is completely satisfied. In order to satisfy the first

condition, the expanded series must terminate at $\ell = MH$. Therefore, Equation (4-51) is reduced to

$$\cos(2MH\theta') = \sum_{\ell=0}^{MH} A_\ell(MH)\ P_{2\ell}(\cos\ \theta') \tag{4-55}$$

and the coefficient $A_\ell(MH)$ is given by (see Appendix C)

$$A_\ell(MH) = (4\ell + 1)\frac{(2MH)(2MH - 2\ell + 2)(2MH - 2\ell + 4)\cdots(2MH + 2\ell - 2)}{(2MH - 2\ell - 1)(2MH - 2\ell + 1)\cdots(2MH + 2\ell + 1)} \tag{4-56}$$

With the series expression of $\cos(2MH\theta')$ in Equation (4-55), the H^{th} harmonic of the far field pattern becomes

$$\begin{aligned} I_H &= 2\int_0^\pi I(\theta')\ \sum_{\ell=0}^{MH} A_\ell(MH)\ P_{2\ell}(\cos\ \theta')\ d\theta' \\ &= 2\sum_{\ell=0}^{MH} A_\ell(MH)\int_0^\pi I(\theta')\ P_{2\ell}(\cos\ \theta')\ d\theta' \\ &= 2\sum_{\ell=0}^{MH} A_\ell(MH)\ K(\ell) \end{aligned} \tag{4-57}$$

where

$$\begin{aligned} K(\ell) &= \int_0^\pi I(\theta')\ P_{2\ell}(\cos\ \theta')\ d\theta' \\ &= \int_0^\pi J_o(ka\ \rho\ \sin\theta')e^{jka\ \cos\ \theta'(\cos\ \theta\ -\ \cos\ \theta_o)} \\ &\quad \cdot\ P_{2\ell}(\cos\ \theta')\ d\theta'\ . \end{aligned} \tag{4-58}$$

Expand the exponential function into its cartesian form of cosine and sine of the exponent. Let us now use the properties of the associated Legendre polynomials, that is, an even function with respect to its argument if the order is even, and odd, otherwise, to reduce Equation (4-58). Thus,

$$K(\ell) = 2\int_0^1 \cos Ax \; J_o(B\sqrt{1 - x^2}) \; P_{2\ell}(x) \; \frac{dx}{\sqrt{1 - x^2}} \qquad (4\text{-}59)$$

where A and B have been defined by Equations (4-38) and (4-39) respectively.

With the expression for I_H analyzed, the far field pattern series, Equation (4-35), is simplified to

$$\begin{aligned}
E(\theta,\phi) &= \frac{MN}{\pi} [I_o + I_1 + I_2 + \cdots + I_H + \cdots] \\
&= \frac{MN}{\pi} [I_o + 2\{\sum_{\ell=0}^{M} A_\ell(M)K(\ell) + \sum_{\ell=0}^{2M} A_\ell(2M)K(\ell) \\
&\quad + \cdots + \sum_{\ell=0}^{MH} A_\ell(MH)K(\ell) + \cdots\}] \\
&= \frac{MN}{\pi} [I_o + 2\{A_o(M) + A_o(2M) + A_o(3M) + \cdots\}K(0) \\
&\quad + 2\{A_1(M) + A_1(2M) + \cdots\}K(1) \\
&\quad + 2\{A_2(M) + A_2(2M) + \cdots\}K(2) + \cdots] \\
&= \frac{MN}{\pi}[I_o + 2(\sum_{p=1}^{\infty} A_o(pM))K(0) \\
&\quad + 2(\sum_{p=1}^{\infty} A_1(pM))K(1) + \cdots] \qquad (4\text{-}60)
\end{aligned}$$

which is in the form of an infinite series. The coefficient of each term is also an infinite series.

Let the series coefficients be defined as follows:

$$C_i = 2 \sum_{p=1}^{\infty} A_i(pM) \tag{4-61}$$

so that the far field series can be written in the form

$$E(\theta,\phi) = \frac{MN}{\pi} [I_o + C_o K(0) + C_1 K(1) + \cdots] \tag{4-62}$$

It is noted that if ℓ is set equal to zero in Equation (4-59) it will result in the form of Equation (4-41) since $P_{2\ell}(x) = 1$ when $\ell = 0$. Therefore,

$$I_o = K(0) \tag{4-63}$$

and the far field pattern series becomes

$$E(\theta,\phi) = \frac{MN}{\pi} [(1 + C_o) I_o + C_1 K(1) + C_2 K(2) + \cdots] \tag{4-64}$$

For a given number of rings, Equation (4-64) shows that the far field pattern is in the form of infinite series with constant coefficients. The i^{th} term of the series, from now on, will be called the i^{th} pattern harmonic.

2. The Coefficients of the Pattern Harmonics

Let us consider a term of a coefficient. For convenience, the term $A_0(M)$ is chosen.

$$A_0(M) = \frac{1}{(2M - 1)(2M + 1)}$$

$$= \frac{1}{4M^2 - 1} \tag{4-65}$$

The form of $A_0(M)$ above immediately guarantees the convergence of the series. Other terms of other coefficients

can be put in this form through the partial fraction method. Since every coefficient is in an infinite series form, let us consider the infinite series [12]

$$\cot \pi Z = \frac{1}{\pi z} - \frac{2Z}{\pi} \sum_{p=1}^{\infty} \frac{1}{p^2 - Z^2} \tag{4-66}$$

The rearrangement of the series into the desired form yields

$$\sum_{p=1}^{\infty} \frac{1}{p^2 - Z^2} = \frac{1}{2Z^2} - \frac{\pi}{2Z} \cot \pi Z \tag{4-67}$$

Substitution of $Z = a/b$ in the above equation results in

$$\sum_{p=1}^{\infty} \frac{b^2}{b^2p^2 - a^2} = \frac{b^2}{2a^2} - \frac{\pi b}{2a} \cot \frac{\pi a}{b}$$

which is simplified to, after multiplying through by a^2/b^2,

$$\sum_{p=1}^{\infty} \frac{a^2}{b^2p^2 - a^2} = \frac{1}{2} - \frac{a\pi}{2b} \cot \frac{a\pi}{b} . \tag{4-68}$$

Equation (4-68) insures that all coefficients of the pattern harmonics can be put in a closed form. Furthermore, the series is absolutely convergent if $b \neq 0$ and $a \neq 0$. An example of solving for C_1 is shown in detail in Appendix D The first few coefficients are shown here in closed form.

$$C_o = 1 - \frac{\pi}{2M} \cot \frac{\pi}{2M} \tag{4-69}$$

$$C_1 = \frac{5\pi}{16M} \left(\cot \frac{\pi}{2M} - 3 \cot \frac{3\pi}{2M}\right) \tag{4-70}$$

$$C_2 = \frac{9\pi}{128M} \left(\cot \frac{\pi}{2M} + \frac{15}{2} \cot \frac{3\pi}{2M} - \frac{35}{2} \cot \frac{5\pi}{2M}\right) \tag{4-71}$$

It should be noted that when M approaches a very large value, all coefficients are evidently reduced to zero. In other words,

$$\lim_{M\to\infty} C_i = 0 \qquad i = 0, 1, 2, 3, \cdots \tag{4-72}$$

This means that for a large number of rings on the array, the pattern series can be approximated by the first term. That is,

$$E(\theta,\phi) \doteq \frac{MN}{\pi} I_o \quad \text{for large } M \tag{4-73}$$

C. Beamwidth

Since the number of rings in the array is designed to be very large, the main beam can be found from the first term of the far field pattern series. Substitution of the expression for I_o, in terms of the product of two zero-order Bessel functions, yields

$$E(\theta,\phi) \doteq MN\, J_o[ka(\sin\omega - \cos\theta + \cos\theta_o)] \cdot J_o[ka(\sin\omega + \cos\theta - \cos\theta_o)] \tag{4-74}$$

The beamwidth of a far field pattern is defined as the two position vectors in a given plane of the main beam where the field falls to $1/\sqrt{2}$ of the main beam peak. The peak field intensity in the main beam is found by replacing θ and ϕ in Equation (4-74) by θ_o and ϕ_o, respectively. Let θ_b and ϕ_b be the spherical coordinates where the beamwidth is to be found. Therefore

$$\frac{E(\theta_b,\phi_b)}{E(\theta_o,\phi_o)} = \frac{1}{\sqrt{2}} \tag{4-75}$$

The far field pattern of an array is a three dimensional figure, but its beamwidth is defined on a planar cut which

is made through the main beam and parallel to its axis. On the cut the far field pattern is now two dimensional. Since the main beam of the pattern in this study is defined in both directions, θ_o and ϕ_o, the pattern is not omnidirectional but rather a pencil beam. Therefore, it is necessary to find its beamwidth in both directions, one in θ and another in ϕ.

1. Beamwidth in the Elevation Angle Plane

In the elevation angle plane, the azimuth angle is fixed at $\phi = \phi_o$. The main beam is scanned along the plane from $\theta = 0$ to $\theta = \pi$. Setting $\phi = \phi_o$ in the Equation (4-48) reduces ω to

$$\omega = \frac{1}{2} \cos^{-1}(\cos\theta \cos\theta_o + \sin\theta \sin\theta_o)$$

$$= \frac{1}{2} (\theta - \theta_o), \quad \text{at} \quad \phi = \phi_o \tag{4-76}$$

which immediately follows that

$$\sin\omega\Big|_{\theta=\theta_o} = 0 \ . \tag{4-77}$$

Consequently,

$$E(\theta_o,\phi_o) = MNJ_o^2(0)$$

$$= MN \ . \tag{4-78}$$

Therefore Equation (4-75) becomes

$$J_o[ka(\sin\omega_b - \cos\theta_b + \cos\theta_o)]J_o[ka(\sin\omega_b + \cos\theta_b - \cos\theta_o)] = \frac{1}{\sqrt{2}} \ . \tag{4-79}$$

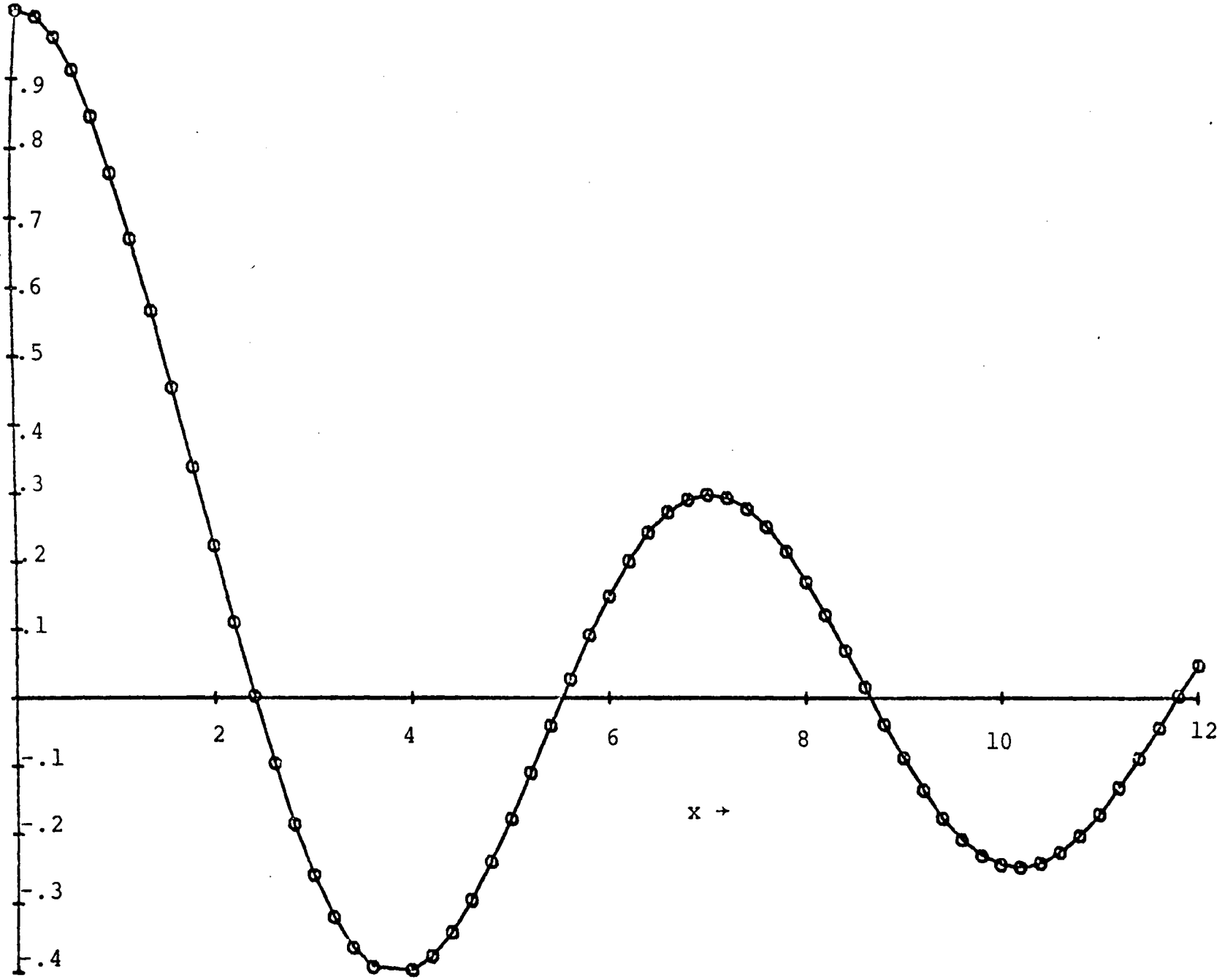

Figure 4-2. The Bessel Function of Zero Order

Before going on, let us turn back and study the variation of the Bessel function of zero order with respect to its argument. Figure 4-2 shows the variation of $J_o(x)$ with respect to x. From this figure, it is evident that the magnitude of $J_o(x)$ reaches the value of zero long before x reaches the value of three. Furthermore, in the case of beamwidth analysis, the magnitude of the Bessel function is always close to 0.707. Although this value is obtained as a result of the multiplication of two Bessel functions together, it must be between 0 and 1, which is non-negative. The probability that both functions could be negative so that their product is positive is ruled out, since the product never goes higher than 0.25.

Consequently, to analyze the beamwidth, the arguments of both Bessel functions are always less than three.

When the argument is never larger than three, the Bessel function of zero order can be approximated by the series [13]

$$J_o(x) = 1 - 2.2499\left(\frac{x}{3}\right)^2 + 1.26562\left(\frac{x}{3}\right)^4 - 0.31638\left(\frac{x}{3}\right)^6 + 0.0444\left(\frac{x}{3}\right)^8 - 0.003944\left(\frac{x}{3}\right)^{10} + 0.00021\left(\frac{x}{3}\right)^{12} + \varepsilon \qquad (4\text{-}80)$$

where

$$|\varepsilon| < 5 \times 10^{-8}.$$

Since the argument under consideration is much less than three, the approximation of $J_o(x)$ to the first two terms is sufficient. Hence

$$J_o(x) \doteq 1 - 2.2499 \left(\frac{x}{3}\right)^2$$

$$\doteq 1 - 2.25 \left(\frac{x}{3}\right)^2 . \qquad (4\text{-}81)$$

With the above approximation, Equation (4-79) becomes

$$\frac{1}{\sqrt{2}} = \left[1 - 2.25 \left(\frac{ka}{3}\right)^2 (\sin \omega_b - \cos \theta_b + \cos \theta_o)^2\right]$$

$$\cdot \left[1 - 2.25 \left(\frac{ka}{3}\right)^2 (\sin \omega_b + \cos \theta_b - \cos \theta_o)^2\right]$$

$$= 1 - \left(\frac{ka}{2}\right)^2 (\sin \omega_b - \cos \theta_b + \cos \theta_o)^2$$

$$- \left(\frac{ka}{2}\right)^2 (\sin \omega_b + \cos \theta_b - \cos \theta_o)^2$$

$$+ \left(\frac{ka}{2}\right)^4 (\sin \omega_b - \cos \theta_b + \cos \theta_o)^2 (\sin \omega_b$$

$$+ \cos \theta_b - \cos \theta_o)^2 . \qquad (4\text{-}82)$$

Again, the last term of Equation (4-82) is much smaller than the others. Therefore, it can be neglected, leaving only the quadratic terms. Expanding, grouping and cancelling the similar terms simplifies Equation (4-82) to

$$\frac{1}{\sqrt{2}} = 1 - \left(\frac{ka}{2}\right)^2 [\sin^2 \omega_b + (\cos \theta_b - \cos \theta_o)^2]$$

$$= 1 - \left(\frac{ka}{2}\right)^2 [\sin^2 \omega_b + 4\sin^2 \left(\frac{\theta_b - \theta_o}{2}\right) \sin^2 \left(\frac{\theta_b + \theta_o}{2}\right)]$$

$$= 1 - \left(\frac{ka}{2}\right)^2 \sin^2 \left(\frac{\theta_b - \theta_o}{2}\right) [1 + 4\sin^2 \left(\frac{\theta_b + \theta_o}{2}\right)] \qquad (4\text{-}83)$$

in which ω_b has been substituted by $(\theta_b - \theta_o)/2$ from Equation (4-76). For the large values of ka, i.e., the case of large numbers of rings, the beamwidth is very small. Therefore, the following approximation can be made,

$$\theta_b + \theta_o \doteq 2\theta_o \tag{4-84}$$

Hence, the Equation (4-82) reduces to

$$(\frac{ka}{2})^2 \sin^2(\frac{\theta_b - \theta_o}{2})[1 + 4\sin^2\theta_o] \doteq 1 - \frac{1}{\sqrt{2}}$$

$$= \frac{\sqrt{2} - 1}{\sqrt{2}}$$

or

$$\sin^2(\frac{\theta_b - \theta_o}{2}) \quad \frac{\sqrt{2}(\sqrt{2} - 1)}{(ka)^2[1 + 4\sin^2\theta_o]} . \tag{4-85}$$

Using the trigonometric identity

$$\cos x = 1 - 2\sin^2\frac{x}{2} , \tag{4-86}$$

we have the halfbeamwidth

$$|\theta_b - \theta_o| = \cos^{-1}[1 - \frac{2\sqrt{2}(\sqrt{2} - 1)}{(ka)^2[1 + 4\sin^2\theta_o]}] \tag{4-87}$$

$$= \cos^{-1}[1 - \frac{1.17157}{(ka)^2(1 + 4\sin^2\theta_o)}] . \tag{4-87a}$$

It is interesting to note that the beamwidth on this planar cut attains its maximum and minimum values at $\theta_o = 0$ and $\theta_o = \pi/2$, respectively. This is consistent with the physical appearance of the spherical array if we consider the planar cut as a linear array and look down at the main beam along the radial direction. At $\theta_o = 0$, the array looks as if it were composed of elements such that they were dense around the main beam but thin at both ends

of the array. Such an arrangement gives a rather large beamwidth [14]. On the other hand, at $\theta_o = \pi/2$, the density of the elements around the main beam is somewhat thinner than at both ends. This results in a smaller beamwidth.

2. Beamwidth in the Plane of Azimuth Angle

In the azimuth angle plane, θ is set equal to θ_o. In addition to this, since the array is arranged in rings around the sphere, the plane on which the beamwidth will be analyzed in terms of the azimuth angle should be the plane of the equator, i.e., $\theta = \theta_o = \pi/2$. Under these conditions, ω is reduced to

$$\omega = \frac{1}{2}(\phi - \phi_o), \quad \theta = \theta_o = \frac{\pi}{2} . \tag{4-88}$$

And from Equation (4-74)

$$E(\tfrac{\pi}{2},\phi) = MNJ_o^2[ka \sin \omega] \tag{4-89}$$

Therefore, at the $1/\sqrt{2}$ th point,

$$J_o^2(ka \sin \omega_b) = \frac{1}{\sqrt{2}}$$

$$J_o(ka \sin \omega_b) = 2^{-\frac{1}{4}} . \tag{4-90}$$

Again, for the case of large numbers of rings,

$$ka \sin \omega_b < 3 . \tag{4-91}$$

Using the same approximation previously employed for the expression of $J_o(ka \sin \omega_b)$ gives

$$2^{-\frac{1}{4}} \doteq 1 - 2.25\left(\frac{ka}{3}\right)^2 \sin^2 \omega_b + 1.266\left(\frac{ka}{3}\right)^4 \sin^4 \omega_b$$

which simplifies to the form of a quadratic equation

$$1.266\left(\frac{ka \sin \omega_b}{3}\right)^4 - 2.25\left(\frac{ka \sin \omega_b}{3}\right)^2 + 0.1591 = 0 \quad . \qquad (4\text{-}92)$$

Solving Equation (4-92) by using the well-known solution of the quadratic equation gives

$$\left(\frac{ka \sin \omega_b}{3}\right)^2 = \frac{2.25 \pm \sqrt{2.25^2 - 4(1.266)(0.1591)}}{2(1.266)}$$

$$= 1.71 \ , \ \ 0.07377 \quad . \qquad (4\text{-}93)$$

With the assumption made earlier that ka sin ω_b is less than three, the only valid solution in Equation (4-93) is 0.07377. Therefore,

$$\sin^2 \omega_b = \frac{0.66397}{(ka)^2} \quad . \qquad (4\text{-}94)$$

Again applying the trigonometric identity, cos $2\omega_b$ = $1 - 2\sin^2 \omega_b$ to Equation (4-94) gives

$$2\omega_b = \cos^{-1}\left[1 - \frac{1.32795}{(ka)^2}\right] \quad . \qquad (4\text{-}95)$$

Substitution of the expression of ω_b in terms of ϕ_b and ϕ_o yields the halfbeamwidth

$$|\theta_b - \theta_o| = \cos^{-1}\left[1 - \frac{1.32795}{(ka)^2}\right] \quad . \qquad (4\text{-}96)$$

It is also interesting to observe that the beamwidth on this plane does not vary with the position of the main beam at all. This is expected because, as the main beam is scanned on the horizontal principal plane, the array as seen by the main beam does not change its configuration.

There is no difference in the array at $\phi = \phi_1$ and $\phi = \phi_2$ as long as they are on the $\theta = \pi/2$ plane.

D. The Approximately Equally-Spaced Spherical Array

It was discussed earlier (Chapter II) that elements in all rings of the approximately equally-spaced spherical array cannot be spaced equally. Otherwise, we would end up with some non-integer number of elements in some rings. Thus, the element spacings are allow fluctuate a little from ring to ring to make the number of antennas in a given ring an integer at all times. By this arrangement, the number of antennas in a ring varies with the ring position and is given by

$$N_m = \frac{2\pi a}{d_m} \sin \theta_m \quad . \tag{4-97}$$

Inserting the number of antennas, N_m, in Equation (4-22), we have

$$E_A(\theta,\phi) = \sum_{m=0}^{M} \frac{2\pi a}{d_m} \sin \theta_m \, J_o(\chi_m) e^{jka \cos \theta_m (\cos \theta - \cos \theta_o)}$$

$$= 2\pi a \sum_{m=0}^{M} \frac{\sin \theta_m}{d_m} J_o(B \sin \theta_m) e^{jA \cos \theta_m} \quad , \tag{4-98}$$

where χ_m, A, and B have been defined in Equations (4-16), (4-38), and (4-39) respectively.

The procedure of the analysis of Equation (4-98) is approximately the same as in the case of the latitude-longitude distribution. Let us start by applying Equation (4-5), with ε taking the value of zero, to

Equation (4-98). Now, changing the variable from ν to θ' through the use of the chain rule, and using the property of equally-spaced rings, we eliminate the derivative $d\nu/d\theta'$. The far field pattern reduces to the integral Equation (4-99),

$$E_A(\theta,\phi) = 2aM \sum_{h=-\infty}^{\infty} \int_0^{\pi} \frac{\sin\theta'}{d(\theta')} J_o(B \sin\theta') \cdot e^{jA\cos\theta' + j2Mh\theta'} d\theta' \quad . \tag{4-99}$$

In this type of element distribution, the element spacings will vary from ring to ring. They will fluctuate around a value, which in this case is the equator element spacing. Analysis in Chapter II reveals that this fluctuation is very small. Most of the element spacings are within one percent of the equator element spacing, with the exception of a few rings which contain small numbers of elements. Therefore, in this analysis, the element spacings are assumed to be the same. That is,

$$d(\theta') = d \quad . \tag{4-100}$$

With this approximation, the far field pattern becomes

$$E_A(\theta,\phi) = \frac{2aM}{d} \sum_{h=-\infty}^{\infty} \int_0^{\pi} \sin\theta' J_o(B \sin\theta') \cdot e^{jA\cos\theta' + j2Mh\theta'} d\theta' \quad . \tag{4-101}$$

1. Pattern Series and Its Coefficients

Through the use of a series expansion for the Bessel function, changing the exponential function into the complex sum of cosine and sine changes the far field pattern expression (4-101), which becomes an infinite series. The sine part of the H^{th} term will cancel the sine part of the minus H^{th} term, leaving only the cosine parts, which combine. Therefore,

$$E_A(\theta,\phi) = \frac{2aM}{d}\left[\int_0^{\pi} I_A(\theta')\,d\theta' + 2\int_0^{\pi} I_A(\theta')\cos(2Mh\theta')d\theta'\right.$$

$$\left. + \cdots + 2\int_0^{\pi} I_A(\theta')\cos(2MH\theta')d\theta' + \cdots\right] , \qquad (4\text{-}102)$$

where

$$I_A(\theta') = \sin\theta'\, J_o(B\sin\theta')\, e^{jA\cos\theta'}$$

$$= \sin\theta'\, I(\theta') , \qquad (4\text{-}103)$$

in which $I(\theta')$ has been defined by Equation (4-36).

Similar to the evaluation of the far field pattern of the latitude-longitude distribution, the integration of the far field pattern series (4-102) has to be integrated term by term. The first term will be denoted I_{oA} and will be integrated by introducing a dummy variable

$$x = \cos\theta' ,$$

then

$$dx = - \sin \theta' \, d\theta'$$

Therefore,

$$I_{OA} = \int_{-1}^{1} \sqrt{1 - x^2} \, J_o(B\sqrt{1 - x^2}) \, e^{jAx} \, \frac{dx}{\sqrt{1 - x^2}}$$

$$= \int_{-1}^{1} J_o(B\sqrt{1 - x^2}) \, e^{jAx} \, dx$$

$$= 2 \int_{0}^{1} J_o \, (B\sqrt{1 - x^2}) \cos Ax \, dx \quad ,$$

where the last integral is obtained by using the fact that the exponential function of a complex exponent is the sum of cosine and sine of the exponent, which are even and odd respectively. The odd function makes the integral vanish while the even function doubles the integral.

From the Table of Integrals [15], the following identity is found

$$\int_{0}^{a} J_o(b\sqrt{a^2 - x^2}) \cos(cx) dx = \frac{\sin(a\sqrt{b^2 + c^2})}{\sqrt{b^2 + c^2}} \quad . \qquad (4\text{-}105)$$

Therefore, the fundamental term of the far field pattern is

$$I_{OA} = 2 \, \frac{\sin(\sqrt{A^2 + B^2})}{\sqrt{A^2 + B^2}} \quad . \qquad (4\text{-}106)$$

As already shown in Appendix B, we have

$$\sqrt{A^2 + B^2} = 2 \, ka \sin \omega \quad . \qquad (4\text{-}107)$$

This gives I_{OA} in its final form:

$$I_{OA} = \frac{\sin\ (2\ ka\ \sin\omega)}{ka\ \sin\ \omega} \quad . \tag{4-108}$$

It should be noted that this expression is similar to the array factor of a uniform linear array, which is given by [18],

$$E_1(\theta) = \frac{\sin\ (\frac{n\psi}{2})}{n\ \sin\ (\frac{\psi}{2})} \quad , \tag{4-109}$$

where

$$\psi = \frac{2\pi s}{\lambda} \cos\ \theta - \psi_o \quad . \tag{4-110}$$

The similarity between the two is that both are the ratios of two sine functions and the argument of the numerator varies much faster than that of the denominator.

Now, let us consider the H^{th} term of the pattern series. This term will be called I_{HA},

$$I_{HA} = 2 \int_0^{\pi} I_A(\theta')\ \cos\ (2MH\theta')\ d\theta' \quad . \tag{4-111}$$

Once more the term $\cos(2MH\theta')$ is expanded into a series of Legendre polynomials of even index.

$$\cos(2MH\theta') = \sum_{l=0}^{MH} A_l(MH) P_{2l}\ (\cos\ \theta') \tag{4-112}$$

where $A_l(MH)$ is as found in Equation (4-56). Inserting the cosine function back in Equation (4-111) and rearranging the integral, the summation becomes

$$I_{HA} = 2 \sum_{l=0}^{MH} A_l(MH)\, K_A(l) \quad , \tag{4-113}$$

where $K_A(l)$ is the integral part and given by

$$K_A(l) = \int_0^{\pi} \sin\theta'\, J_o(B \sin\theta') e^{jA\cos\theta'} P_{2l}(\cos\theta')\, d\theta' \quad , \tag{4-114}$$

or in terms of the dummy variable $x = \cos\theta'$

$$K_A(l) = 2 \int_0^{1} \cos Ax\, J_o(B\sqrt{1 - x^2}) P_{2l}(x)\, dx \ . \tag{4-115}$$

Substitution of Equations (4-108) and (4-113) into the pattern series (4-102) results in a series similar to the one given by Equation (4-60).

$$\begin{aligned} E_A(\theta,\phi) &= \frac{2aM}{d} \Big[I_{OA} + 2\Big(\sum_{p=1}^{\infty} A_o(pM)\Big) K_A(0) \\ &\quad + 2\Big(\sum_{p=1}^{\infty} A_1(pM)\Big) K_A(1) + 2\Big(\sum_{p=1}^{\infty} A_2(pM)\Big) K_A(2) + \cdots \Big] \\ &= \frac{2aM}{d} \left[I_{OA} + C_o K_A(0) + C_1 K_A(1) + \cdots \right] \\ &= \frac{2aM}{d} \left[(1 + C_o) I_{OA} + C_1 K_A(1) + C_2 K_A(2) + \cdots \right] \quad , \end{aligned} \tag{4-116}$$

C_o, C_1, C_2, $\cdots$ are the pattern harmonic coefficients and have already been defined by Equations (4-69), (4-70) and (4-71) respectively. $K_A(0) = I_{OA}$ has also been used.

Again, in the case of a large number of elements, the far field pattern for the approximately equally-spaced

array will reduce to the first term of Equation (4-116) only

$$E_A(\theta,\phi) \doteq \frac{2aM}{d} I_{OA} \quad , \quad \text{for large M}$$

$$= \frac{2aM}{d} \frac{\sin(2ka \sin \omega)}{ka \sin \omega}$$

$$= \frac{4aM}{d} \frac{\sin u}{u} \quad , \tag{4-117}$$

where

$$u = 2ka \sin \omega \quad . \tag{4-118}$$

2. Beamwidth

a. Beamwidth in the Elevation Angle Plane

For a large number of elements, only the first term of the far field series is sufficient to evaluate the beamwidth.

$$E_A(\theta,\phi) = \frac{2aM}{d} \frac{\sin (2ka \sin \omega)}{ka \sin \omega} \quad . \tag{4-119}$$

In order to compute the beamwidth in the elevation angle plane, the aximuth angle is fixed at $\phi = \phi_o$. This leads to

$$\omega = \frac{1}{2}(\theta - \theta_o) \quad , \quad \text{at} \quad \phi = \phi_o \tag{4-120}$$

Therefore, the

$$\omega_b = \frac{1}{2}(\theta_b - \theta_o) \quad , \tag{4-121}$$

where the subscript b stands for the beamwidth.

Thus, as found in Equation (4-75), we have

$$\frac{E_A(\theta_b,\phi_b)}{E_A(\theta_o,\phi_o)} = \frac{1}{\sqrt{2}}$$

$$\frac{\sin u_b}{u_b} = \frac{1}{\sqrt{2}} \qquad (4\text{-}122)$$

Solving the above equation numerically by applying the method of linear iteration [19] gives

$$u_b = 1.39156 \quad . \qquad (4\text{-}123)$$

The half beamwidth is immediately found to be

$$|\theta_b - \theta_o| = 2 \sin^{-1} \left(\frac{0.69578}{ka}\right) \qquad (4\text{-}124)$$

For a small beamwidth, it can be approximated to

$$|\theta_b - \theta_o| \doteq \frac{1.39156}{ka} \qquad (4\text{-}125)$$

Another way to solve for the beamwidth is to expand the function sin u_b into an infinite series of u_b. Then

$$\frac{1}{\sqrt{2}} = 1 - \frac{u_b^2}{3!} + \frac{u_b^4}{5!} - \frac{u_b^6}{7!} + \cdots \qquad (4\text{-}126)$$

In the neighborhood of the mainbeam axis, u_b is small. Therefore, the series can be approximated by neglecting all terms in Equation (4-126) except the first two terms. Then

$$u_b^2 \doteq 3! \left(1 - \frac{1}{\sqrt{2}}\right)$$

$$= 3\sqrt{2} \left(\sqrt{2} - 1\right) \quad .$$

Or, in terms of sin ω_b

$$\sin^2 \omega_b = \frac{3\sqrt{2} \left(\sqrt{2} - 1\right)}{4(ka)^2} \quad . \qquad (4\text{-}127)$$

But

$$\text{Cos } 2\omega_b = 1 - 2 \sin^2 \omega_b$$

$$= 1 - \frac{3\sqrt{2}\ (\sqrt{2} - 1)}{2(ka)^2} .$$

Then

$$|\theta_b - \theta_o| = \cos^{-1}[1 - \frac{3\sqrt{2}\ (\sqrt{2} - 1)}{2(ka)^2}] , \qquad (4\text{-}128)$$

$$= \cos^{-1}[1 - \frac{0.87868}{2(ka)^2}] . \qquad (4\text{-}128a)$$

Equations (4-124) and (4-128) reveal that the beamwidth of the approximately equally-spaced array does not vary with the position of the main beam. This implies that the array can be electronically scanned 360 degrees in this planar cut without changing the far field pattern. In a practical situation, the main beam will change slightly as it is scanned about the sphere. This is due to the fact that the spacing is not purely uniform. At the far observation point, however, the array, as seen by the observer, looks highly uniform. This makes the far field pattern almost the same regardless of the position of the main beam in that planar cut.

b. Beamwidth in the Azimuth Angle Plane

To derive the beamwidth in this plane, the elevation angle θ is fixed at $\pi/2$. Then the expression for ω becomes

$$\omega = \frac{1}{2}(\phi - \phi_o) \quad , \quad \text{at} \quad \theta = \theta_o = \frac{\pi}{2} \, . \tag{4-129}$$

The expression for ω in the $\theta = \theta_o = \pi/2$ plane immediately shows that the shape of the main beam on this azimuth plane is exactly the same as found in the elevation angle plane. Therefore, the beamwidth can be found simply by replacing θ_b by ϕ_o, respectively, in the expression for the beamwidth in the elevation angle plane. Hence,

$$|\phi_b - \phi_o| = 2 \sin^{-1} \left[\frac{0.69578}{ka}\right] \, , \tag{4-130}$$

for the exact beamwidth, and

$$|\phi_b - \phi_o| = \cos^{-1} \left[1 - \frac{0.87868}{(ka)^2}\right] \, , \tag{4-131}$$

as an approximation.

CHAPTER V

NUMERICAL RESULTS AND DISCUSSIONS

A. Method of Computation

This chapter presents the numerical analysis of the developments in the preceding chapters. All numerical data were obtained through the extensive use of the IBM/360 computer. The programmings are Fortran IV under both Wat4 and Os. control cards. Wat4 is employed in all general programmings, while Os. is called for when a subroutine or a plot program is needed.

Before we analyze the far field patterns, let us look at the equations once more. They are

$$E(\theta,\phi) = \frac{MN}{\pi} [(1 + C_o)I_o + C_1K(1) + C_2K(2) + \cdots]$$

for the latitude-longitude distribution, and

$$E_A(\theta,\phi) = \frac{MN}{\pi} [(1 + C_o)I_{o_A} + C_1K_A(1) + C_2K_A(2) + \cdots]$$

for the approximately equally-spaced distribution.

It can be seen that the pattern harmonics of both types of distributions, $K(\ell)$ and $K_A(\ell)$ respectively, are still in integral form. Since they can not be at present integrated into a closed form, it is totally necessary that they be integrated numerically. For convenience in finding the right method to integrate them, $K(\ell)$ and

$K_A(\ell)$ are put in the form of the dummy variable $x = \cos\theta'$.

$$K(\ell) = 2\int_0^1 \cos Ax\, J_o(B\sqrt{1-x^2})P_{2\ell}(x)\,\frac{dx}{\sqrt{1-x^2}}\,, \qquad (5\text{-}1)$$

and

$$K_A(\ell) = 2\int_0^1 \cos Ax\, J_o(B\sqrt{1-x^2})P_{2\ell}(x)\,dx\,. \qquad (5\text{-}2)$$

There are several methods of numerical integration, for example, the rectangular rule, trapezoidal rule, Simpson's rule, etc. In order to choose the right method for the above two equations, one should note that the integrand of $K(\ell)$ makes the integral improper at $x = 1$. But it is guaranteed by Equation (4-58) that this integral is definitely finite. In programming, however, the computer rejects any division by zero. Therefore, any numerical integration method that requires the integrand to be evaluated at the end points fails to qualify. Fortunately, there is one method which does not require the integrand to be evaluated there, and yet gives a highly accurate result when compared to other methods. It is the method of Gaussian Quadrature.

The principal of the Gaussian Quadrature integration is as follows [20].

The interval of integration to be evaluated is transformed from [a,b] to [-1,1] through the substitution

$$x = \frac{1}{2}(b - a)t + \frac{1}{2}(a + b) \tag{5-3}$$

so that

$$\int_a^b f(x)\,dx = \frac{b - a}{2} \int_{-1}^{1} F(t)\,dt \tag{5-4}$$

where F(t) is the transform of f(x) through the Equation (5-3). Then the integration is evaluated to be

$$\int_{-1}^{1} F(t)\,dt = \sum_{n=1}^{N} A_n F(t_n) \quad , \tag{5-5}$$

where N is the number of points at which F(t) is found. The higher N is, the more accurate the result will be.

For the evaluation of the integral through the use of the five-point Gaussian formula, t_n and A_n are given by [20],

$$\begin{aligned} t_4 &= -t_0 = 0.90617985 \\ t_3 &= -t_1 = 0.53846931 \\ t_2 &= 0.0 \\ A_4 &= A_0 = 0.23692689 \\ A_3 &= A_1 = 0.47862867 \\ A_2 &= 0.56888888 \quad . \end{aligned} \tag{5-6}$$

The only disadvantage of this method is that t_n and A_n, as can be seen from (5-6), are irrational numbers. This does not have any effect on a computer since it can store any number without limitation. The main advantage is

the great accuracy of this method. The five-point Gaussian formula gives approximately the same accuracy as the 20-division Simpson's rule.

Upon applying the method to $K(\mathbb{1})$ and $K_A(\mathbb{1})$, the variable x is transformed into t by Equation (5-3)

$$x = \frac{t + 1}{2} , \tag{5-7}$$

and the integrand becomes

$$F(t) = F_1(t)F_2(t)F_3(t)/F_4(t) \tag{5-8}$$

where

$$F_1(t) = \cos A \left(\frac{t + 1}{2}\right) \tag{5-9}$$

$$F_2(t) = J_o \left(B \frac{\sqrt{1 - 2t - t^2}}{2}\right) \tag{5-10}$$

$$F_3(t) = P_{21} \left(\frac{t + 1}{2}\right) \tag{5-11}$$

and

$$F_4(t) = \frac{\sqrt{1 - 2t - t^2}}{2} \qquad \text{for } K(\mathbb{1}) \tag{5-12a}$$

$$= 1 \qquad \text{for } K_A(\mathbb{1}) \tag{5-12b}$$

The five-point formula was employed to perform the task in this case. Therefore, the integration is found to be

$$\begin{aligned} \text{Integration} = 2 \{ & 0.23692689 \, [F(-0.90617985) \\ & + F(0.90617885)] + 0.47862867 \\ & \cdot [F(-0.53846931) + F(0.53846931)] \\ & + 0.568888889 \, F(0) \} . \end{aligned} \tag{5-13}$$

B. The Pattern Harmonics

The H^{th} pattern harmonic is defined in Chapter IV by

$$I_H = C_H K(H) \tag{5-13}$$

in which C_H denotes its coefficient. Since the magnitude of C_H depends totally on the number of rings, M, it is interesting to look at the magnitudes of these coefficients as a function of M. Furthermore, as was mentioned before, their magnitudes approach zero when M becomes a very large value. There is a range of M that is between the so-called large and small number of rings.

Figure 5-1 shows the variations of the magnitudes of the first few coefficients versus M. It can be seen that the coefficients of the higher harmonics are large in magnitude when the array consists of only a few rings, but decreases rapidly to an almost vanishing value as M increases.

Figures 5-2 and 5-3 show the magnitudes of the first few pattern harmonics as a function of M. Again, the magnitudes of these harmonics are seen to decrease as M increases. Furthermore, the higher the harmonic, the smaller its magnitude will be. At the region of small M, it may be noticed that some harmonic magnitudes are larger than that of the fundamental. This is the region of invalidity since the far field pattern in this study is defined only for large M.

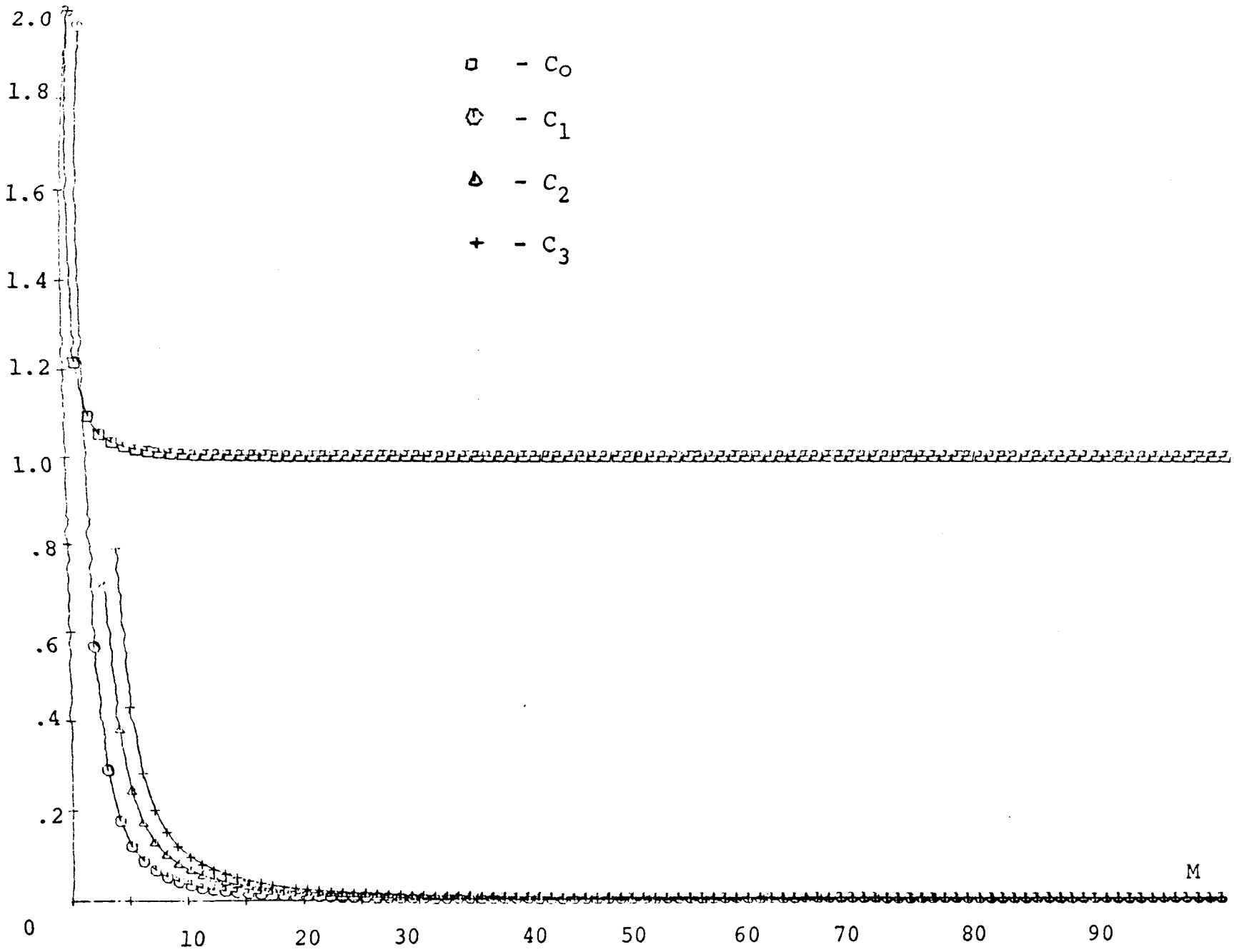

Figure 5-1. The Magnitudes of C's versus M

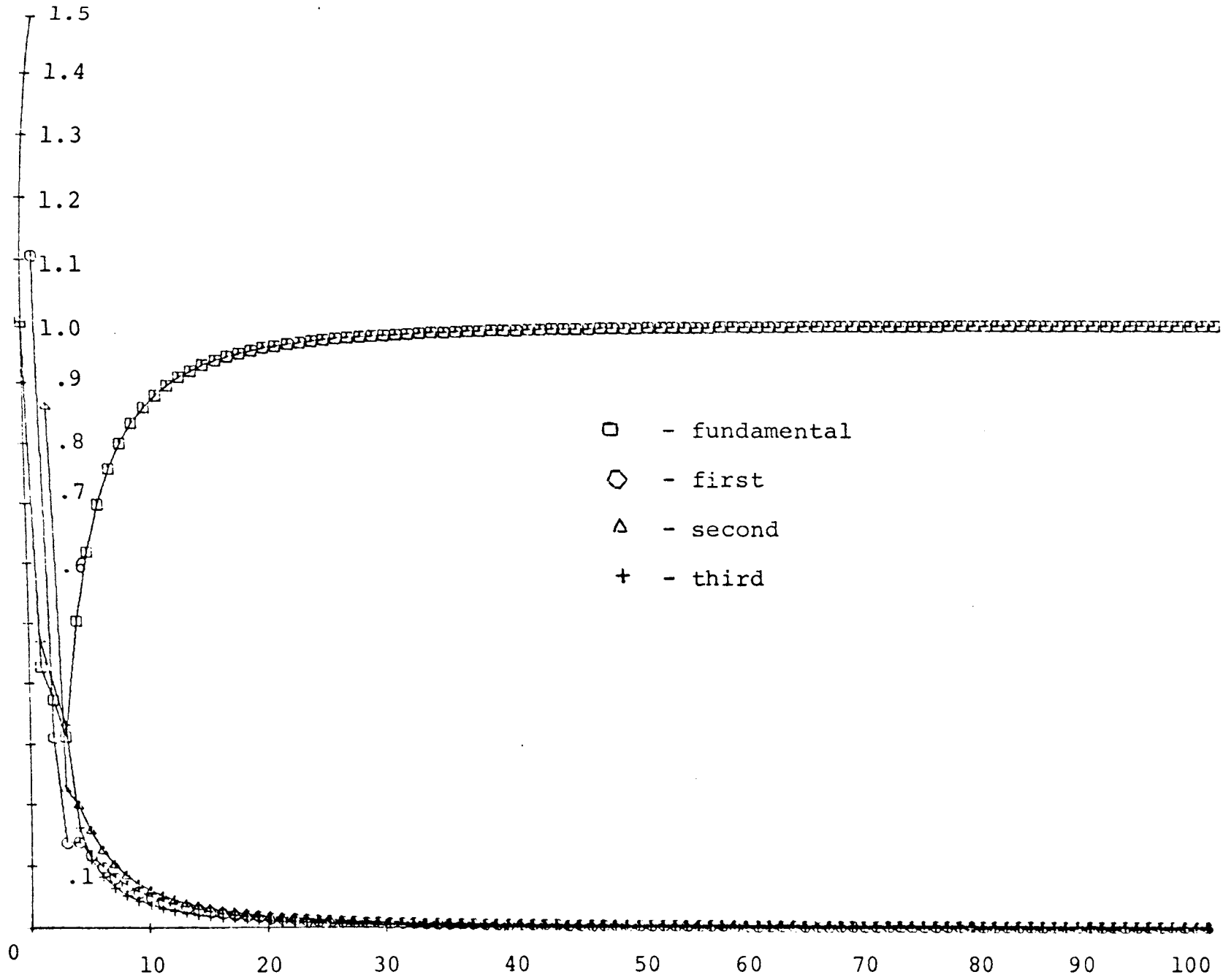

Figure 5-2. The Latitude-Longitude Far Field Pattern Harmonics as a Function of M

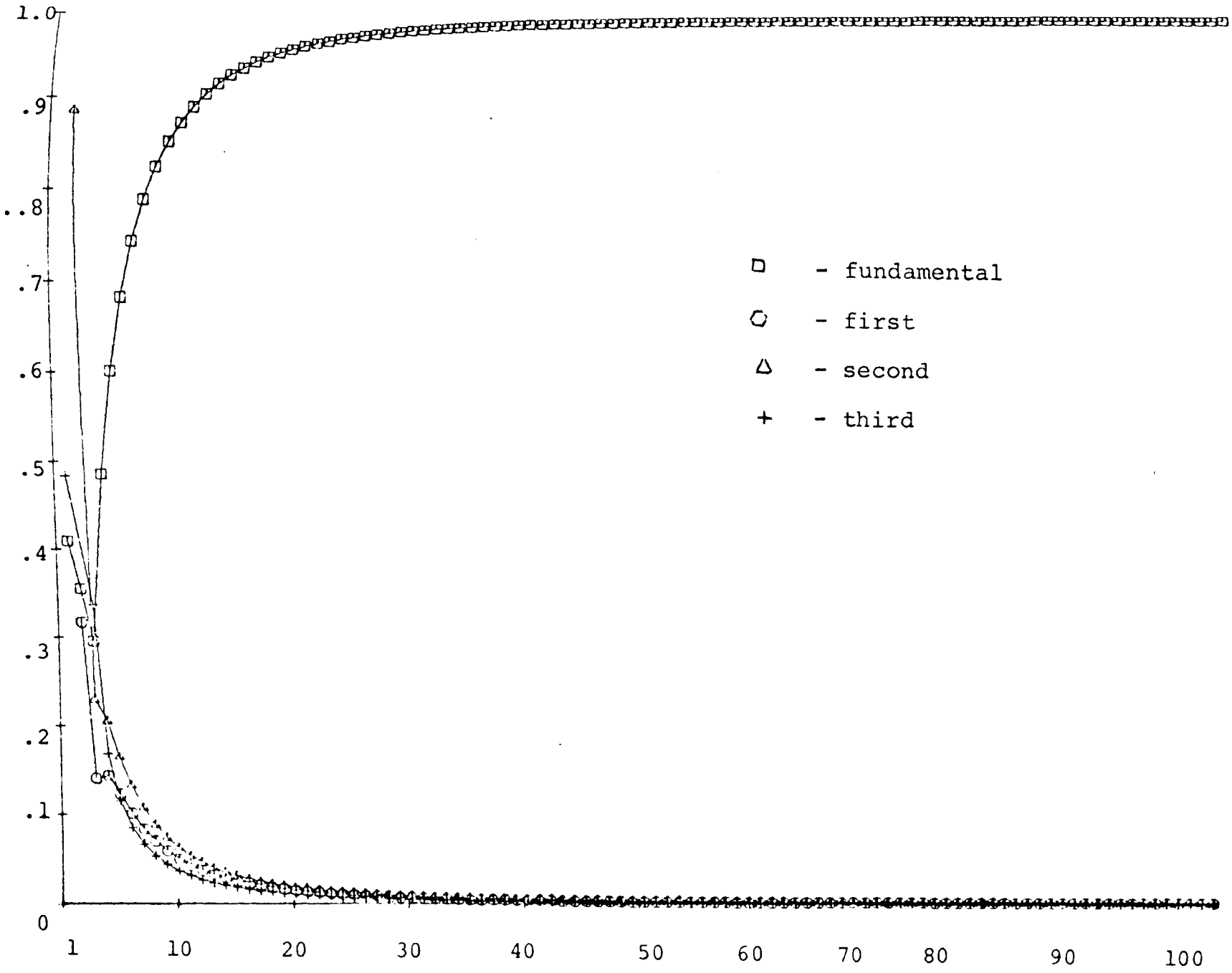

Figure 5-3. The Approximately Equally-Spaced Far Field Pattern Harmonics as a Function of M

The application determines the critical range of M for the definition "large number of rings". Since the main purpose of this analysis is to illustrate the principle involved, accuracy is not foremost in our calculations. The first four terms of the far field pattern series will be used in computing the far field patterns. To satisfy the large number of ring requirements, M will be chosen to be 20 to minimize the computing time with a fairly good accuracy for the four-term approximation. This value of M will be used in all computations made.

With M = 20, Figures 5-4, 5-5, and 5-6 show the comparison along the pattern harmonics on various planes for the latitude-longitude (LL) distribution. Figures 5-7, 5-8, and 5-9 show the same plots for the approximately equally-spaced (AES) distribution. From these figures, one thing is obvious; that the fundamental term almost completely dominates the other harmonics which decrease rapidly to a nearly vanishing value at large angles away from the main beam.

C. Far Field Pattern Analysis

Figure 5-10 shows the flow chart used in the pattern computation programming. In order to bound the pattern between -1 and 1, it is at every point normalized such that the main beam is unity. For convenience in programming, the evaluation begins at the main beam, and the value obtained there is used as the normalizing factor.

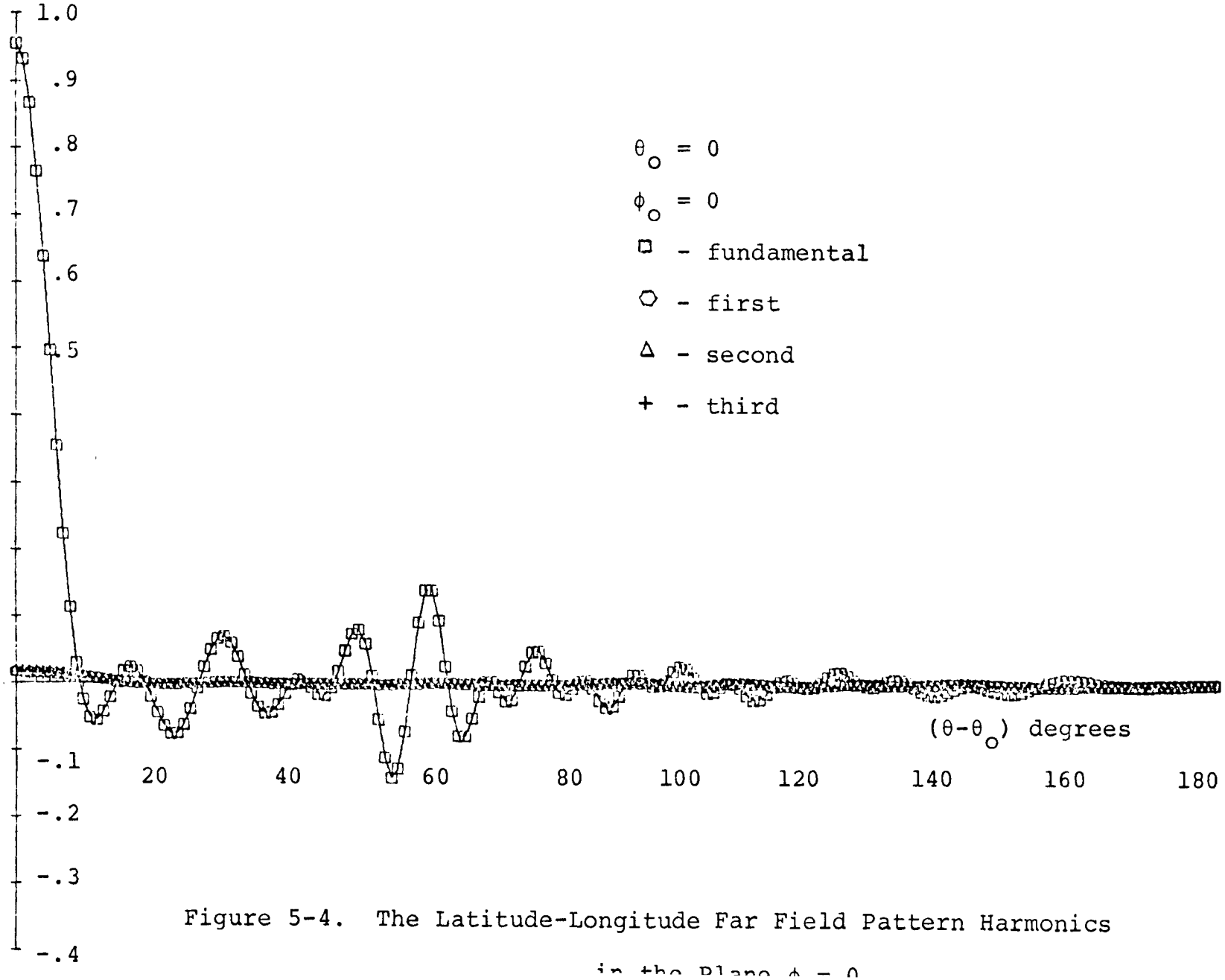

Figure 5-4. The Latitude-Longitude Far Field Pattern Harmonics in the Plane $\phi = 0$

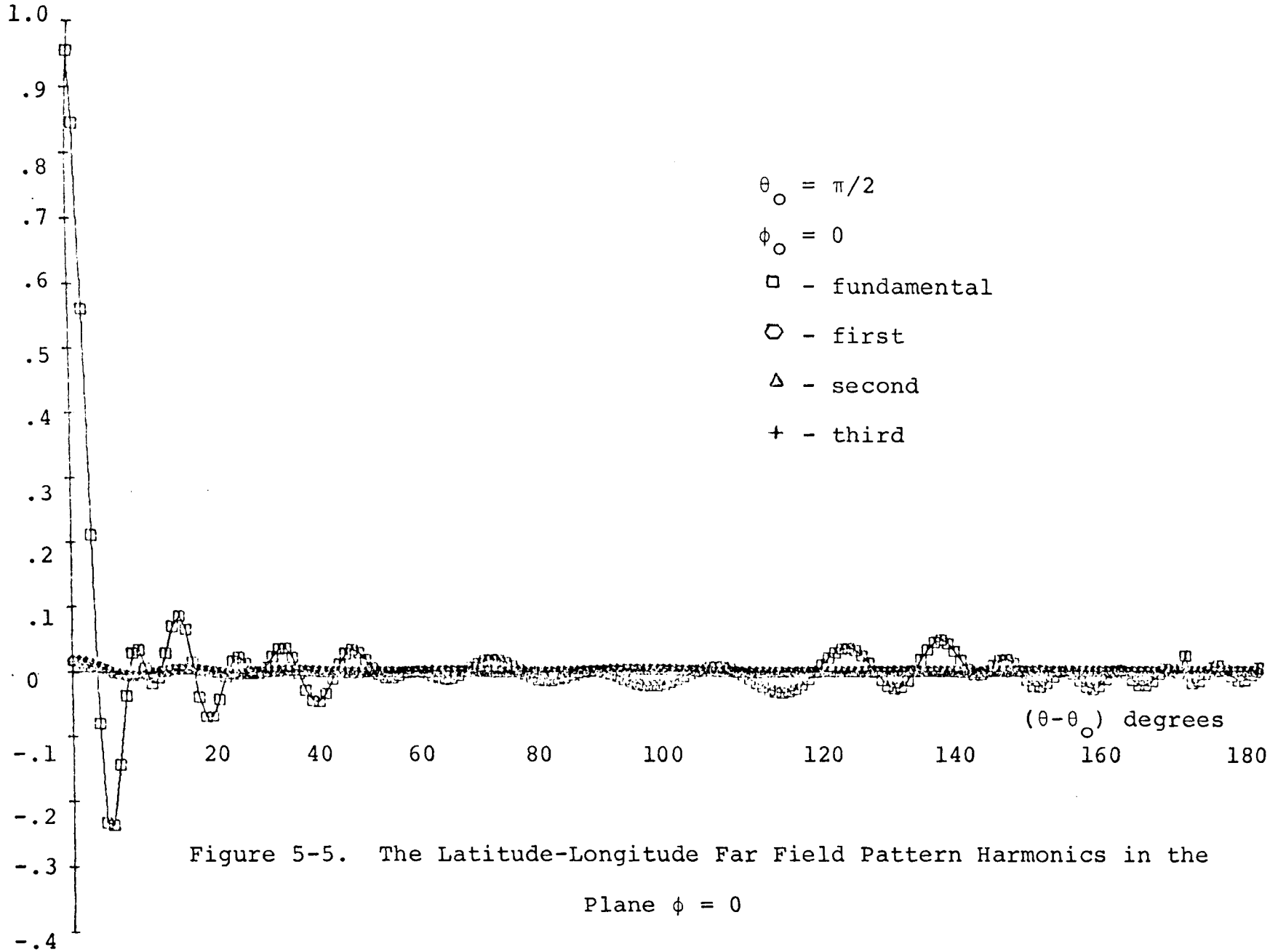

Figure 5-5. The Latitude-Longitude Far Field Pattern Harmonics in the Plane $\phi = 0$

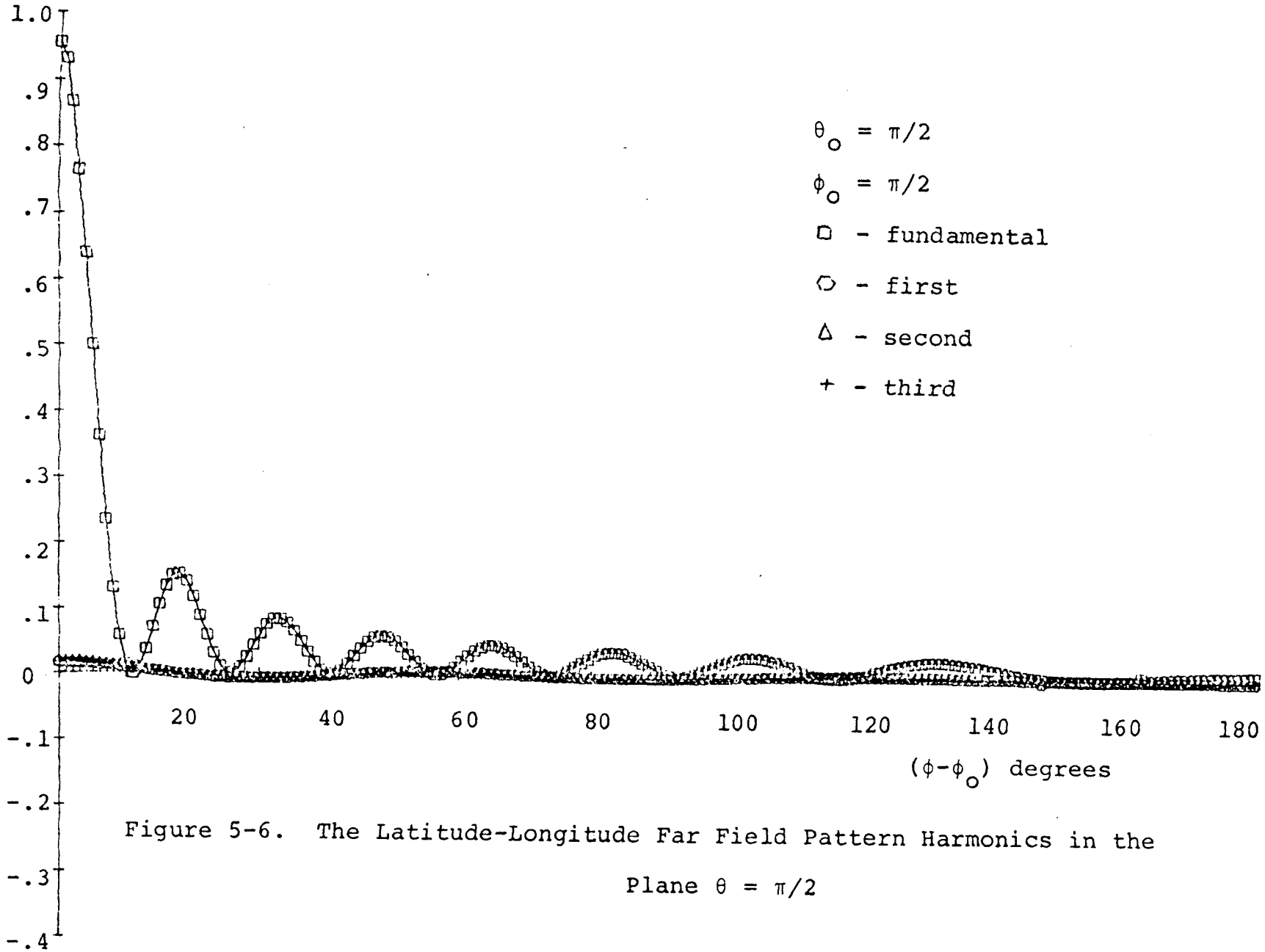

Figure 5-6. The Latitude-Longitude Far Field Pattern Harmonics in the Plane $\theta = \pi/2$

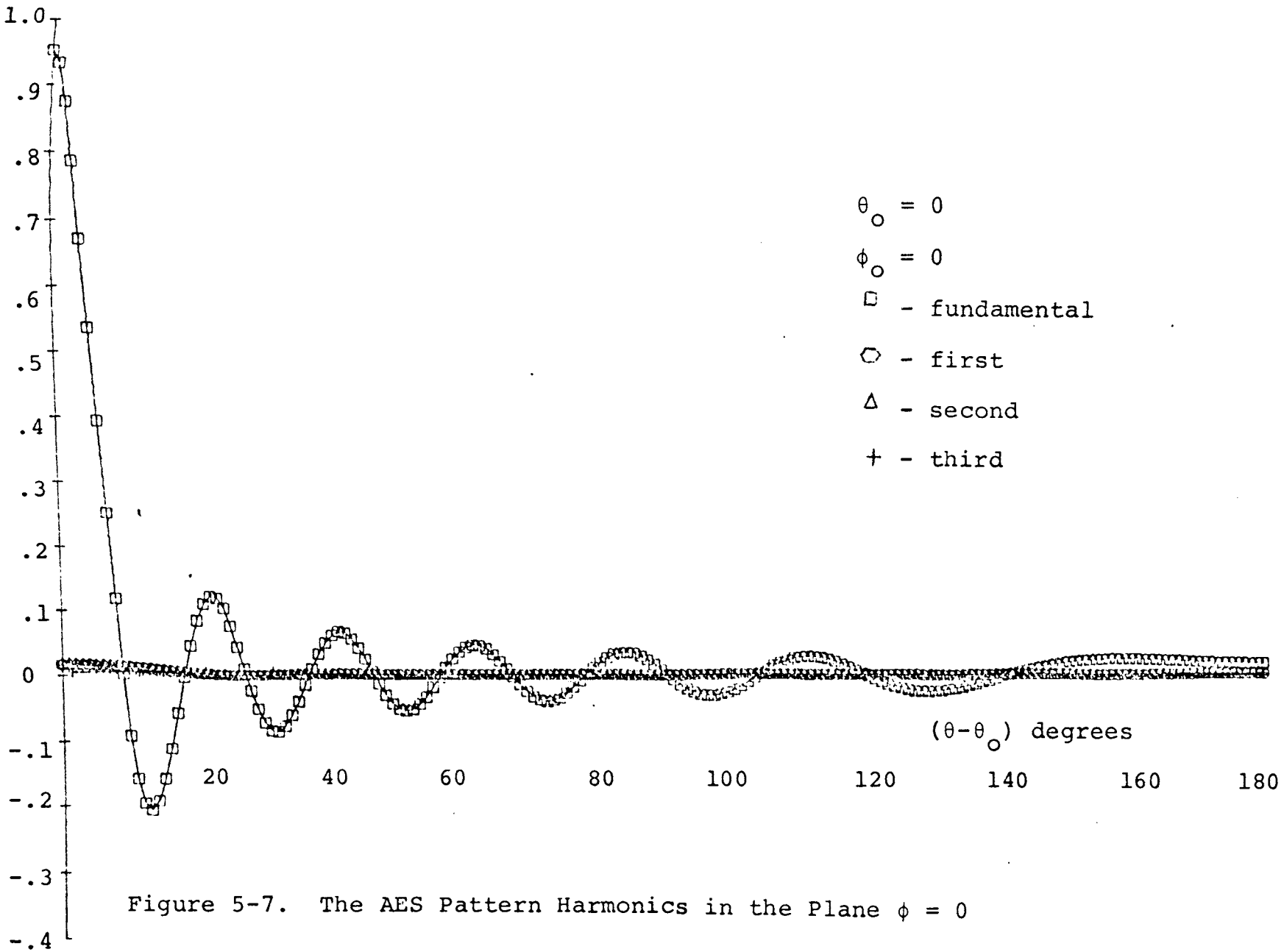

Figure 5-7. The AES Pattern Harmonics in the Plane $\phi = 0$

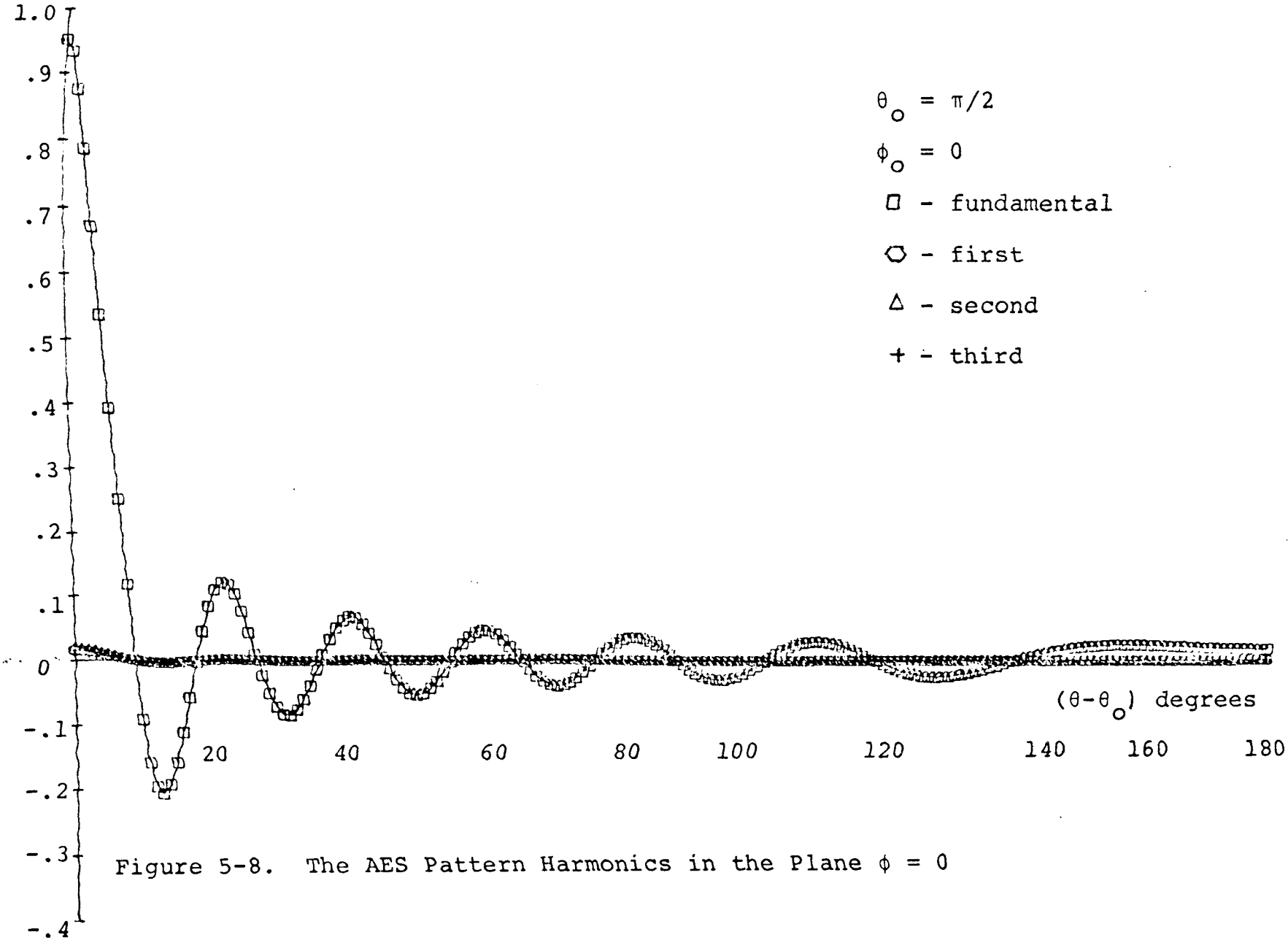

Figure 5-8. The AES Pattern Harmonics in the Plane $\phi = 0$

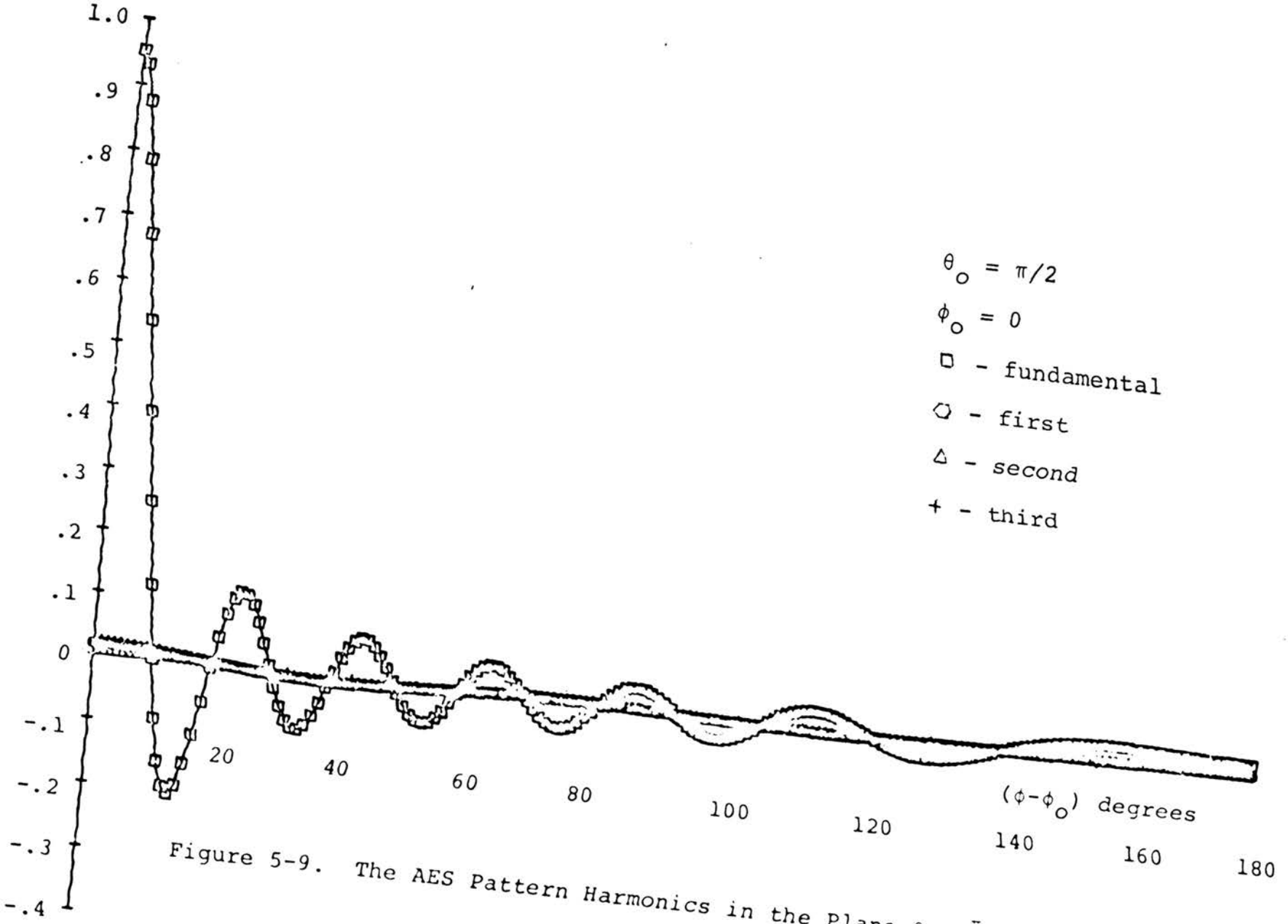

Figure 5-9. The AES Pattern Harmonics in the Plane $\theta = \frac{\pi}{2}$

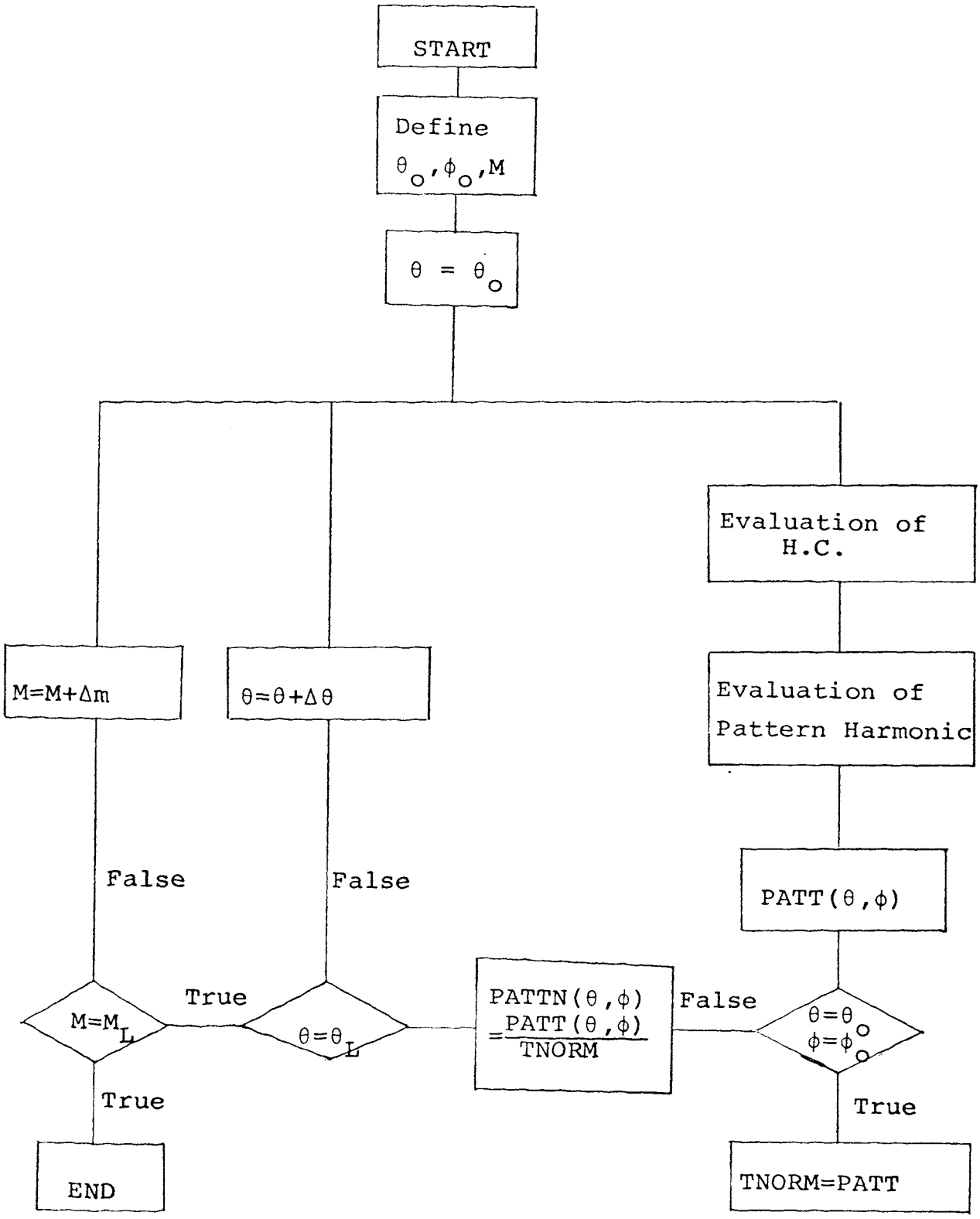

Figure 5-10. The Far Field Pattern Programming Flow Chart

The pattern is not always symmetrical due to the asymmetrical arrangement of antennas in the array. Because of this fact, it becomes necessary to evaluate the pattern around the sphere (i.e., 360 degrees from the mainbeam).

The computer programming for the pattern evaluation is under an Os. control card. The Os. is employed so that the subroutine for Bessel functions and Legendre polynomials can be called from the subroutine area. The program is shown in Appendix F.

The arguments of the Bessel functions from Equation (4-46) can be negative at some points. This does not affect the value of the Bessel functions since they are even functions. In the program, however, since the computer does not store any values of Bessel functions of a negative agrument, it is necessary that their arguments be under the absolute sign. Yet a problem still exists since the absolute sign makes the argument approach zero from the negative side. Consequently, the value of $J_o(x)$ at $x = 0$ is computed to be zero instead of unity, as it should be. In order to avoid this problem, the number 0.00005 is added to the argument of the Bessel function so that it approaches zero from the positive end.

Figure 5-11 illustrates the approximated pattern of the LL element distribution in the plane $\phi = 0$ with the mainbeam positioned at $\theta_o = \pi/6$, $\pi/4$, and $\pi/3$. From this figure, it can be seen that the pattern changes shape slightly. The beamwidth becomes broader as the mainbeam

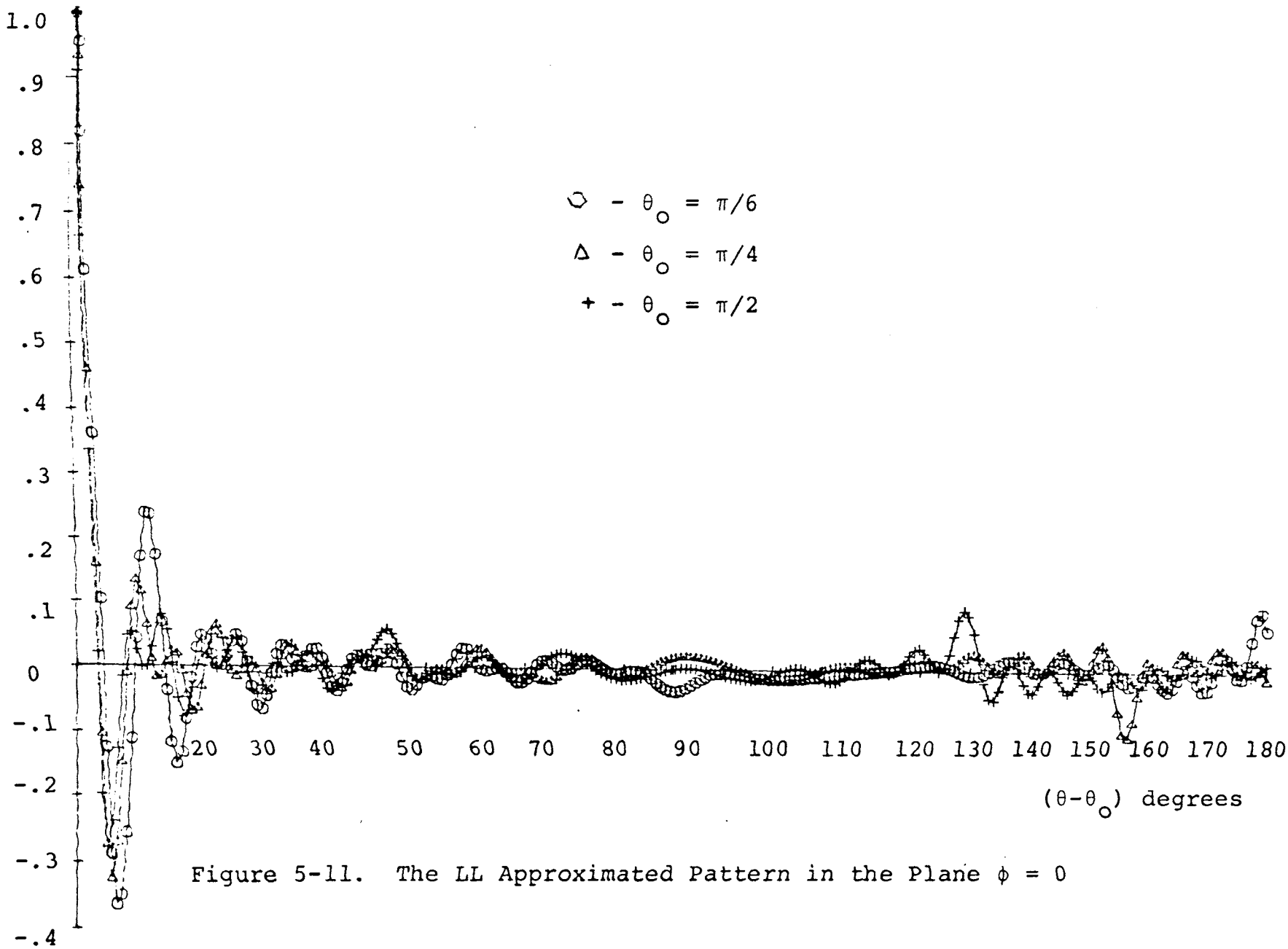

Figure 5-11. The LL Approximated Pattern in the Plane $\phi = 0$

moves from $\pi/6$ to $\pi/3$. The far field pattern of the AES element distribution at various positions of the mainbeam is not shown since it is not a function of the mainbeam position. This has been proven in Chapter IV.

Figures 5-12a, b, and c show the approximated pattern of the LL distribution around the sphere in the plane $\theta = \pi/2$. The purpose here is to investigate the radiation pattern in the region away from the mainbeam. The mainbeam is fixed at $\theta_o = \pi/2 = \phi_o$. Part a shows the pattern in the region 0-120 degrees from the mainbeam axis, part b in the region 120-240 degress and part c 240-360 degrees. Figures 5-13a, b, and c show the same plots for the AES element distribution in the plane $\phi = 0$ with the mainbeam at $\theta_o = 0 = \phi_o$. The approximated pattern for the AES element distribution in the plane $\theta = \pi/2$ with the mainbeam at $\theta_o = \pi/2$ is shown in Figure 5-14.

From these figures, it is observed that there are no high grating lobes in the far field patterns. This indicates that most of the power supplied to the spherical antenna array is in the mainbeam. The highest grating lobe of the far field pattern in the ϕ-plane is 0.0464 (normalized) or -26.67 db for the LL element distribution and 0.0259 (normalized) or -31.734 db for the AES element distribution.

The sidelobe of the LL element distribution is found to be 0.24838 (-12.096 db) in the plane $\theta = \pi/2$. In the $\phi = \pi/2$ plane, the sidelobes are very small while the

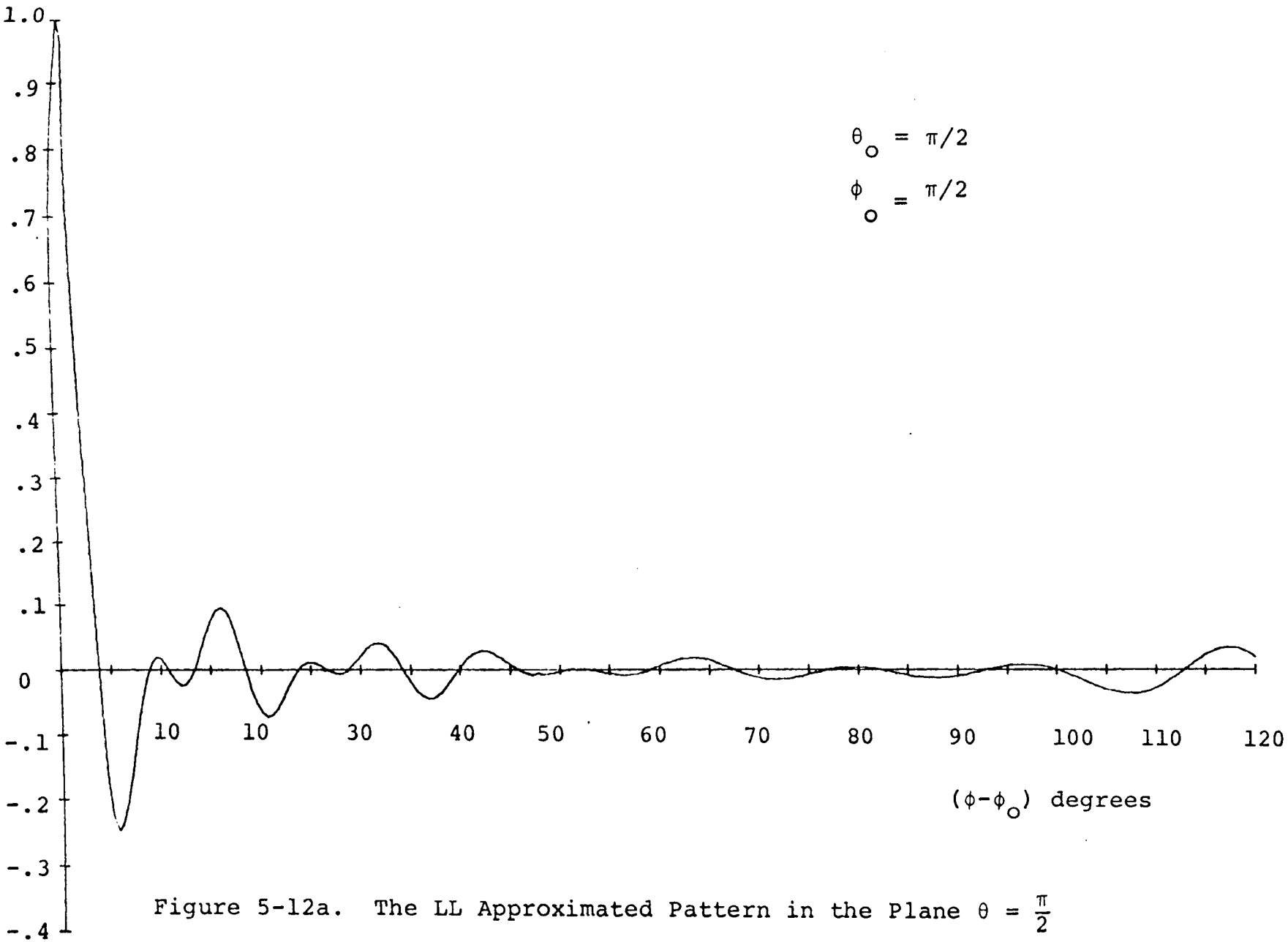

Figure 5-12a. The LL Approximated Pattern in the Plane $\theta = \frac{\pi}{2}$

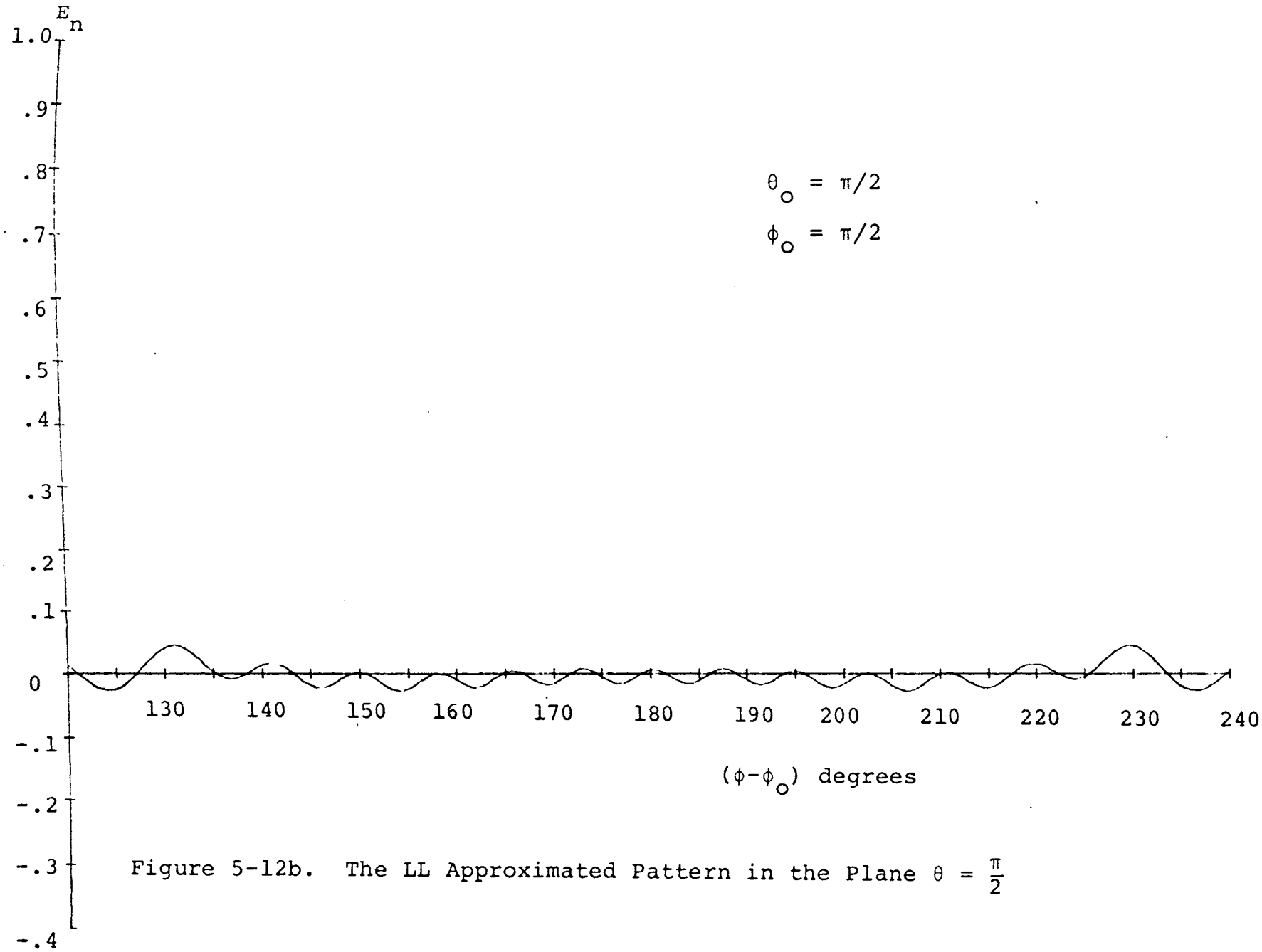

Figure 5-12b. The LL Approximated Pattern in the Plane $\theta = \frac{\pi}{2}$

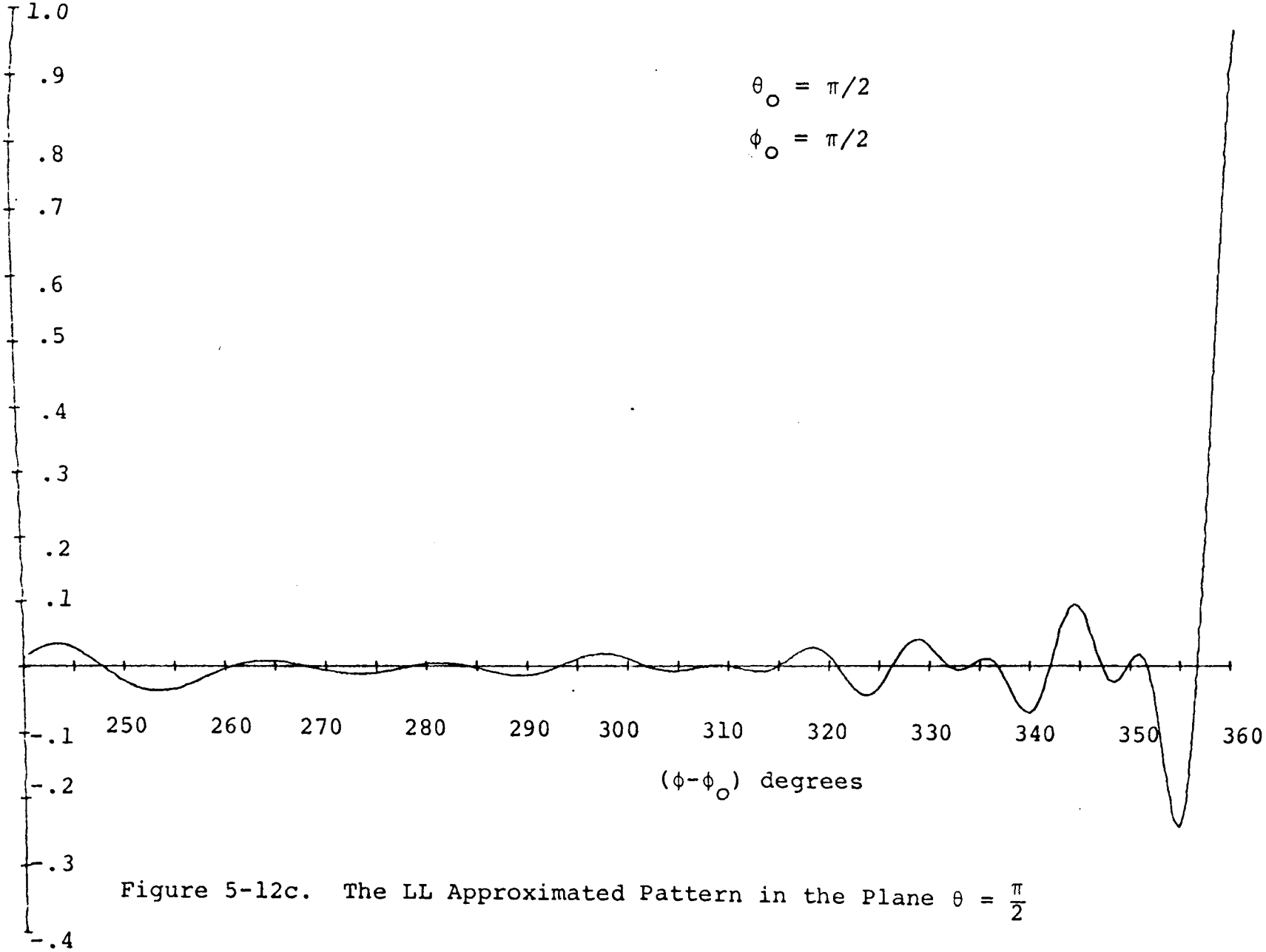

Figure 5-12c. The LL Approximated Pattern in the Plane $\theta = \frac{\pi}{2}$

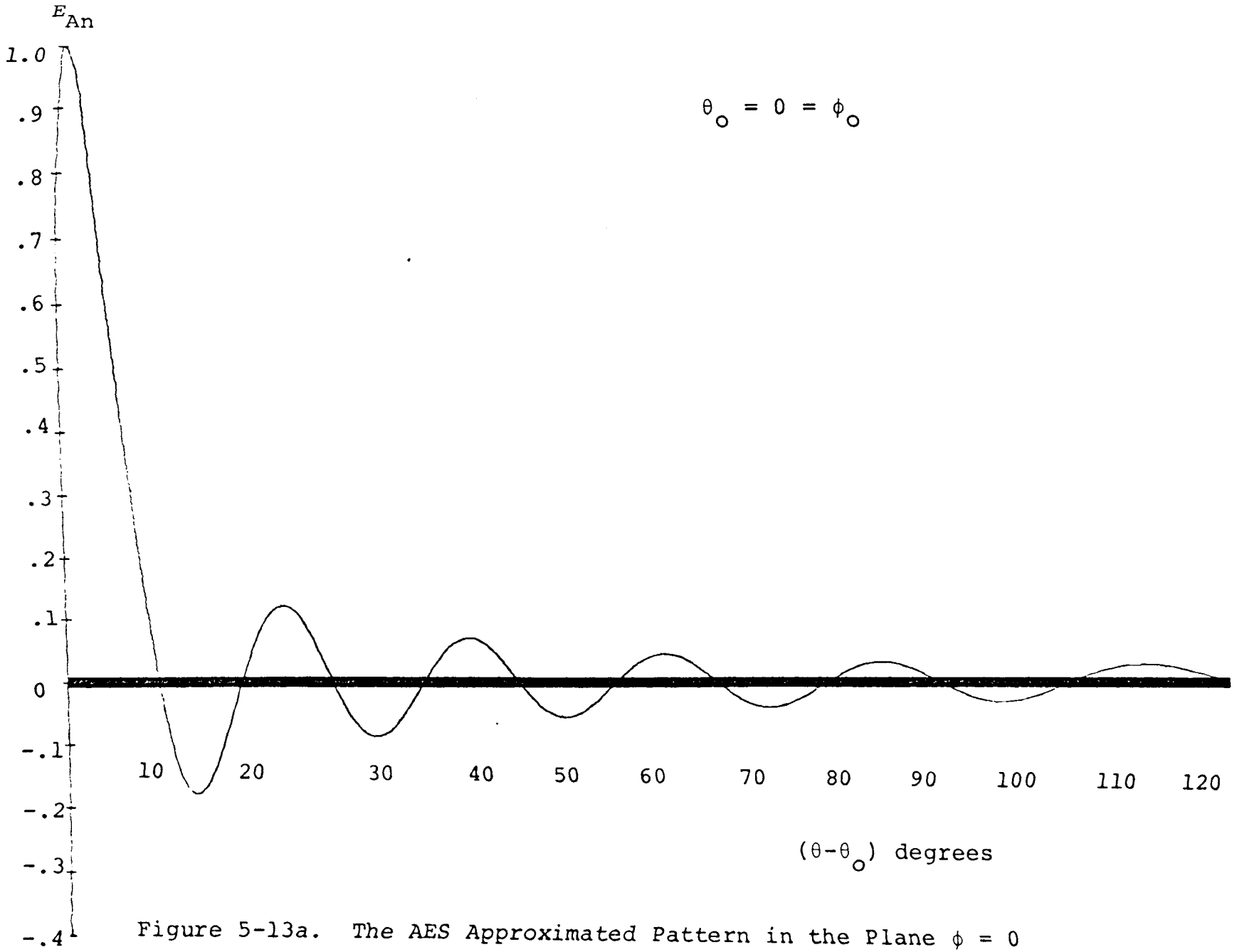

Figure 5-13a. *The AES Approximated Pattern in the Plane* $\phi = 0$

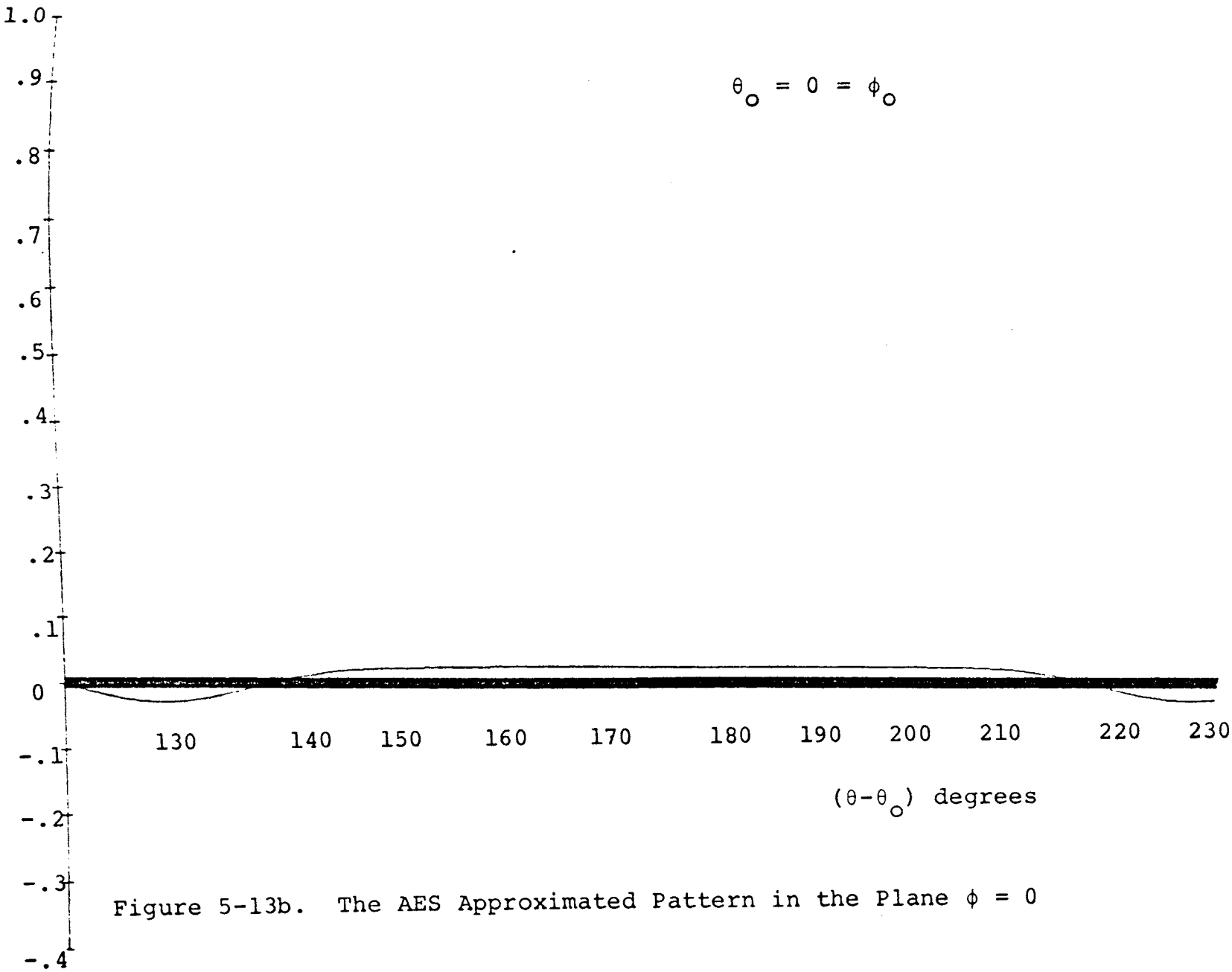

Figure 5-13b. The AES Approximated Pattern in the Plane $\phi = 0$

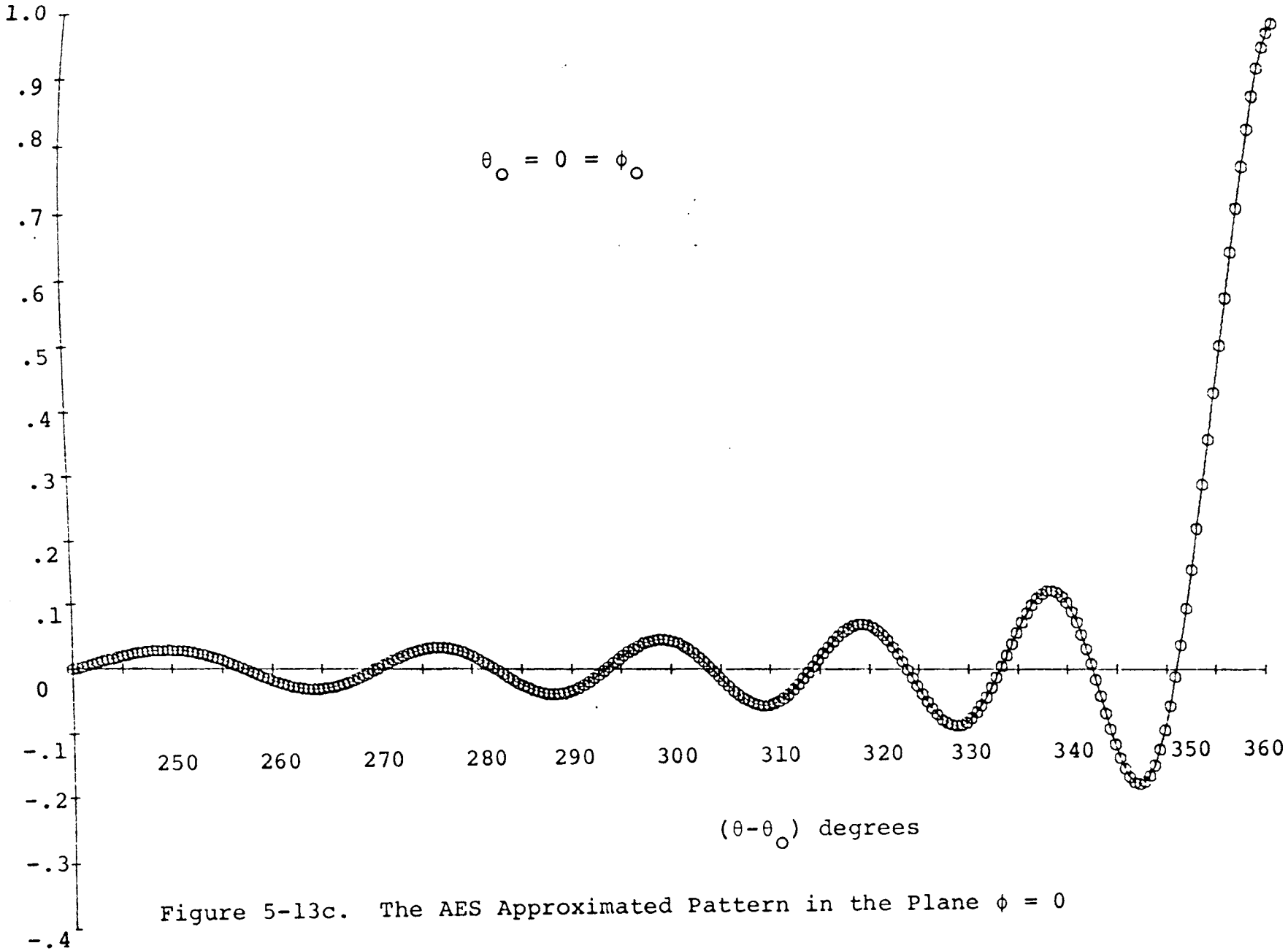

Figure 5-13c. The AES Approximated Pattern in the Plane $\phi = 0$

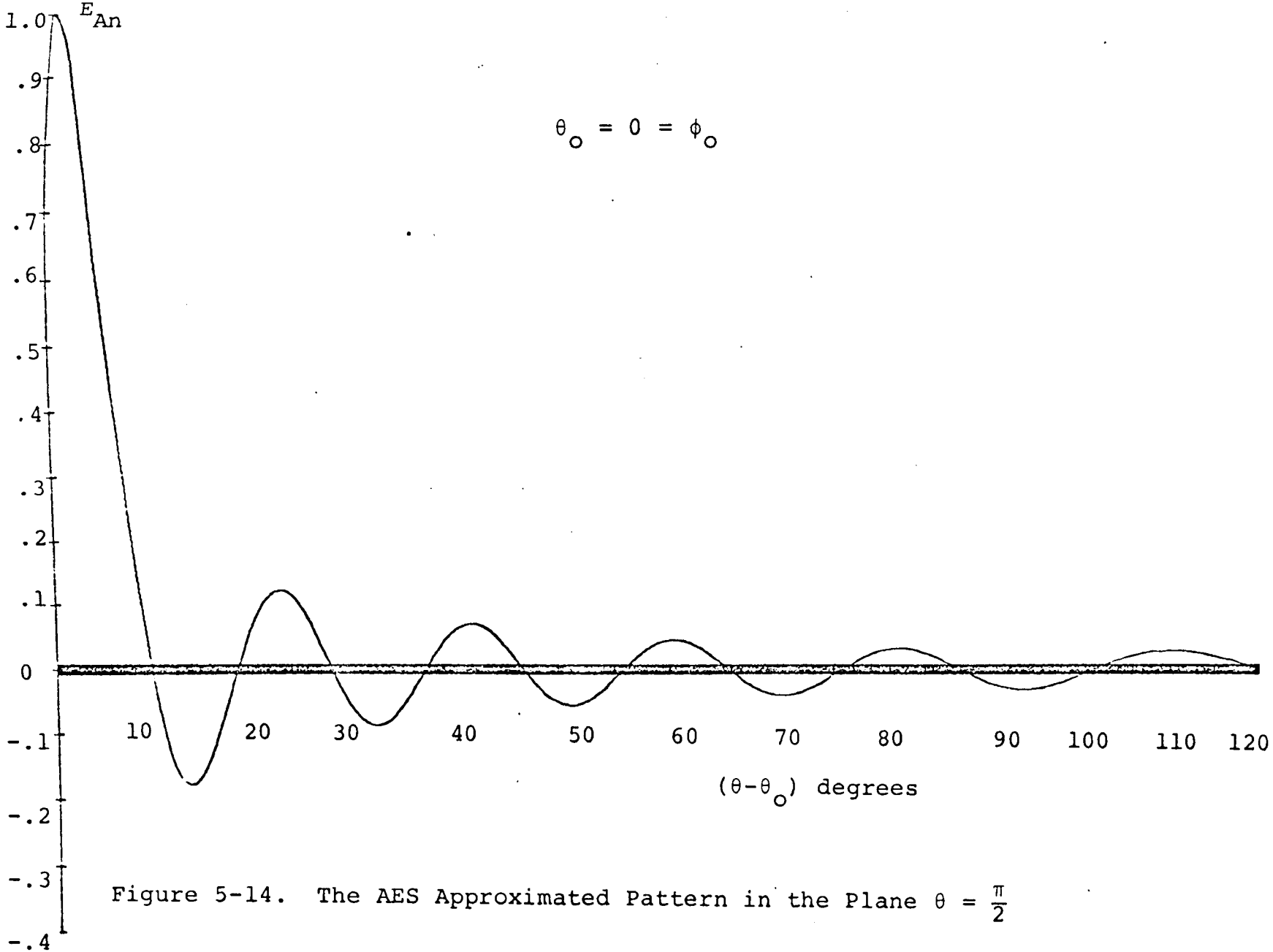

Figure 5-14. The AES Approximated Pattern in the Plane $\theta = \frac{\pi}{2}$

grating lobe increases in magnitude at a point approximately 60 degrees from the mainbeam. Their magnitudes are observed to be 0.06184 (-24.174 db) for the sidelobe and 0.16969 (-15.4020 db) for the maximum grating lobe.

In the far field patterns of the AES element distribution, as shown in Figures 5-13a, b, and c, and 5-14, the patterns in both principal planes are exactly the same. Their sidelobe is 0.1788 (-15.952 db).

From these figures, the general pattern of a spherical antenna array seems to contain a large region of flat grating lobes and, for this study, was found to be symmetrical around the mainbeam. The high grating lobe which appears in the pattern of the LL element distribution in the elevation angle plane occurs because in that particular plane the array contains the characteristic of an edge array which has high grating lobes in its pattern [21]. (It should be noted that the element currents at the poles of the array are N times stronger than that of each individual element.) This high grating lobe does not appear in the AES distribution pattern since the array does not contain such characteristics in any plane.

In order to show the validity of the approximation, the approximated patterns of both element distributions are compared to the true far field pattern. For convenience, the comparison will be made at the mainbeam only. It is made at this point, since here it is easy to find the far

field pattern of the true beam. From Chapter III, the far field pattern at the mainbeam is given by

$$E(\theta_o,\phi_o) = \sum_{m=0}^{M} \sum_{n=1}^{N_m} I_{mn}$$

In this study, I_{mn} is assumed to be uniformly unity. Therefore, the far field pattern is found to be

$$E(\theta_o,\phi_o) = (M + 1)N$$

for the LL element distribution. This is actually the total number of elements in the spherical array. For the AES element distribution, this term can be found by summing all elements in all rings. For the case of M = 20, the total number of elements in the AES element distribution is found to be 510.

Figures 5-15 and 5-16 show the approximated far field pattern and the true far field pattern for various values of M. The former is for the LL element distribution, the latter for the AES element distribution. Both figures show that the approximated far field pattern for large M does not differ from the true far field pattern. The figures also show the invalid range of small M, in which the far field patterns are not accurate for such approximations.

D. Beamwidth

The expressions for the beamwidth as analyzed in Chapter IV are

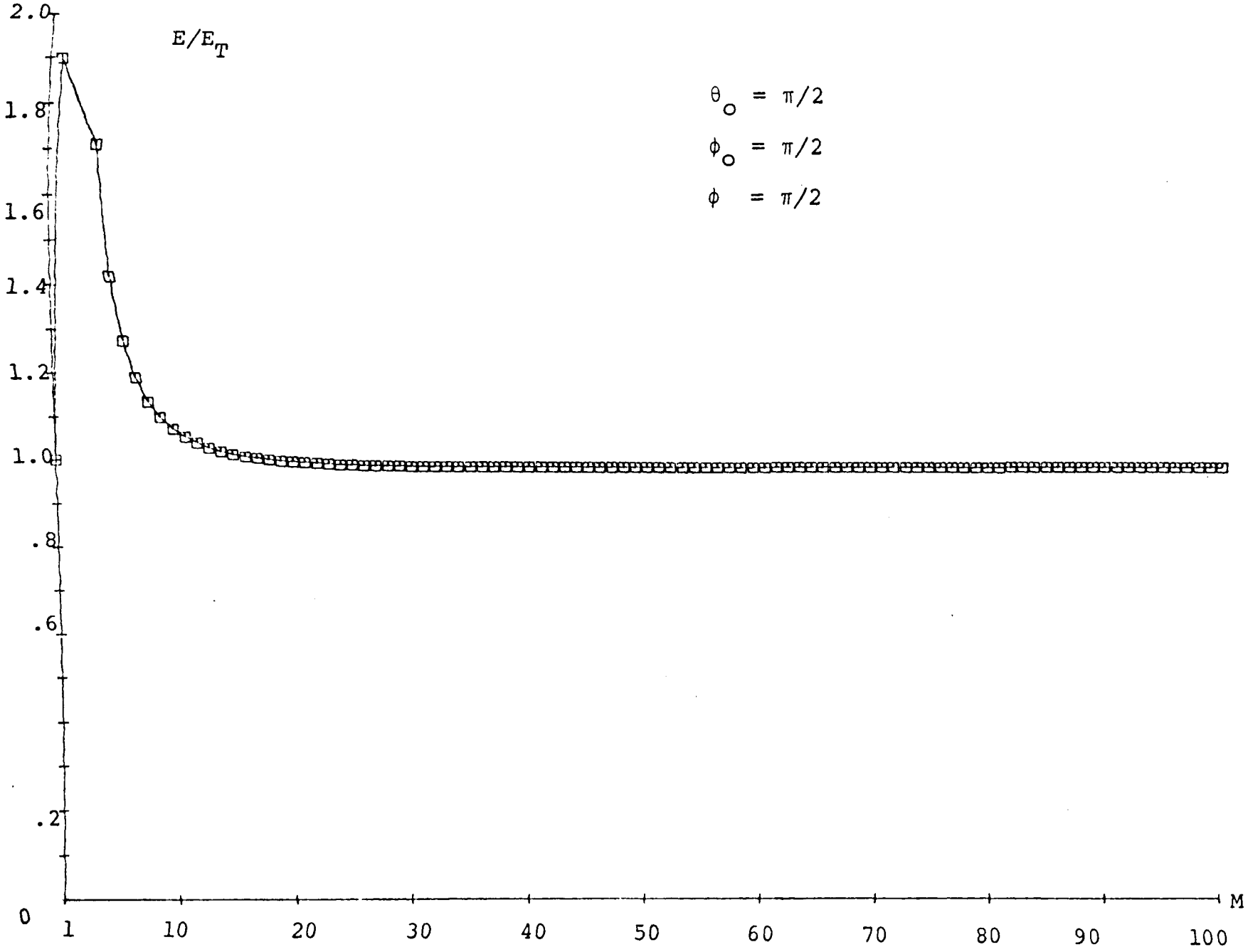

Figure 5-15. Comparison of the LL Approximated Far Field Pattern to the True One

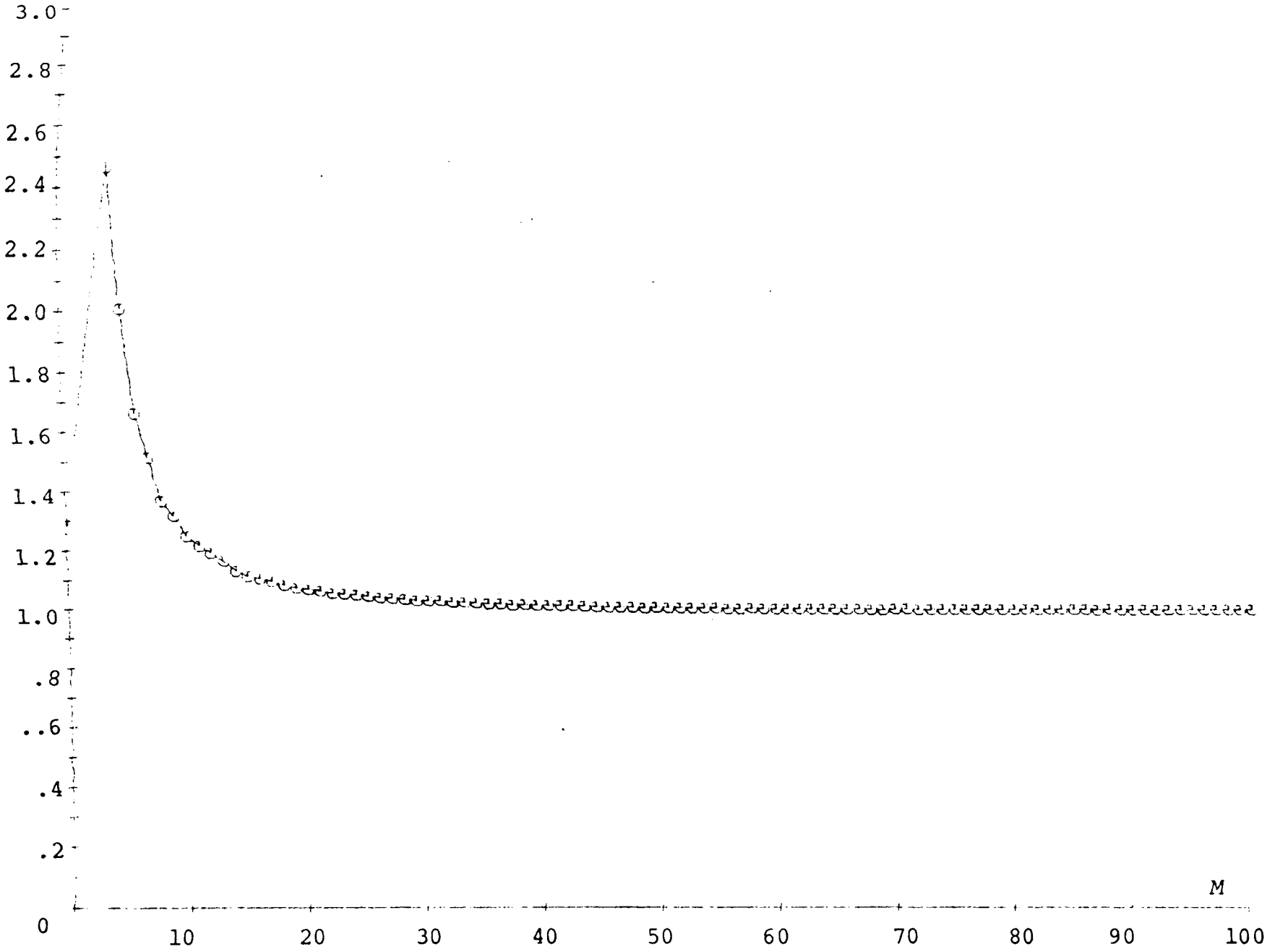

Figure 5-16. Comparison of the AES Approximated Far Field Pattern to the True One at the Main Beam

$$BW = 2 \cos^{-1} \left[1 - \frac{1.17157}{(ka)^2(1 + 4\sin^2\theta_o)}\right]$$

in the elevation angle plane, and

$$BW = 2 \cos^{-1} \left[1 - \frac{1.32795}{(ka)^2}\right]$$

in the azimuth angle plane. Both are for the LL element distribution. The appearance of the spherical array, as seen from a distant point on the mainbeam axis, changes as the mainbeam is scanned along a plane. At $\theta_o = 0$, the spherical array looks like a two-dimensional array with a high element density about the mainbeam axis, but with a gradually thinner density away from this location. This gives rise to the broad beam. On the other hand, at $\theta_o = \pi/2$, the element density is high around the edge of the array but rather thin at the mainbeam axis. This leads to a narrow beamwidth. Between the period of $\pi/2$, the beamwidth varies within these two extremes.

In the azimuth angle plane, however, the beamwidth does not vary with the position of the mainbeam. Thus, the beamwidth of the AES element distribution is independent of θ_o in both planes. This is due to the fact that in these particular planes the spherical arrays look like a uniform array. Therefore, the beamwidth in these planes can not be controlled by positioning the mainbeam. Its width is entirely dependent on the signal frequency used in the spherical array. The beamwidths are found to be

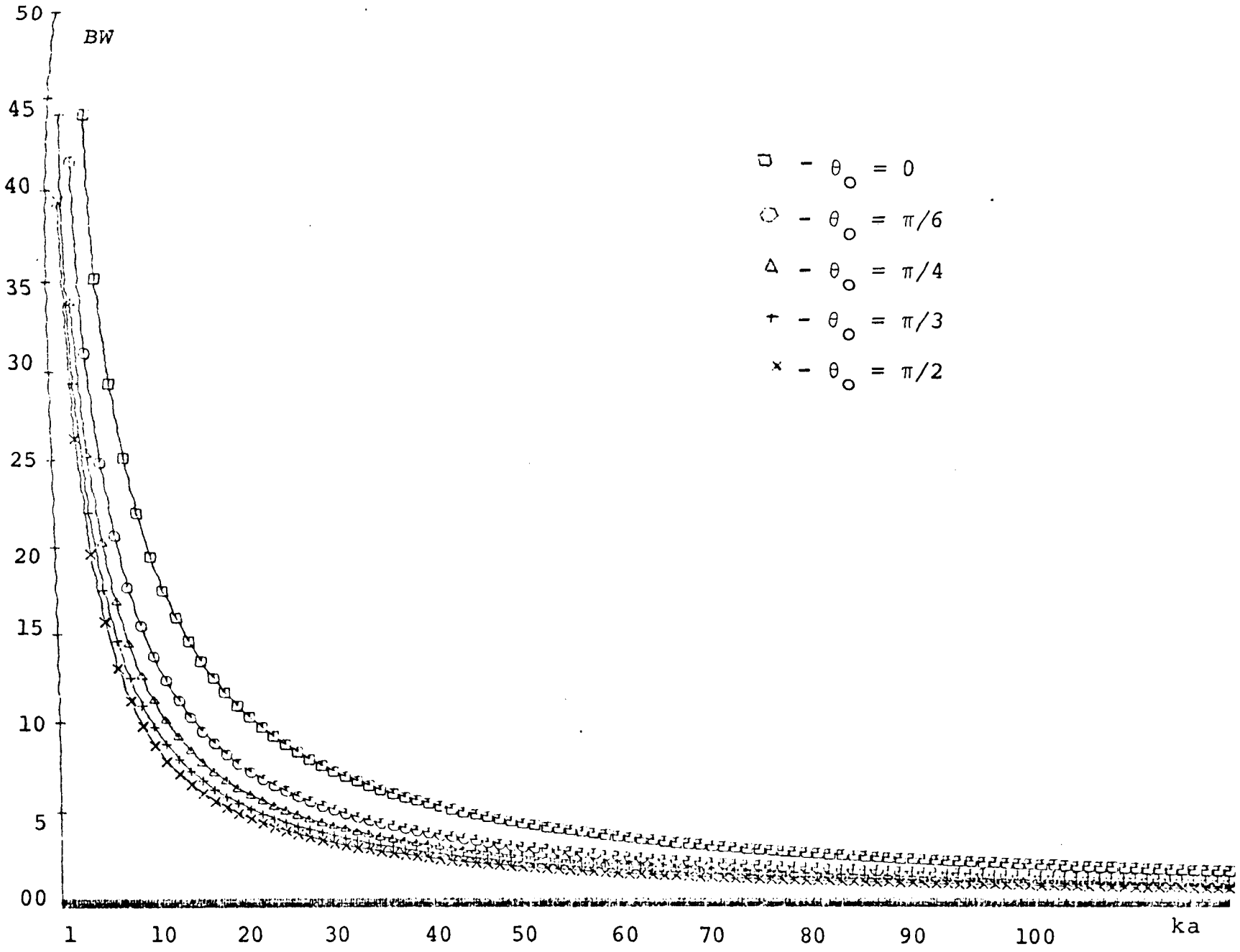

Figure 5-17. The LL Beamwidth as a Function of ka in the Plane of ϕ = Constant

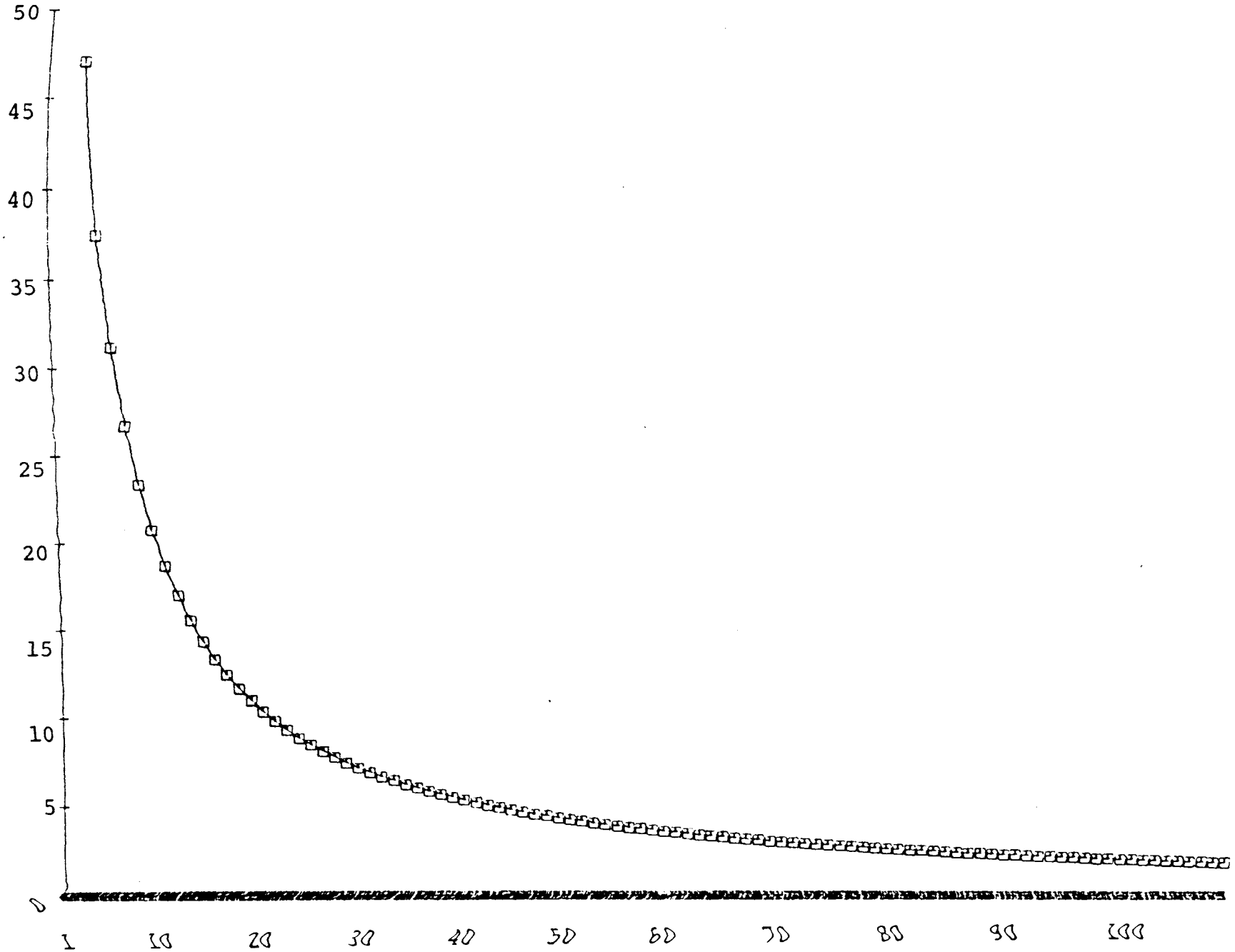

Figure 5-18. The LL Beamwidth as a Function of ka in the Plane $\theta = \frac{\pi}{2}$

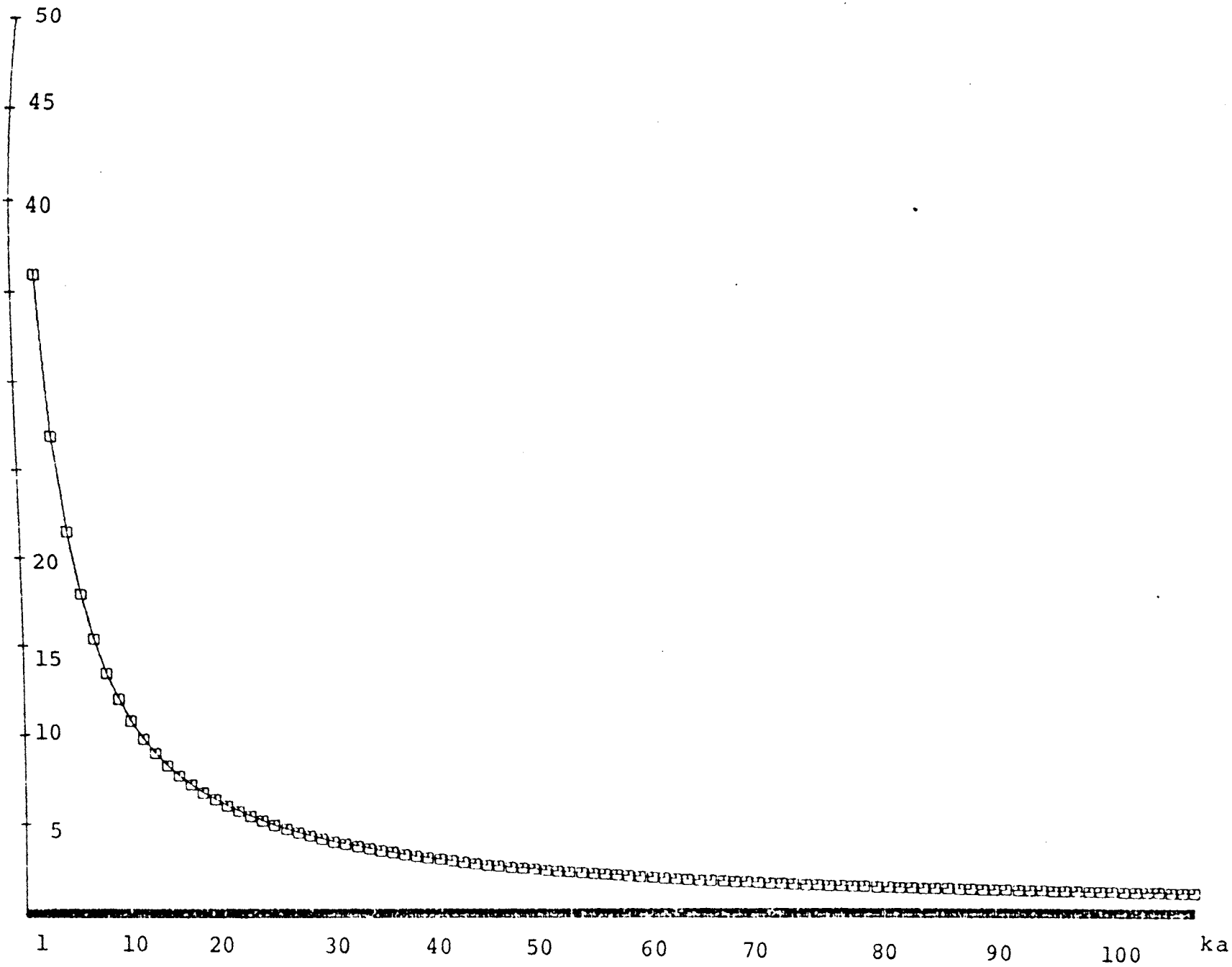

Figure 5-19. The AES Beamwidth as a Function of ka in Both Planes

9.34 degrees for the LL element distribution and 5.3712 degrees for the AES element distribution.

E. The Scanning Property of the Spherical Array

In addition to the details in the beamwidth discussion in the above section, Equations (4-88) and (4-89) for the LL element distribution, and (4-108) for the AES element distribution, show that the pattern of both spherical arrays remain constant with respect to the mainbeam position. This is due to the fact that the radiation pattern varies as a function of the difference of the angles with the mainbeam position as a reference. From these facts, it leads to the conclusion that in the azimuth angle plane, for the LL element distribution, and both planes for the AES element distribution, the spherical array can be scanned in all directions without losing or introducing any pattern changes due to scanning.

For the LL element distribution, in the case of the elevation angle plane, the pattern obviously changes its shape while being scanned. However, comparison between the patterns with $\theta_o = \pi/6$, $\pi/4$, and $\pi/3$ show that the change in sidelobe when the pattern is scanned is very small. Therefore, the introduction of any pattern changes should not be very significant.

CHAPTER VI

CONCLUSIONS AND RECOMMENDATIONS

A. Conclusions

The far field radiation pattern of an isotropic spherical antenna array with two types of element distributions, a latitude-longitude distribution and an approximately equally-spaced distribution, have been theoretically investigated using Poisson's Sum Formula. An approximation was made only for the case of a large number of elements.

The far field radiation pattern results in the form of a convergent infinite series whose harmonic amplitudes are much smaller than the fundamental term when the number of elements is large. In the case of a large number of elements, the far field radiation patterns are given by

$$E(\theta,\phi) = MN\, J_o[ka(\sin\omega - \cos\theta + \cos\theta_o)]J_o[ka(\sin\omega + \cos\theta - \cos\theta_o)]$$

for the latitude-longitude distribution, and

$$E_A(\theta,\phi) = \frac{2aM}{d}\,\frac{\sin(2ka\,\sin\,\omega)}{ka\,\sin\,\omega}$$

for the approximately equally-spaced distribution.

The expressions of beamwidths in various planes were obtained in closed forms. For the latitude-longitude element distribution, they are given by

$$BW = 2 \cos^{-1} \left[1 - \frac{1.17157}{(ka)^2 (1 + 4\sin^2 \theta_o)}\right]$$

in the plane of the elevation angle, and

$$BW = 2 \cos^{-1} \left[1 - \frac{1.32795}{(ka)^2}\right]$$

in the plane of the azimuth angle.

For the approximately equally-spaced element distribution, they are given by

$$BW = 2 \cos^{-1} \left[1 - \frac{0.87868}{(ka)^2}\right]$$

in both planes.

Numerical analysis was performed by selecting arbitrarily the number of rings to be 21 to minimize the computing time and yet to provide good accuracy. Only the first four terms of the far field radiation pattern series were taken into consideration. Better accuracy may be obtained by simply adding more terms of the series. The beamwidth was also analyzed numerically at this number of rings.

The far field radiation patterns of both types of element distributions do not vary with the mainbeam locations except for the case of the latitude-longitude distribution in the elevation angle plane. However, the

pattern change in that plane is very insignificant. Results also show that the radiation patterns contain no large grating lobes. The range of these low grating lobes is rather large, particularly in the region of 50 to 310 degrees.from the mainbeam axis. The sidelobes remain almost constant for a large number of elements while the mainbeams remain very narrow; approximately 5 degrees.

Even though mutual coupling among elements has been neglected, the results of both types of element distributions are practically desirable. The mutual coupling, however, can not be forgotten in practice, especially when the element spacing is less than halfwavelength. This makes the approximately equally-spaced distribution the only one applicable since the average element spacing is halfwavelength.

B. Recommendations

This research covered a spherical array of isotropic point sources since the interest was only in the far field pattern created by a spherical array.

The current distribution of the spherical array was assumed uniform. Nonuniform current distribution would be a very interesting case since another degree of freedom is added to the problem.

The nonuniform element spacing as well as the ring spacing should prove to be of interest for investigation.

With these degrees of freedom, however, the problem could be extremely difficult mathematically. Some special functions might be required in order to solve such a problem.

In addition to these problems, there is a problem of polarization produced by the array of polarized elements. As cited in the literature, Sengupta, et al. [3] worked on the array of circularly polarized elements and concluded that the array of such elements are circularly polarized in all directions if each element is circularly polarized. Wolff [2] worked on a general array of linearly polarized elements. With these reports on two extreme conditions, a question arises, "How does a spherical array change the polarizability of its elements?" Or, to put it in a simpler word, "Can a spherical array improve the polarizability of its elements?"

The author of this paper has performed elementary work on the polarization of a spherical array of a general element distribution of crossed dipoles (see Appendix E). The far field pattern becomes

$$E(\theta,\phi) = \sum_{m,n} C_{mn}(\theta,\phi) e^{j[ka(\psi_{mn}-\Delta_{mn})+(\xi_{mn}-\eta_{mn})]} \qquad (6\text{-}1)$$

where $C_{mn}(\theta,\phi)$ is the complex magnitude which is a function of the spherical coordinates θ and ϕ. If we separate the radiation pattern into two parts, in θ and ϕ directions, we obtain,

$$E(\theta,\phi) = S_\theta \bar{a}_\theta + j\, S_\phi \bar{a}_\phi \quad , \tag{6-2}$$

which is elliptically polarized with the axial ratio

$$AR = \left| \frac{S_\theta}{S_\phi} \right| \quad . \tag{6-3}$$

The general expression of $E(\theta,\phi)$ in Equation (6-1) shows that it is similar to the case of nonuniform current distribution. Therefore, if we could solve the problem of nonuniform element current distribution, the same method should help solving the polarization problem by considering it as an array of a complex element current distribution.

BIBLIOGRAPHY

1. Hoffman, M., "Conventions for the Analysis of Spherical Arrays," IEEE Transactions on Antennas and Propagation, Vol. AP-11, No. 4, July 1963, pp. 390-393.

2. Wolff, E. A., "Antenna Analysis," New York, New York, John Wiley and Sons, inc., 1966, pp. 283-285.

3. Sengupta, D. L., Smith, T. M., and Larson, R. W., "Radiation Characteristics of a Spherical Array of Circularly Polarized Elements," IEEE Transactions on Antennas and Propagation, Vol. AP-16, No. 1, January 1968, pp. 2-7.

4. Ishimaru, A., "Theory of Unequally-Spaced Arrays," IEEE Transactions on Antennas and Propagation, Vol. AP-10, No. 5, November 1962, pp. 691-702.

5. Morse, P. N. and Feshbach, H., "Methods of Theoretical Physics," McGraw-Hill Book Company, New York, New York, 1963, pp. 466.

6. Olmsted, J. M. H., "Advanced Calculus," Appleton-Century-Crofts, Inc., New York, New York, 1961, pp. 69.

7. Watson, G. N., "A Treatise on the Theory of Bessel Functions," McMillan Company, New York, New York, 1945, p. 20.

8. Gradshteyn, I. S. and Ryzhik, I. M., "Table of Integrals, Series, and Products," Academic Press, New York, New York, 1965, p. 757.

9. Sanson, G., Diamond, A. H., and Hill, E., "Orthogonal Functions," Interscience Publishers, Inc., New York, 1959, p. 193.

10. Rainville, E. D., "Special Functions," McMillan Company, New York, 1960, pp. 174-176.

11. See Reference 8, p. 824.

12. See Reference 8, p. 36.

13. Abramowitz, M. and Stegun, I. A., "Handbook of Mathematical Functions with Formulas, Graphs and Mathematical Tables," U.S. Department of Commerce, National Bureau of Standards, AM-55, Washington, D. C., 1966, p. 369.

14. Krause, J. D., "Antennas," McGraw-Hill Book Company, Inc., New York, 1960, pp. 93-95.

15. See Reference 8, p. 737.

16. Knittel, G. H., "Choosing the Number of a Phased Array for Hemispherical Scan Coverage," IEEE Transactions on Antennas and Propagation, Vol. AP-13, November 1965, pp. 878-882.

17. Du, L. J. and Tai, C. T., "Radiation Pattern of Four Symmetrically Located Sources on a Perfectly Conducting Sphere," Ohio State Research Foundation, Columbus, Ohio, Rept. 1961-10, 1964.

18. Silver, S., "Microwave Antenna Theory and Design," Dover Publications, Inc., New York, 1965, p. 264.

19. Conte, S. D., "Elementary Numerical Analysis," McGraw-Hill Book Company, Inc., New York, New York, 1965, pp. 19-26.

20. See Reference 19, pp. 138-143.

21. See Reference 14, p. 94.

22. Yoothanom, N., "Polarization of a Crossed Dipole," Unpublished research, November, 1967.

23. Sengupta, D. L., Ferris, J. E., and Smith, T. M., "Experimental Study of a Spherical Array of Circularly Polarized Elements," Proceedings IEEE, Vol. 56, No. 11, November 1968, pp. 2048-2051.

24. Smith, T. M., "An Approximation of a Spherical Array by a Continuous Field Distribution in a Spherical Aperture," Radiation Lab., University of Michigan Internal Mem., 7577-511-M, 1966.

APPENDIX A

EQUALLY-SPACED SPHERICAL ARRAYS

A. Ring-Type Division

Let a sphere be divided into n equal stripes. The ring of each stripe is also divided into m subintervals whose chord is equal to the distance between two adjacent rings. For convenience, let the rings be in the horizontal position. Figure A-1a and b shows the top view and the cross-sectional front view of such division, respectively. C denotes the length of the chord connecting two adjacent elements and θ the angle subtended by the chord at the center o of the sphere whose radius is denoted by a. In the front view, a perpendicular is drawn from an element to the polar axis and r denotes its length. Let the length of the line connecting this intersection and the center o be z.

Therefore, for the first ring to be considered

$$\theta = \frac{\pi}{n} \tag{A-1}$$

$$r = a \sin \theta \tag{A-2}$$

and

$$Z = a \cos \theta \tag{A-3}$$

Then, the chord length C is found by

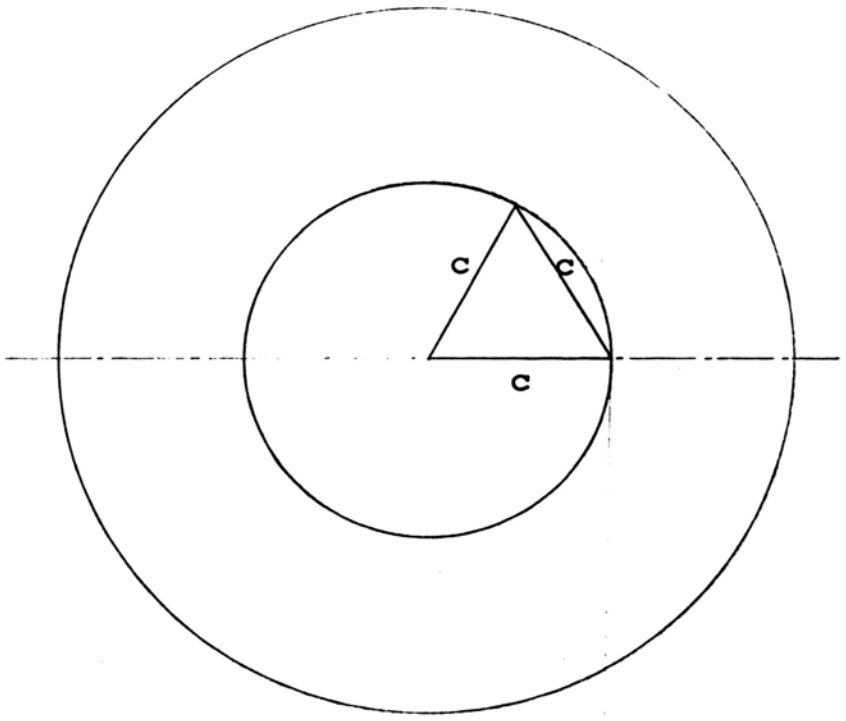

Figure A-1a. Top View

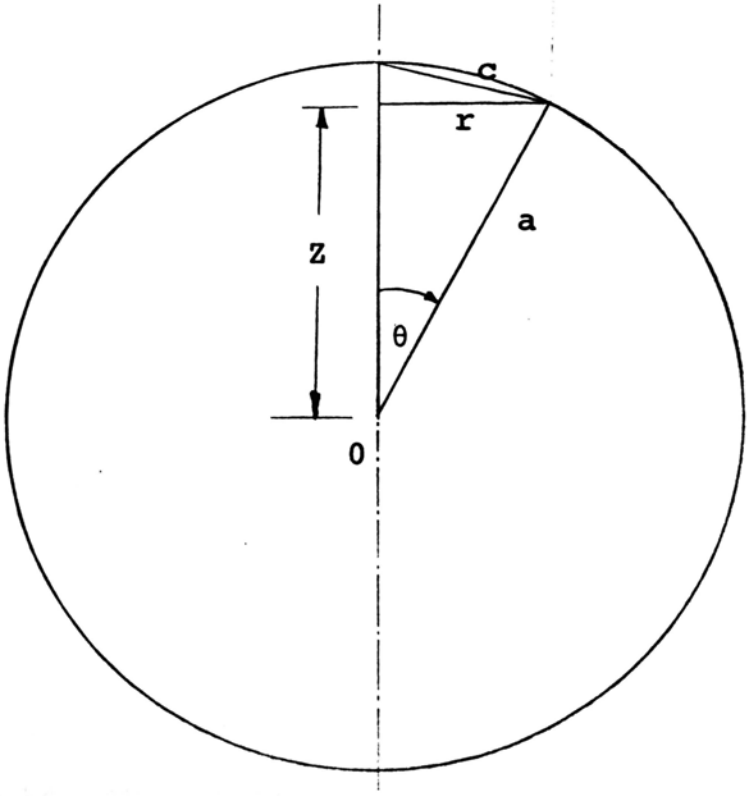

Figure A-1b. Cross-Sectioned Front View

$$C^2 = r^2 + (a - Z)^2$$

$$= 2a^2(1 - \cos \theta)$$

$$= 4a^2 \sin^2 \frac{\theta}{2}$$

Taking the square root of both sides gives

$$C = 2a \sin \frac{\theta}{2} \tag{A-4}$$

where only the positive sign of the square root is taken since C must be positive and $0 \leq \theta \leq \pi$.

Since the ring is also divided into m equal sub-intervals, each of these must subtend the angle of $2\pi/m$ at the polar axis. Figure A-2 shows the cross-sectioned top view of the sphere to show the ring with its radius r. Therefore, from Figure A-2,

$$C = 2r \sin (\frac{\pi}{m}) \tag{A-5}$$

Equating Equation (A-4) to (A-5) with the expression of θ and r from (A-1) and (A-2) gives

$$2a \sin (\frac{\pi}{2n}) = 2a \sin (\frac{\pi}{n}) \cdot (\frac{\pi}{m}) \tag{A-6}$$

Using the trigonometric identity

$$\sin \theta = 2 \sin \frac{\theta}{2} \cos \frac{\theta}{2} \tag{A-7}$$

to reduce Equation (A-6) to

$$1 = 2 \cos (\frac{\pi}{2n}) \sin (\frac{\pi}{m}) \tag{A-8}$$

Since m and n must always be integers, it is evident that Equation (A-8) can not be satisfied for all n except for n = 2. Therefore, the above assumption is firmly contradicted.

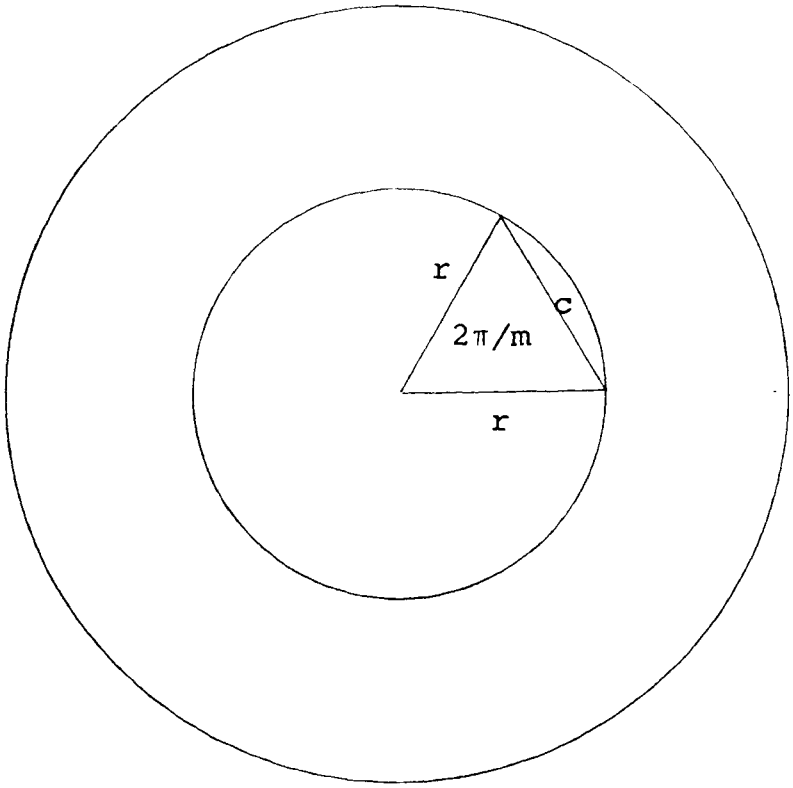

Figure A-2. Cross-Sectioned Top View of the First Ring

B. Polygon-Type Division

In the polygon-type division, the angle θ at the center of the sphere is not restricted to be π over an integer. To distinguish it from the previous θ, let it be called θ_1. Therefore, Figures A-1a, b, and A-2 can still be employed with the replacement of θ by θ_1.

Replacing π/n in Equation (A-8) by θ_1 gives

$$1 = 2 \cos \left(\frac{\theta_1}{2}\right) \sin \left(\frac{\pi}{m}\right) \tag{A-9}$$

or

$$\theta_1 = 2 \cos^{-1} \left[\frac{1}{2 \sin \left(\frac{\pi}{m}\right)}\right] . \tag{A-10}$$

Evaluating θ_1 from Equation (A-10) for each m shows that

$$\begin{aligned} m &= 1 \quad \theta_1 = \text{no solution} \\ m &= 2 \quad \theta_1 = 120° \\ m &= 3 \quad \theta_1 = 109.52° \\ m &= 4 \quad \theta_1 = 90° \\ m &= 5 \quad \theta_1 = 63.42° \\ m &= 6 \quad \theta_1 = 0° \\ m &> 6 \quad \theta_1 = \text{imaginary} \end{aligned} \tag{A-11}$$

For the purpose of a spherical array, the value m = 5 is certainly chosen so that there will be as many elements as possible in the array. This means that the first ring circumscribes a pentagon whose sides are equal to the length of the line connecting the nearest pole to one of its vertices. The same procedure working from another pole

will give its first ring circumscribing another pentagon which is congruent to the first one. Rotate the two pentagons around the polar axis until the connections between their elements form equitriangles. Note that the connections of each pentagon to its corresponding pole already form equitriangles. The final polygon which is obviously circumscribed by the sphere is an icosahedron. The picture of this geometrical structure is shown in Figure 1-1.

APPENDIX B

EVALUATION OF THE ARGUMENTS IN EQUATION (4-45)

It has been given that

$$A = ka(\cos\theta - \cos\theta_o) \tag{B-1}$$

$$B = ka\,\rho \quad . \tag{B-2}$$

Therefore, after substituting the expression of ρ^2 from (3-11),

$$\begin{aligned} A^2 + B^2 &= (ka)^2\{(\cos\theta - \cos\theta_o)^2 + \rho^2\} \\ &= (ka)^2\{\cos^2\theta - 2\cos\theta\cos\theta_o + \cos^2\theta_o - \sin^2\theta \\ &\quad + \sin^2\theta_o - 2\sin\theta\sin\theta_o\cos(\phi - \phi_o) \\ &= 2(ka)^2\{1 - (\cos\theta\cos\theta_o + \sin\theta\sin\theta_o\cos(\phi-\phi_o))\} \end{aligned} \tag{B-3}$$

Defining

$$\cos 2\omega \equiv \cos\theta\cos\theta_o + \sin\theta\sin\theta_o\cos(\phi - \phi_o) \quad . \tag{B-4}$$

Then Equation (B-3) is simplified to

$$\begin{aligned} A^2 + B^2 &= 2(ka)^2(1 - \cos 2\omega) \\ &= 4(ka)^2\sin^2\omega \quad . \end{aligned} \tag{B-5}$$

Hence

$$\sqrt{A^2 + B^2} = 2(ka)\sin\omega \quad . \tag{B-6}$$

Therefore,

$$\frac{1}{2}\sqrt{A^2 + B^2} - A = ka(\sin\omega - \cos\theta + \cos\theta_o) \quad , \quad \text{(B-7)}$$

$$\frac{1}{2}\sqrt{A^2 + B^2} + A = ka(\sin\omega + \cos\theta - \cos\theta_o) \quad \text{(B-8)}$$

APPENDIX C

EVALUATION OF THE COEFFICIENT $A_m(MH)$

Substituting Equation (4-53) into Equation (4-52) gives

$$A_m(MH) = \frac{4m+1}{4}\left\{\frac{2(2MH+1-2m+1)(2MH+1-2m+3)\cdots(2MH+1+2m-1)}{(2MH+1-2m)(2MH+1-2m+2)\cdots(2MH+1+2m)}\right.$$

$$\left. - \frac{2(2MH-1-2m+1)(2MH-1-2m+3)\cdots(2MH-1+2m-1)}{(2MH-1-2m)(2MH-1-2m+2)\cdots(2MH-1+2m)}\right\}$$

$$= \frac{4m+1}{2}\left\{\frac{(2MH-2m+2)(2MH-2m+4)\cdots(2MH+2m)}{(2MH-2m+1)(2MH-2m+4)\cdots(2MH+2m+1)}\right.$$

$$\left. - \frac{(2MH-2M)(2MH-2m+2)\cdots(2MH+2m-2)}{(2MH-2m-1)(2MH-2m+1)\cdots(2MH+2m-1)}\right\} \qquad \text{(C-1)}$$

It has been noted that both terms contain common factors. Factoring them out leaves the last ratio of the first term and the first ratio of the second term.

$$A_m(MH) = \frac{4m+1}{2}\,\frac{(2MH-2m+2)(2MH-2m+4)\cdots(2MH+2m-2)}{(2MH-2m+1)(2MH-2m+4)\cdots(2MH+2m-1)}$$

$$\cdot \left(\frac{2MH+2m}{2MH+2m+1} - \frac{2MH-2m}{2MH-2m-1}\right) \qquad \text{(C-2)}$$

Let us consider at the moment the last factor of Equation (C-2)

$$\frac{2MH+2m}{2MH+2m+1} - \frac{2MH-2m}{2MH-2m-1}$$

$$= \frac{(2MH+2m)(2MH-2m-1)-(2MH-2m)(2MH+2m+1)}{(2MH+2m+1)(2MH-2m-1)}$$

$$= \frac{4(MH)^2+4MHm-4MHm+2MH-4m^2-2m-4(MH)^2+4MHm+2MH-4MHm+4m^2+2m}{(2MH-2m+1)(2MH-2m-1)}$$

$$= \frac{4(MH)}{(2MH+2m+1)(2MH-2m-1)} \qquad (C-3)$$

Then, the final form of the m^{th} coefficient of the Legendre series, $A_m(MH)$, can be written

$$A_m(MH)$$

$$= (4m + 1) \frac{(2MH)(2MH-2m+2)(2MH-2m+4)\cdots(2MH+2m-2)}{(2MH-2m-1)(2MH-2m+1)\cdots(2MH+2m+1)} \qquad (C-4)$$

APPENDIX D

THE CLOSED FORM OF THE PATTERN COEFFICIENT C_1

As defined by Equation (4-61b)

$$C_1 = 2 \sum_{p=1}^{\infty} A_1(pM) \quad . \tag{D-1}$$

From Equation (C-4)

$$A_1(pM) = \frac{5(2pM)(2pM)}{(2pM-3)(2pM-1)(2pM+1)(2pM+3)}$$

$$= \frac{20p^2M^2}{(4p^2M^2-9)(4p^2M^2-1)}$$

$$= 5 \frac{4p^2M^2}{(4p^2M^2 - 9)(4p^2M^2 - 1)}$$

$$= 5\ G(pM) \tag{D-2}$$

where

$$G(pM) \equiv \frac{4p^2M^2}{(4p^2M^2 - 9)(4p^2M^2 - 1)} \tag{D-3}$$

Now setting

$$G(pM) = \frac{A}{4p^2M^2 - 9} + \frac{B}{4p^2M^2 - 1} \tag{D-4}$$

and solving for A and B gives

$$A = (4p^2M^2 - 9)G(pM)\Big|_{4p^2M^2=9}$$

$$= \frac{9}{8}$$

$$B = (4p^2M^2 - 1)G(pM)\Big|_{4p^2M^2=1}$$

$$= -\frac{1}{8}$$

Therefore,

$$A_1(pM) = \frac{5}{8}\left[\frac{9}{4p^2M^2 - 9} - \frac{1}{4p^2M^2 - 1}\right] \qquad \text{(D-5)}$$

and

$$C_1 = \frac{5}{4}\left[\sum_{p=1}^{\infty} \frac{9}{4p^2M^2 - 9} - \sum_{p=1}^{\infty} \frac{1}{4p^2M^2 - 1}\right] \qquad \text{(D-6)}$$

Now applying Equation (4-68) with

$$a = 3 ,$$

$$b = 2M ,$$

for the first series, and

$$a = 1 ,$$

$$b = 2M ,$$

for the second one gives

$$C_1 = \frac{5}{4}\left[\frac{1}{2} - \frac{3\pi}{4M}\cot\left(\frac{3\pi}{2M}\right) - \frac{1}{2} + \frac{\pi}{4M}\cot\left(\frac{\pi}{2M}\right)\right]$$

$$= \frac{5\pi}{16M}\left[\cot\left(\frac{\pi}{2M}\right) - 3\cot\left(\frac{3\pi}{2M}\right)\right] \qquad \text{(D-7)}$$

APPENDIX E

POLARIZABILITY OF A SPHERICAL ANTENNA ARRAY

The complete expression for the far field electric field produced at the far field point $P(r_o, \theta, \phi)$ by a spherical antenna array of identical elements is given by [3]

$$E(\theta,\phi) = \sum_{m,n} E_{mn}(\theta',\phi') e^{j(ka\cos\theta' - \psi_{mn}')} \frac{e^{j(\omega t - kR)}}{R} \tag{E-1}$$

where the primed coordinates indicate the local system of each element as shown in Figure E-1. The primed origin is located at each element, the polar axis z' is along the direction of the pattern minimum of the individual element and the x' axis is taken in the z-z' plane.

$E_{mn}(\theta',\phi')$ is the individual element pattern in primed coordinates, which assumes the general expression of

$$E_{mn}(\theta',\phi') = \bar{e}_{\theta'} f_1(\theta',\phi') + \bar{e}_{\phi'} f_2(\theta',\phi') e^{-j\delta} \tag{E-2}$$

in which f_1 and f_2 are real functions and δ is a constant specifying the state of polarization of the element field pattern, $\bar{e}_{\theta'}$ and $\bar{e}_{\phi'}$ are two unit vectors in the θ' and ϕ' directions, respectively.

It is necessary that the primed coordinates system be transformed into the unprimed coordinate system.

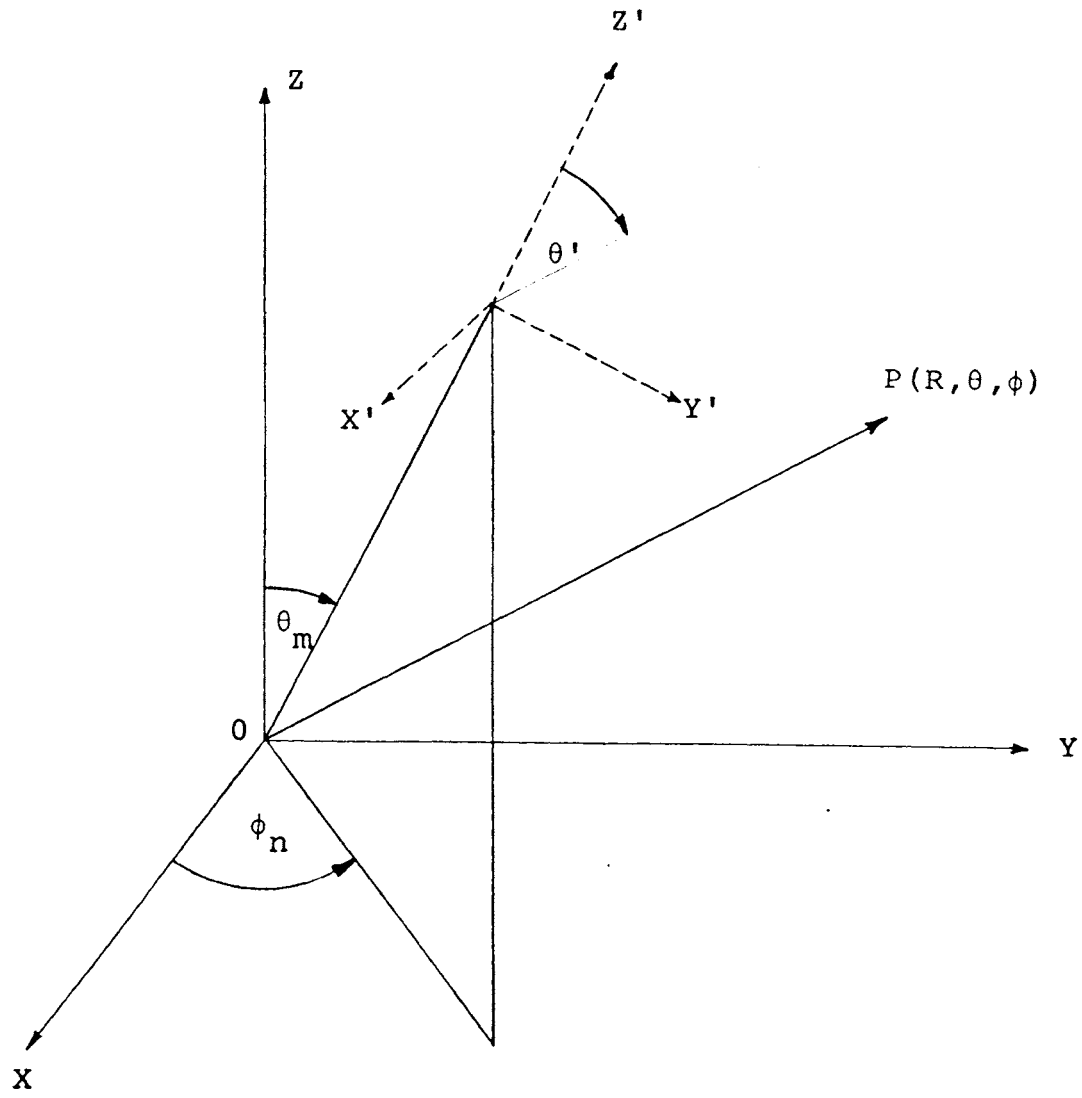

Figure E-1. Illustration of the Local System (x',y',z') in the Main System (x,y,z)

Segupta, et al. [3] have reported the necessary transformation relations as follows:

$$\cos\theta' = \sin\theta_m \sin\theta \cos(\phi - \phi_n) + \cos\theta_m \cos\theta$$

$$\cos\phi' = \frac{\cos\theta_m \sin\theta \cos(\phi - \phi_n) - \sin\theta_m \cos\theta}{\sin\theta \sin(\phi - \phi_n)}$$

$$\bar{e}_{\theta'} = -\frac{\cos\theta \sin\theta_m \cos(\phi - \phi_n) - \sin\theta \cos\theta_m}{\sin\theta'} \bar{e}_\theta + \frac{\sin\theta_m \sin(\phi - \phi_n)}{\sin\theta'} \bar{e}_\phi \qquad \text{(E-3)}$$

$$\bar{e}_{\phi'} = -\frac{\sin\theta_m \sin(\phi - \phi_n)}{\sin\theta'} \bar{e}_\theta - \frac{\cos\theta \sin\theta_m \cos(\phi - \phi_n) - \sin\theta \cos\theta_m}{\sin\theta'} \bar{e}_\phi$$

Let an element of the antenna array be a crossed dipole with 90 degrees out of phase. This element gives the radiation of an elliptical polarization and is given by [22]

$$E_{mn}(\theta',\phi') = \cos\theta'(\cos\phi' + j \sin\phi') \bar{e}_{\theta'} - (\sin\phi' - j \cos\phi') \bar{e}_{\phi'}$$

$$= (\cos\theta' \bar{e}_{\theta'} + j \bar{e}_{\phi'}) e^{j\phi'} \qquad \text{(E-4)}$$

with the axial ratio being

$$AR = |\cos\theta'| \quad . \qquad \text{(E-5)}$$

Substituting Equations (E-3) and (E-4) into (E-1), and after some algebraic manipulation, we have

$$E(\theta,\phi) = \sum_{m,n} [A_{mn}(\theta,\phi) + B_{mn}(\theta,\phi)] e^{j\phi' + j(ka \cos\theta' - \psi_{mn}')} \qquad \text{(E-6)}$$

where

$$A_{mn}(\theta,\phi) = \sin\theta_m \sin(\phi - \phi_n)[\cot\theta' \bar{e}_\phi - \frac{j}{\sin\theta'} \bar{e}_\theta]$$

$$B_{mn}(\theta,\phi) = [\sin\theta \cos\theta_m \cos\theta \sin\theta_m \cos(\phi - \phi_n)]$$

$$\cdot [\cot\theta' \bar{e}_\theta + \frac{j}{\sin\theta'} \bar{e}_\phi]$$

At $\theta = \theta_o$ and $\phi = \phi_o$,

$$E(\theta_o,\phi_o) = \sum_{m,n} [A_{mn}(\theta,\phi) + B_{mn}(\theta,\phi)] \quad .$$

Therefore

$$\phi' + ka\cos\theta' - \psi_{mn}' = 0 \quad ,$$

then

$$\psi_{mn}' = \phi' + ka\cos\theta' \Big|_{\substack{\theta=\theta_o \\ \phi=\phi_o}} \tag{E-7}$$

Let

$$C_{mn}(\theta,\phi) = A_{mn}(\theta,\phi) + B_{mn}(\theta,\phi) \quad ,$$

then

$$E(\theta,\phi) = \sum_{m,n} C_{mn}(\theta,\phi) e^{j(\phi'+ka\cos\theta')-j(\phi'+ka\cos\theta')} \Big|_{\substack{\theta_o \\ \phi_o}}$$

$$= \sum_{m,n} C_{mn}(\theta,\phi) e^{jka[\cos\theta'-\cos'(\theta_o,\phi_o)]+j[\phi'-\phi'(\theta_o,\phi_o)]}$$

$$= \sum_{m,n} C_{mn}(\theta,\phi) e^{jka[\psi_{mn}-\Delta_{mn}]+j[\xi_{mn}-\eta_{mn}]}$$

$$= \sum_{m,n} C_{mn}(\vartheta,\phi) e^{j[ka(\psi_{mn}-\Delta_{mn})+(\xi_{mn}-\eta_{mn})]} \qquad (E-8)$$

where

$$\psi_{mn} = \cos\vartheta\cos\theta_m + \sin\theta\sin\theta_m\cos(\phi-\phi_n)$$

$$\Delta_{mn} = \psi_{mn}(\theta_o,\phi_o)$$

$$\xi_{mn} = \tan^{-1}\left[\frac{\sin\theta\sin(\phi-\phi_n)}{\sin\theta\cos\theta_m\cos(\phi-\phi_n) - \sin\theta_m\cos\theta}\right]$$

$$\eta_{mn} = \xi_{mn}(\theta_o,\phi_o)$$

APPENDIX F

COMPUTER PROGRAMS

```
C       NARONG YOOTHANOM          PHD DISSERTATION
CC      THE SPACING DEVIATIONS IN THE APPROXIMATELY
CC      EQUALLY-SPACED ARRAY.
        DIMENSION  D20(20),D40(40),D60(60),D80(80),D100(100)
        CALL PENPOS ('NARONG YOOTHANOM',16,1)
        READ(1,15) XPOSIN,YPOSIN,TZERO,YZERO,TMIN,TMAX
       1,YMIN,YMAX,DT,DY
     15 FORMAT(10F6.1)
        CALL NEWPLT(XPOSIN,YPOSIN,10.0)
        CALL ORIGIN(TZERO,YZERO)
        CALL TSCALE(TMIN,TMAX,8.0)
        CALL YSCALE(YMIN,YMAX,6.0)
        CALL TAXIS(DT)
        CALL YAXIS(DY)
        PI = 3.14159
     10 DO 500 M=20,100,20
        K = M-1
        DO 700 I=1,K
        RNM = 2.*M*SIN(I*PI/M)
        NM = RNM+0.5
        RATIO = RNM/NM
        DEVIA = (RATIO-1)*100.
     30 IF(M-20) 10,20,40
     20 D20(I) = DEVIA
        GO TO 700
     40 IF(M-40) 30,50,60
     50 D40(I) = DEVIA
        GO TO 700
     60 IF(M-60) 40,70,80
     70 D60(I) = DEVIA
        GO TO 700
     80 IF(M-80) 60,90,100
     90 D80(I) = DEVIA
        GO TO 700
    100 IF(M-100) 80,110,120
    110 D100(I) = DEVIA
    700 CONTINUE
    500 CONTINUE
    120 CALL TPLT(D20,19,1,1)
        CALL TPLT(D40,39,1,2)
        CALL TPLT(D60,59,1,3)
        CALL TPLT(D80,79,1,4)
        CALL TPLT(D100,99,1,5)
        CALL SYM(4.0,2.0,0.14,'DEVIA',0.0,5)
        CALL ENDPLT
        CALL LSTPLT
        CALL EXIT
        END
```

```
CC     NARONG YOOTHANOM        PHD DISSERTATION
CC       THE HARMONIC COEFFICIENTS AS A FUNCTION OF M.
       DIMENSION  CC(100),C1(100),C2(100),C3(100)
       PI = 3.14159
       DO 500 M=1,100
       CC(M) =  2.-(PI/(2.*M))*COTAN(PI/(2.*M))
       C1(M) =  5.*PI*(COTAN(PI/(2.*M))-3.*COTAN(3.*PI/
      1(2.*M)))/(16.*M)
       C2(M) =  9.*PI*(COTAN(PI/(2.*M))+7.5*COTAN(3.*PI/
      1(2.*M))-17.5*COTAN(5.*PI/(2.*M)))/(128.*M)
  500 C3(M) =  (13*PI/(2048.*M))*(5.*COTAN(PI/(2.*M))+
      121.*COTAN(3.*PI/(2.*M))+105.*COTAN(5.*PI/(2.*M))
      2-231.*COTAN(7.*PI/(2.*M)))
       CALL TPLT(CC,100,1,0)
       CALL TPLT(C1,100,1,1)
       CALL TPLT(C2,100,1,2)
       CALL TPLT(C3,100,1,3)
       CALL ENDPLT
       CALL LSTPLT
       CALL EXIT
       END
```

```
C       NARONG YOOTHANOM          PHD DISSERTATION
CC      THE FIRST FEW PATTERN HARMONICS AS A FUNCTION OF M.
        DIMENSION  TERM(50),Y(30),PATT(300),PHO(300)
       1,PH1(300),PH2(300),PH3(300)
        F1(T) = COS((T+1.)*A/2.)
        F(T) = F1(T)*F2*F3
        CALL PENPOS ('NARONG YOOTHANOM',16,1)
        READ(1,10) XPOSIN,YPOSIN,TZERO,YZERO,TMIN,TMAX,
       1YMIN,YMAX,DT,DY
    10 FORMAT(10F6.1)
        CALL NEWPLT(XPOSIN,YPOSIN,10.0)
        CALL ORIGIN(TZERO,YZERO)
        CALL TSCALE(TMIN,TMAX,8.0)
        CALL YSCALE(YMIN,YMAX,6.0)
        CALL TAXIS(DT)
        CALL YAXIS(DY)
        PI = 3.14159
        THETAO = PI/2.
        PHIO = 0.
        PHI = PHIO
        THETA = PI/2.
        KA = 20
        DO 70 M=1,100
        A = KA*(COS(THETA)-COS(THETAO))
        RHO = SQRT(SIN(THETA)**2+SIN(THETAO)**2-2.*SIN
       1(THETA)*SIN(THETAO)*COS(PHI-PHIO))
        B = KA*RHO
        C0 = 2.-(PI/(2.*M))*COTAN(PI/(2.*M))
        C1 = 5.*PI*(COTAN(PI/(2.*M))-3.*COTAN(3.*PI/(2.*M)
       1))/(16.*M)
        C2 = 9.*PI*(COTAN(PI/(2.*M))+7.5*COTAN(3.*PI/(2.*M)
       1)-17.5*COTAN(5.*PI/(2.*M)))/(128.*M)
        C3= (13*PI/(2048.*M))*(5.*COTAN(PI/(2.*M))+21.*
       1COTAN(3.*PI/(2.*M))+105.*COTAN(5.*PI/(2.*M))-231.
       2*COTAN(7.*PI/(2.*M)))
        AAA= SQRT(A**2+B**2)
        IF(AAA) 3,4,3
     3  TIO = 2.*SIN(AAA)/AAA
        GO TO 5
     4  TIO = 2.
     5  T0 = -0.90617985
        T1 = -0.53846931
        T2 = 0.0
        T3 = -T1
        T4 = -T0
        A0 = 0.23692689
        A1 = 0.47862867
        A2 = 0.56888888
        A3 = A1
        A4 = A0
        DO 50 L=1,3
    72  T = T0
    60  BA = ABS(B*SQRT(3.-2.*T-T**2)/2.)+0.00005
        CALL BESJ(BA,0,F2,0.00005,0)
```

```
      X = (T+1.)/2.
      K = 2*L
      CALL LEP(Y,X,K+1)
      F3 = Y(K+1)
      IF(T-T0)72,73,74
   73 T = T1
      GO TO 60
   74 IF(T-T1)73,81,82
   81 T=T2
      GO TO 60
   82 IF(T-T2) 81,90,91
   90 T=T3
      GO TO 60
   91 IF(T-T3) 90,94,95
   94 T=T4
      GO TO 60
   95 TERM(L)=( A0*F(T0)+A1*F(T1)+A2*F(T2)+A3*F(T3)+A4*
     1F(T4))*2.
   50 CONTINUE
      PATT(M) = C0*TI0+C1*TERM(1)+C2*TERM(2)+C3*TERM(3)
      PH0(M) = C0*TI0/PATT(M)
      PH1(M) = C1*TERM(1)/PATT(M)
      PH2(M) = C2*TERM(2)/PATT(M)
      PH3(M) = C3*TERM(3)/PATT(M)
      AA = PH0(M)
      BB = PH1(M)
      CC = PH2(M)
      DD = PH3(M)
      DI = 180.*PHI/PI
      WRITE(3,100)DI,AA,BB,CC,DD
  100 FORMAT(5F20.4)
   70 CONTINUE
      CALL TPLT(PH3,100,1,3)
      CALL TPLT(PH2,100,1,2)
      CALL TPLT(PH1,100,1,1)
      CALL TPLT(PH0,100,1,0)
      CALL SYM(3.0,4.0,.14,'AES-3',0.0,5)
      CALL ENDPLT
      CALL LSTPLT
      CALL EXIT
      END
```

```
C       NARONG YOOTHANOM              PHD DISSERTATION
CC      THE LL APPROXIMATED PATTERN ON THE PLANE OF THE
CC      ELEVATION ANGLE WITH VARIOUS POSITIONS OF THE
CCC     MAINBEAMS.
C       TWO DIMENSIONAL PLOT
        DIMENSION TERM(50),Y(30),PATT(400),PATTN(400),
       1PATTN1(300),PATTN2(300),PATTN3(300)
        F1(T) = COS((T+1.)*A/2.)
        F4(T) = SQRT(3.-2.*T-T**2)/2.
        F(T) = F1(T)*F2*F3/F4(T)
        CALL PENPOS ('NARONG YOOTHANOM',16,1)
        READ(1,10) XPOSIN,YPOSIN,TZERO,YZERO,TMIN,TMAX,
       1YMIN,YMAX,DT,DY
    10 FORMAT(10F6.1)
        CALL NEWPLT(XPOSIN,YPOSIN,10.0)
        CALL ORIGIN(TZERO,YZERO)
        CALL TSCALE(TMIN,TMAX,8.0)
        CALL YSCALE(YMIN,YMAX,6.0)
        CALL TAXIS(DT)
        CALL YAXIS(DY)
        PI = 3.14159
        THETA0 = PI/6.
        PHI0 =0.
        THETAX = PI/180.
        PHI = 0.
        DO 20 J=1,3
        THETA = THETA0
        M=20
        N = 2*M
        KA = 0.628*N
        DO 70 I=1,240
        A = KA*(COS(THETA)-COS(THETA0))
        RHO = SQRT(SIN(THETA)**2+SIN(THETA0)**2-2.*SIN
       1(THETA)*SIN(THETA0)*COS(PHI-PHI0))
        B = KA*RHO
        C0 = 2.-(PI/(2.*M))*COTAN(PI/(2.*M))
        C1 = 5.*PI*(COTAN(PI/(2.*M))-3.*COTAN(3.*PI/(2.*M)
       1))/(16.*M)
        C2 = 9.*PI*(COTAN(PI/(2.*M))+7.5*COTAN(3.*PI/(2.*M)
       1)-17.5*COTAN(5.*PI/(2.*M)))/(128.*M)
        C3= (13*PI/(2048.*M))*(5.*COTAN(PI/(2.*M))+21.*COTAN
       1(3.*PI/(2.*M))+105.*COTAN(5.*PI/(2.*M))-231.*COTAN
       2(7.*PI/(2.*M)))
        Z1 = ABS(0.5*SQRT(A**2+B**2)-A) +0.00005
        Z2 = ABS(0.5*SQRT(A**2+B**2)+A) +0.00005
        CALL BESJ(Z1,0,BES10,0.00005,0)
        CALL BESJ(Z2,0,BES20,0.00005,0)
        TI0 = PI*BES10*BES20
        T0 = -0.90617985
        T1 = -0.53846931
        T2 = 0.
        T4 = -T0
        T3 = -T1
        A0 = 0.23692689
```

```
      A1 = 0.47862867
      A2 = 0.568888888
      A3 = A1
      A4 = A0
      DO 250 L = 1,3
   72 T = T0
   60 BA = ABS(B*SQRT(3.-2.*T-T**2)/2.)+0.00005
      CALL BESJ(BA,0,F2,0.00005,0)
      X = (T+1.)/2.
      K = 2*L
      CALL LEP(Y,X,K+1)
      F3 = Y(K+1)
      IF(T-T0)72,73,74
   73 T = T1
      GO TO 60
   74 IF(T-T1)73,81,82
   81 T = T2
      GO TO 60
   82 IF(T-T2)81,90,91
   90 T = T3
      GO TO 60
   91 IF(T-T3)90,94,95
   94 T = T4
      GO TO 60
   95 TERM(L) = 2.*(A0*F(T0)+A1*F(T1)+A2*F(T2)+A3*F(T3)
     1+A4*F(T4))
  250 CONTINUE
      PATT(I) = M*N*(C0*T10+C1*TERM(1)+C2*TERM(2)+C3*
     1TERM(3))/PI
      PATTN(I) = PATT(I)/PATT(1)
   25 IF(THETA0-PI/6.) 30,30,40
   30 PATTN1(I) = PATTN(I)
      GO TO 70
   40 IF(THETA0-PI/4.) 25,50,61
   50 PATTN2(I) = PATTN(I)
      GO TO 70
   61 IF(THETA0-PI/3.) 40,65,75
   65 PATTN3(I) = PATTN(I)
   70 THETA = THETA+THETAX
   20 THETA0 = THETA0+PI/12.
   75 CALL TPLT(PATTN1,240,1,1)
      CALL TPLT(PATTN2,240,1,2)
      CALL TPLT(PATTN3,240,1,3)
      CALL SYM(4.0,4.0,0.14,'LL-12',0.0,5)
      CALL ENDPLT
      CALL LSTPLT
      CALL EXIT
```

```
C      NAPONG YOOTHANOM          PHD DISSERTATION
CC     COMPARISON OF THE FIRST FEW PATTERN HARMONICS AS
CC     A FUNCTION OF THE SPACE COORDINATES.
       DIMENSION  TERM(50),Y(30),PATT(300),PHC(300)
      1,PH1(300),PH2(300),PH3(300)
       F1(T) = COS((T+1.)*A/2.)
       F4(T) = SQRT(3.-2.*T-T**2)/2.
       F(T) = F1(T)*F2*F3 /F4(T)
       CALL PENPOS ('NAPONG YOOTHANOM',16,1)
       READ(1,10) XPOSIN,YPOSIN,TZERO,YZERO,TMIN,TMAX,
      1YMIN,YMAX,DT,DY
    10 FORMAT(10F6.1)
       CALL NEWPLT(XPOSIN,YPOSIN,10.0)
       CALL ORIGIN(TZERO,YZERO)
       CALL TSCALE(TMIN,TMAX,8.0)
       CALL YSCALE(YMIN,YMAX,6.0)
       CALL TAXIS(DT)
       CALL YAXIS(DY)
       PI = 3.14159
       THETA0 = PI/2.
       PHI0 = 0.
       THETA = PI/2.
       PHI = PHI0
       PHIX = PI/180.
       M = 20
       DO 700 I=1,180
       N = 2*M
       KA = 0.628*N
       A = KA*(COS(THETA)-COS(THETA0))
       RHO = SQRT(SIN(THETA)**2+SIN(THETA0)**2-2.*SIN
      1(THETA)*SIN(THETA0)*COS(PHI-PHI0))
       B = KA*RHO
       C0 = 2.-(PI/(2.*M))*COTAN(PI/(2.*M))
       C1 = 5.*PI*(COTAN(PI/(2.*M))-3.*COTAN(3.*PI/(2.*M)
      1))/(16.*M)
       C2 = 9.*PI*(COTAN(PI/(2.*M))+7.5*COTAN(3.*PI/(2.*M)
      1)-17.5*COTAN(5.*PI/(2.*M)))/(128.*M)
       C3= (13*PI/(2048.*M))*(5.*COTAN(PI/(2.*M))+21.*
      1COTAN(3.*PI/(2.*M))+105.*COTAN(5.*PI/(2.*M))-231.
      2*COTAN(7.*PI/(2.*M)))
       Z1 = ABS(0.5*SQRT(A**2+B**2)-A)+0.00005
       Z2 = ABS(0.5*SQRT(A**2+B**2)+A)+0.00005
       CALL BESJ(Z1,0,BES10,0.00005,0)
       CALL BESJ(Z2,0,BES20,0.00005,0)
       TI0 = PI*BES10*BES20
     5 T0 = -0.90617985
       T1 = -0.53846931
       T2 = 0.0
       T3 = -T1
       T4 = -T0
       A0 = 0.23692689
       A1 = 0.47862867
       A2 = 0.56888888
       A3 = A1
```

```
      A4 = AC
      DO 50 L=1,3
   72 T = T0
   60 BA = ABS(B*SQRT(3.-2.*T-T**2)/2.)+0.00005
      CALL BESJ(BA,C,F2,0.00005,0)
      X = (T+1.)/2.
      K = 2*L
      CALL LEP(Y,X,K+1)
      F3 = Y(K+1)
      IF(T-T0)72,73,74
   73 T = T1
      GO TO 60
   74 IF(T-T1)73,81,82
   81 T=T2
      GO TO 60
   82 IF(T-T2) 81,90,91
   90 T=T3
      GO TO 60
   91 IF(T-T3) 90,94,95
   94 T=T4
      GO TO 60
   95 TERM(L)=( AC*F(T0)+A1*F(T1)+A2*F(T2)+A3*F(T3)+A4*
     1F(T4))*2.
   50 CONTINUE
      PATT(I) = C0*TI0+C1*TERM(1)+C2*TERM(2)+C3*TERM(3)
      PH0(I) = C0*TI0/PATT(I)
      PH1(I) = C1*TERM(1)/PATT(I)
      PH2(I) = C2*TERM(2)/PATT(I)
      PH3(I) = C3*TERM(3)/PATT(I)
      AA = PH0(I)
      BB = PH1(I)
      CC = PH2(I)
      DD = PH3(I)
      DI = 180.*PHI/PI
      WRITE(3,100)DI,AA,BB,CC,DD
  100 FORMAT(5F20.4)
  700 PHI = PHI+PHIX
      CALL TPLT(PH0,100,1,0)
      CALL TPLT(PH1,100,1,1)
      CALL TPLT(PH2,100,1,2)
      CALL TPLT(PH3,100,1,3)
      CALL SYM(3.0,4.0,.14,'LLL-4',0.0,5)
      CALL ENDPLT
      CALL LSTPLT
      CALL EXIT
      END
//
```

```
C       NARONG YOOTHANOM            PHD DISSERTATION
        DIMENSION  TERM(50),Y(30),PATT(300),PATTN(300)
        F1(T) = COS((T+1.)*A/2.)
        F(T) = F1(T)*F2*F3
        CALL PENPOS ('NARONG YOOTHANOM',16,1)
        READ(1,15) XPOSIN,YPOSIN,TZERO,YZERO,TMIN,TMAX
       1,YMIN,YMAX,DT,DY
     15 FORMAT(10F6.1)
        CALL NEWPLT(XPOSIN,YPOSIN,10.0)
        CALL ORIGIN(TZERO,YZERO)
        CALL TSCALE(TMIN,TMAX,8.0)
        CALL YSCALE(YMIN,YMAX,6.0)
        CALL TAXIS(DT)
        CALL YAXIS(DY)
        PI = 3.14159
        THETAX = PI/(2.*180.)
        PHIO = 0.
        THETAO = 0.
        PHI =0.
        M = 20
        THETA = THETAO
        KA = M
        DO 70 I=1,240
        A = KA*(COS(THETA)-COS(THETAO))
        RHO = SQRT(SIN(THETA)**2+SIN(THETAO)**2-2.*SIN
       1(THETA)*SIN(THETAO)*COS(PHI-PHIO))
        B = KA*RHO
        CO = 2.-(PI/(2.*M))*COTAN(PI/(2.*M))
        C1 = 5.*PI*(COTAN(PI/(2.*M))-3.*COTAN(3.*PI/
       1(2.*M)))/(16.*M)
        C2 = 9.*PI*(COTAN(PI/(2.*M))+7.5*COTAN(3.*PI/
       1(2.*M))-17.5*COTAN(5.*PI/(2.*M)))/(128.*M)
        C3= (13*PI/(2048.*M))*(5.*COTAN(PI/(2.*M))+21.*
       1COTAN(3.*PI/(2.*M))+105.*COTAN(5.*PI/(2.*M))
       2-231.*COTAN(7.*PI/(2.*M)))
        AA = SQRT(A**2+B**2)
        IF(AA) 3,4,3
      3 TIO = 2.*SIN(AA)/AA
        GO TO 5
      4 TIO = 2.
      5 TO = -0.90617985
        T1 = -0.53846931
        T2 = 0.
        T4 = -TO
        T3 = -T1
        AO = 0.23692689
        A1 = 0.47862867
        A2 = 0.568888888
        A3 = A1
        A4 = AO
        DO 50 L=1,3
     72 T = TO
     60 BA = ABS(B*SQRT(3.-2.*T-T**2)/2.)+0.00005
        CALL BESJ(BA,C,F2,0.00005,0)
```

```
      X = (T+1.)/2.
      K = 2*L
      CALL LEP(Y,X,K+1)
      F3 = Y(K+1)
      IF(T-T0)72,73,74
   73 T = T1
      GO TO 60
   74 IF(T-T1)73,81,82
   81 T = T2
      GO TO 60
   82 IF(T-T2)81,90,91
   90 T = T3
      GO TO 60
   91 IF(T-T3)90,94,95
   94 T = T4
      GO TO 60
   95 TERM(L) = 2.*(AC*F(T0)+A1*F(T1)+A2*F(T2)+A3*F(T3)
     1+A4*F(T4))
   50 CONTINUE
      PATT(I) = CC*TIO+C1*TERM(1)+C2*TERM(2)+C3*TERM(3)
      TNORM = PATT(1)
      PATTN(I) = PATT(I)/TNORM
   70 THETA = THETA+THETAX
      ZZ = PATT(1)
      WRITE(3,100) ZZ,(PATTN(I),I=1,240)
  100 FORMAT(6F20.4)
      CALL TPLT(PATTN,240,1,M)
      CALL SYM(1.5,4.0,0.21,'AES-15',0.0,6)
      CALL ENDPLT
      CALL LSTPLT
      CALL EXIT
      END
```

```
C       NARONG YOOTHANOM              PHD DISSERTATION
CC      THE AES APPROXIMATED PATTERN ON THE PLANE OF THE
CC      AZIMUTH ANGLE.
        DIMENSION  TERM(50),Y(30),PATT(300),PATTN(300)
        F1(T) = COS((T+1.)*A/2.)
        F(T) = F1(T)*F2*F3
        CALL PENPOS ('NARONG YOOTHANOM',16,1)
        READ(1,15) XPOSIN,YPOSIN,TZERO,YZERO,TMIN,TMAX
       1,YMIN,YMAX,DT,DY
     15 FORMAT(10F6.1)
        CALL NEWPLT(XPOSIN,YPOSIN,10.0)
        CALL ORIGIN(TZERO,YZERO)
        CALL TSCALE(TMIN,TMAX,8.0)
        CALL YSCALE(YMIN,YMAX,6.0)
        CALL TAXIS(DT)
        CALL YAXIS(DY)
        PI = 3.14159
        THETAO =PI/2.
        PHIO = 0.
        PHI = PHIO
        THETA = PI/2.
        PHIX = PI/180.
        DO 70 I=1,180
        M = 20
        KA = M
        A = KA*(COS(THETA)-COS(THETAO))
        RHO = SQRT(SIN(THETA)**2+SIN(THETAO)**2-2.*SIN
       1(THETA)*SIN(THETAO)*COS(PHI-PHIO))
        B = KA*RHO
        C0 = 2.-(PI/(2.*M))*COTAN(PI/(2.*M))
        C1 = 5.*PI*(COTAN(PI/(2.*M))-3.*COTAN(3.*PI/(2.*M)
       1))/(16.*M)
        C2 = 9.*PI*(COTAN(PI/(2.*M))+7.5*COTAN(3.*PI/(2.*M))
       1-17.5*COTAN(5.*PI/(2.*M)))/(128.*M)
        C3= (13*PI/(2048.*M))*(5.*COTAN(PI/(2.*M))+21.*
       1COTAN(3.*PI/(2.*M))+105.*COTAN(5.*PI/(2.*M))-
       2231.*COTAN(7.*PI/(2.*M)))
        AA = SQRT(A**2+B**2)
        IF(AA) 3,4,3
      3 TIO = 2.*SIN(AA)/AA
        GO TO 5
      4 TIO = 2.
      5 T0 = -0.90617985
        T1 = -0.53846931
        T2 = 0.
        T4 = -T0
        T3 = -T1
        A0 = 0.23692689
        A1 = 0.47862867
        A2 = 0.568888888
        A3 = A1
        A4 = A0
        DO 250 L = 1,3
     72 T = T0
```

```
 60 BA = ABS(B*SQRT(3.-2.*T-T**2)/2.)+0.00005
    CALL BESJ(BA,0,F2,0.00005,0)
    X = (T+1.)/2.
    K = 2*L
    CALL LEP(Y,X,K+1)
    F3 = Y(K+1)
    IF(T-T0)72,73,74
 73 T = T1
    GO TO 60
 74 IF(T-T1)73,81,82
 81 T = T2
    GO TO 60
 82 IF(T-T2)81,90,91
 90 T = T3
    GO TO 60
 91 IF(T-T3)90,94,95
 94 T = T4
    GO TO 60
 95 TERM(L) = 2.*(A0*F(T0)+A1*F(T1)+A2*F(T2)+A3*F(T3)
   1+A4*F(T4))
250 CONTINUE
    PATT(I) = (C0*T10+C1*TERM(1)+C2*TERM(2)+C3*TERM(3))
    TNORM = PATT(1)
    PATTN(I) = PATT(I)/TNORM
 70 PHI = PHI+PHIX
    WRITE(3,100) TNORM,(PATTN(I),I=1,240)
100 FORMAT(6F20.4)
    CALL TPLT(PATTN,180,1,1)
    CALL SYM(1.5,4.0,.21,'AES-17',0.0,6)
    CALL ENDPLT
    CALL LSTPLT
    CALL EXIT
    END
```

```
C      NARONG YOOTHANOM          PHD DISSERTATION
CC     COMPARISON OF THE AES APPROXIMATED PATTERN TO THE
CC     TRUE ONE AT THE MAINBEAM AT VARIOUS M.
       DIMENSION  TERM(50),Y(30),PATT(125),PATTN(125)
       F1(T) = COS((T+1.)*A/2.)
       F4(T) = SQRT(3.-2.*T-T**2)/2.
       F(T) = F1(T)*F2*F3/F4(T)
       CALL PENPOS ('NARONG YOOTHANOM',16,1)
       READ(1,15) XPOSIN,YPOSIN,TZERO,YZERO,TMIN,TMAX
     1,YMIN,YMAX,DT,DY
    15 FORMAT(10F6.1)
       CALL NEWPLT(XPOSIN,YPOSIN,10.0)
       CALL ORIGIN(TZERO,YZERO)
       CALL TSCALE(TMIN,TMAX,8.0)
       CALL YSCALE(YMIN,YMAX,6.0)
       CALL TAXIS(DT)
       CALL YAXIS(DY)
       PI = 3.14159
       PHIO = PI/2.
       THETAO = PI/2.
       PHI = PI/2.
       THETA = THETAO
       THETAX = PI/180.
       DO 500 M=1,100
       KA = M
       A = KA*(COS(THETA)-COS(THETAO))
       RHO = SQRT(SIN(THETA)**2+SIN(THETAO)**2-2.*SIN
     1(THETA)*SIN(THETAO)*COS(PHI-PHIO))
       B = KA*RHO
       C0 = 2.-(PI/(2.*M))*COTAN(PI/(2.*M))
       C1 = 5.*PI*(COTAN(PI/(2.*M))-3.*COTAN(3.*PI/(2.*M)
     1))/(16.*M)
       C2 = 9.*PI*(COTAN(PI/(2.*M))+7.5*COTAN(3.*PI/(2.*M))
     1-17.5*COTAN(5.*PI/(2.*M)))/(128.*M)
       C3= (13*PI/(2048.*M))*(5.*COTAN(PI/(2.*M))+21.*
     1COTAN(3.*PI/(2.*M))+105.*COTAN(5.*PI/(2.*M))-
     2231.*COTAN(7.*PI/(2.*M)))
       AA = SQRT(A**2+B**2)
       IF(AA) 3,4,3
     3 TIO = 2.*SIN(AA)/AA
       GO TO 5
     4 TIO = 2.
     5 T0 = -0.90617985
       T1 = -0.53846931
       T2 = 0.
       T4 = -T0
       T3 = -T1
       A0 = 0.23692689
       A1 = 0.47862867
       A2 = 0.568888888
       A3 = A1
       A4 = A0
       DO 250 L = 1,3
    72 T = T0
```

```
 60 BA = ABS(B*SQRT(3.-2.*T-T**2)/2.)+0.00005
    CALL BESJ(BA,0,F2,0.00005,0)
    X = (T+1.)/2.
    K = 2*L
    CALL LEP(Y,X,K+1)
    F3 = Y(K+1)
    IF(T-T0)72,73,74
 73 T = T1
    GO TO 60
 74 IF(T-T1)73,81,82
 81 T = T2
    GO TO 60
 82 IF(T-T2)81,90,91
 90 T = T3
    GO TO 60
 91 IF(T-T3)90,94,95
 94 T = T4
    GO TO 60
 95 TERM(L) = 2.*(AC*F(T0)+A1*F(T1)+A2*F(T2)+A3*F(T3)
   1+A4*F(T4)
250 CONTINUE
    PATT(M) =  (CC*TI0+C1*TERM(1)+C2*TERM(2)+C3*
   1TERM(3))*2.*M**2/PI
    NORM = 2
    MM = M-1
    DO 700 I=1,MM
    RNM = 2.*M*SIN(I*PI/M)
    NM = RNM+0.5
700 NORM = NORM+NM
    IF(M-20) 11,12,11
 12 WRITE(3,101) NORM
101 FORMAT(F20.4)
 11 PATTN(M) = PATT(M)/NORM
    P = PATTN(M)
500 WRITE(3,100) M,P
100 FORMAT(I20,F20.4)
    CALL TPLT(PATTN,100,1,1)
    CALL SYM(3.0,4.0,0.21,'AES-18',0.0,6)
    CALL ENDPLT
    CALL LSTPLT
    CALL EXIT
    END
```

```
C      NARONG YOOTHANOM          PHD DISSERTATION
CC       THE LATITUDE-LONGITUDE DISTRIBUTION
CC         THE BEAMWIDTH ON THE PLANE OF THE ELEVATION ANGLE.
       DIMENSION    BWC(120),BW1(120),BW2(120),BW3(120),
      1BW4(120)
       CALL PENPOS ('NARONG YOOTHANOM',16,1)
       READ(1,10) XPOSIN,YPOSIN,TZERO,YZERO,TMIN,TMAX,
      1YMIN,YMAX,DT,DY
   10 FORMAT(10F6.1)
       CALL NEWPLT(XPOSIN,YPOSIN,10.0)
       CALL ORIGIN(TZERO,YZERO)
       CALL TSCALE(TMIN,TMAX,8.0)
       CALL YSCALE(YMIN,YMAX,6.0)
       CALL TAXIS(DT)
       CALL YAXIS(DY)
       PI = 3.14159
       T0 =0.
       T1 = PI/6.
       T2 = PI/4.
       T3 = PI/3.
       T4 = PI/2.
       DO 700 KA=1,100
       A0 = 1.-1.17157/((KA**2)*(1.+4.*SIN(T0)**2))
       A1 = 1.-1.17157/((KA**2)*(1.+4.*SIN(T1)**2))
       A2 = 1.-1.17157/((KA**2)*(1.+4.*SIN(T2)**2))
       A3 = 1.-1.17157/((KA**2)*(1.+4.*SIN(T3)**2))
       A4 = 1.-1.17157/((KA**2)*(1.+4.*SIN(T4)**2))
       B0 = 2.*ARCOS(A0)*180./PI
       B1 = 2.*ARCOS(A1)*180./PI
       B2 = 2.*ARCOS(A2)*180./PI
       B3 = 2.*ARCOS(A3)*180./PI
       B4 = 2.*ARCOS(A4)*180./PI
       BW0(KA) = B0
       BW1(KA) = B1
       BW2(KA) = B2
       BW3(KA) = B3
       BW4(KA) = B4
  700 WRITE(3,100) KA,B0,B1,B2,B3,B4
  100 FORMAT(I10,5F15.4)
       CALL TPLT(BW0,100,1,0)
       CALL TPLT(BW1,100,1,1)
       CALL TPLT(BW2,100,1,2)
       CALL TPLT(BW3,100,1,3)
       CALL TPLT(BW4,100,1,4)
       CALL SYM(2.0,3.0,0.14,'THETA-PLANE',0.0,11)
       CALL ENDPLT
       CALL LSTPLT
       CALL EXIT
       END
```

```
C       NARONG YOOTHANOM          PHD DISSERTATION
CC      THE LL DISTRIBUTION SPHERICAL ARRAY.
CC      THE BEAMWIDTH ON THE PLANE OF THE AZIMUTH ANGLE AS
CC      A FUNCTION OF KA.
        DIMENSION    BW(120)
        CALL PENPOS ('NARONG YOOTHANOM',16,1)
        READ(1,15) XPOSIN,YPOSIN,TZERO,YZERO,TMIN,TMAX
       1,YMIN,YMAX,DT,DY
   15 FORMAT(10F6.1)
        CALL NEWPLT(XPOSIN,YPOSIN,10.0)
        CALL ORIGIN(TZERO,YZERO)
        CALL TSCALE(TMIN,TMAX,8.0)
        CALL YSCALE(YMIN,YMAX,6.0)
        CALL TAXIS(DT)
        CALL YAXIS(DY)
        PI = 3.14159
        DO 700 KA = 1,100
        A = 1.-1.32795/(KA**2)
        B = 2.*ARCOS(A)*180./PI
        BW(KA) = B
  700 WRITE(3,100) KA,B
  100 FORMAT(I20,F20.4)
        CALL TPLT(BW,100,1,0)
        CALL SYM(1.5,4.0,.21,'LL-20',0,5)
        CALL SYM(2.0,3.0,0.14,'PHI-PLANE',0.0,9)
        CALL ENDPLT
        CALL LSTPLT
        CALL EXIT
        END
```

```
C      NARONG YOOTHANOM          PHD DISSERTATION
CC        THE APPROXIMATELY EQUALLY-SPACED  SPHERICAL ARRAY.
CC        THE BEAMWIDTH ON THE PRINCIPAL PLANES.
       DIMENSION    BW(120)
       CALL PENPOS ('NARONG YOOTHANOM',16,1)
       READ(1,15) XPOSIN,YPOSIN,TZERO,YZERO,TMIN,TMAX
      1,YMIN,YMAX,DT,DY
   15 FORMAT(10F6.1)
       CALL NEWPLT(XPOSIN,YPOSIN,10.0)
       CALL ORIGIN(TZERO,YZERO)
       CALL TSCALE(TMIN,TMAX,8.0)
       CALL YSCALE(YMIN,YMAX,6.0)
       CALL TAXIS(DT)
       CALL YAXIS(DY)
       PI = 3.14159
       DO 700 KA = 1,100
       A = 1.-0.87868/(2.*KA**2)
       B = 2.*ARCOS(A)*180./PI
       BW(KA) = B
  700 WRITE(3,100) KA,B
  100 FORMAT(I20,F20.4)
       CALL TPLT(BW,100,1,0)
       CALL SYM(1.5,4.0,.21,'AES',0.0,3)
       CALL SYM(2.0,3.0,0.14,'PHI-THETA',0.0,9)
       CALL ENDPLT
       CALL LSTPLT
       CALL EXIT
       END
```

VITA

Narong Yoothanom was born on April 13, 1942, in the city of Kanchanaburi, Thailand. He received his primary and secondary education at the Visutharangsi School of Kanchanaburi. Upon receiving a scholarship from Chulalongkorn University, Bangkok, Thailand, he spent four years from 1960 to 1964 in the College of Engineering, after which he was graduated with a Bachelor of Science Degree in Electrical Engineering with First Class Honors in March, 1964.

Having been granted a Fellowship from the Anandhamahidol Foundation, Thailand, in September, 1965, he entered Stanford University, California, from which he received a Master of Science Degree in Electrical Engineering in June, 1966. He transferred to the University of Missouri -- Rolla in the following September to begin his postgraduate work in Electrical Engineering.

Since May, 1964, the author has been holding the position of Instructor with the Department of Electrical Engineering at Chulalongkorn University, Thailand, where he is mostly involved in Electromagnetic Theory and Advanced Electronics. During the Summer of 1966, he was employed as a research engineer at Stanford Research Institute, working mainly with the antenna pattern in a dense jungle. Since September, 1968, he has been with

the Department of Electrical Engineering, University of Missouri -- Rolla, as a graduate assistant.

Mr. Yoothanom was a recipient of two Medal Awards from the King of Thailand, the copper one in 1963 and the golden one in 1964. He is a member of The Engineering Association of Thailand and The Institute of Electrical and Electronics Engineers, with the specialized groups of Antennas and Propagation and Microwave Theory and Technique.